INVESTIGATION OF DIACYLGLYCEROL KINASE EPSILON

INVESTIGATING THE ROLES OF A PUTATIVE TRANSMEMBRANE DOMAIN OF MAMMALIAN DIACYLGLYCEROL KINASE EPSILON

By

ARMELA OVIDIA DICU, B.Sc.

A Thesis

Submitted to the School of Graduate Studies

In Partial Fulfillment of the Requirements

For the Degree

Master of Science

McMaster University

MASTER OF SCIENCE (2006) McMaster University

(Biochemistry and Biomedical Sciences) Hamilton, Ontario, Canada

TITLE: Investigating the roles of a putative transmembrane domain of mammalian diacylglycerol kinase epsilon

AUTHOR: Armela Ovidia Dicu, B.Sc. (University of Waterloo)

SUPERVISOR: Dr. Richard M. Epand

NUMBER OF PAGES: i-xv, 1-108.

ABSTRACT

An area of current research interest involves the diacylglycerol kinase (DGK) family. Diacylglycerol kinases (DGKs) are a group of enzymes that phosphorylate diacylglycerol (DAG), a second messenger involved in cell signaling. The product of this reaction, phosphatidic acid (PA), also has signaling roles. An interesting isoform is DGKε, that although it has no identifiable regulatory domains other than the C1 domains. In addition, the catalytic domain is homologous to that of other DGK isoforms; however, DGKε exhibits an unusual specificity toward acyl chains of DAG, selectively phosphorylating an arachidonoyl-DAG substituted at the *sn*-2 position. Recently, researchers have identified an N-terminal hydrophobic domain of about 19 amino-acids in human DGKε. The present study attempted to identify the function of the N-terminal putative transmembrane domain of human DGKε and its relationship to the activity and substrate specificity of this enzyme by designing a truncated form of DGKε lacking the putative transmembrane domain.

We have shown that the putative transmembrane domain of DGKε is not required for enzyme activity or for substrate specificity. In a mixed micellar assay the enzyme-catalyzed reaction followed surface dilution kinetics with respect to diacylglycerol and followed Michaelis-Menten kinetics with respect to ATP. The results show that the truncated form of the enzyme maintains substrate specificity for lipids with an arachidonoyl moiety present at the *sn*-2 position. The truncation increased the catalytic rate constant for all three substrates used in this study. It appears unlikely that the putative transmembrane domain, a segment unique to DGKε, has no functional role. It is possible that the hydrophobic segment may have a role in enzyme regulation by associating the enzyme in oligomers that are inactive in quiescent cells and get activated upon dissociation into monomers by increased levels of DAG in the membrane. We have shown that

the presence of higher molecular species in the gel is not dependent on the presence or absence of the putative transmembrane domain. The only difference between the full-length and truncated enzyme is the monomer to dimer ratio. It appears likely that another segment of DGKε besides the putative transmembrane domain may be involved in oligomerization and that oligomerization is either transient or very weak. The absence of the hydrophobic domain of DGKε seems to cause no drastic changes either in the activity, the substrate specificity, or the state of oligomerization of the enzyme.

Therefore, the next question is whether the hydrophobic domain of DGKε inserts itself in the membrane as a transmembrane helix or it only helps associate the enzyme to the surface of the membrane. We studied the topology of the N-terminal domain of DGKε in intact and permeabilized cells by indirect immunofluorescent microscopy. The results show that the N-terminal domain of the protein is present in the cytosol. The data supports a model in which the hydrophobic domain of DGKε forms a hydrophobic loop that attaches to the inner layer of the plasma membrane or that the hydrophobic domain attaches to the inner leaflet through its non-polar surface of a horizontal helix. The first hypothesis is supported by the presence of a Pro residue in the middle of the hydrophobic domain. This Pro would introduce a kink in the helix creating a loop, but the absence of one or more glycine residues proximal to proline may hinder the formation of the loop. The second hypothesis is sustained by the presence of a polar surface on one side of the helical wheel. This orientation indicates the presence of a slightly horizontal helix attached to the surface of the inner layer of the plasma membrane.

Regardless of the orientation of the helix, the weak association of the enzyme with the membrane is supported by previous data on the ease of extractability of the enzyme with high salts and on the Triton X-114 phase partitioning.

ACKNOWLEDGEMENTS

First and foremost I would like to thank my supervisor, Dr. Richard M. Epand. Dr. Epand's knowledge and expertise were valuable resources throughout my Masters. He not only offered me great supervision, but he was also a great mentor for me. I will always value the knowledge and the confidence I developed working on my project in his lab. Secondly, I would like to thank my committee members, Dr. Ray Truant and Dr. Radhey S. Gupta, for challenging and advising me throughout my project. This project would not have been possible without the help of Dr. Matthew K. Topham, our collaborator from Huntsman Cancer Institute in Utah. I would like to thank him for leading my first steps into this project. He not only helped me gain procedural knowledge but also believe in my abilities. I would also like to thank past and present members of the Epand lab, and especially to Dr. Raquel F. Epand, for offering me a great example of passion for science and research. I will be indebted forever to all the people that helped me get so far in my career and helped me believe in myself.

Last but not least, I would like to thank my family, especially my mom, for being so patient with me and for being so supportive of my career choices. Finally, I would not have made it thus far without the support and love of my friends. Thank you all for keeping me grounded and for being so supportive and patient with me.

TABLE OF CONTENTS

LIST OF FIGURES

LIST OF TABLES

LIST OF ABBREVIATIONS

ACA	aminocaproic acid
ATP	adenosine triphosphate
BAP	bacterial alkaline phosphatase
BSA	bovine serum albumine
C1	cys-rich domains
CD	circular dichroism
CERK	ceramide kinases
C1P	ceramide-1-phosphate
CRD	cys-rich domains
CS	calf serum
DAG	diacylglycerol
DGK	diacylglycerol kinase
DGKε	epsilon isoform of DGK
DGKΔε	a truncated form of DGKε lacking a segment of 40 amino acids at the N-terminus
DMEM	Dulbecco's modified Eagle's medium
DOG	1, 2-dioleoyl-*sn*-glycerol
DOPC	1, 2-dioleoylphosphatidylcholine
DSS	disuccinimidyl suberate
DTT	dithiothreitol
EDTA	ethylenediamine-tetraacetic acid
EGTA	ethyleneglycol-tetraacetic acid
ER	endoplasmic reticulum
FBS	fetal bovine serum

FLAG	an N-terminal FLAG epitope tag
FRET	fluorescence resonance energy transfer
GTP	guanosine triphosphate
HIS	a C-terminal His tag
HRP	horse-radish peroxidase
IP_3	inositol 1, 4, 5-trisphosphate
LUV	large unilamellar vesicles
MAG	monoacylglycerol
MOPS	3-(N-Morpholino)-propanesulfonic acid
NHS	N-hydroxysuccinimide
OG	octyl-β-glucoside
PA	phosphatidic acid
PAGE	polyacrylamide-gel electrophoresis
PBS	phosphate buffer saline
PC	phosphatidylcholine
PCR	polymerase chain reaction
PE	phosphatidylethanolamine
PFO	perfluoro-octanoic acid
PH	pleckstrin homology domain
PI	phosphatidylinositide
PIP_2	phosphatidylinositol-4, 5-bisphosphate
PI-K	phosphatidylinositol kinase
PIPK	phosphatidylinositol phosphate kinases
PKC	protein kinase C

PKD	protein kinase D
PLC	phospholipase C
POPC	1-palmitoyl-2-oleoyl-sn-glycero-3-phosphocoline
PVDF	polyvinylidene fluoride
SAG	1-stearoyl-2-arachidonoyl-*sn*-glycerol
SAM	sterile alpha motif
SLG	1-stearoyl-2-linoleoyl-*sn*-glycerol
S1P	sphingosine-1-phosphate
SPHK	shingosine kinases
TCA	trichloroacetic acid
TPA	12-O-tetradecanoylphorbol 13-acetate

Chapter 1. Introduction

Cellular signaling

Each cell in a multicellular organism has been programmed during development to respond to specific extracellular signals produced by other cells. These signals act in various combinations to regulate the behavior of the cell. Cell signaling requires a set of receptor proteins that get activated by the extracellular signal molecules. There are three classes of cell-surface receptors: ion-channel linked receptors, G-protein linked receptors, and enzyme-linked receptors (Alberts *et al.*, 2002).

G-protein linked receptors form the largest class of cell-surface receptors. They transmit a signal into the cell interior by activating chains of intracellular signaling proteins. Many of these signaling proteins are activated ON and OFF by phosphorylation or GTP binding (Alberts *et al.*, 2002). An important class of relay molecules is the class of GTP-binding proteins (G proteins). These G proteins are attached to the cytoplasmic side of the plasma membrane where they couple the receptors to enzymes or ion channels. Some G proteins activate the inositol phospholipid signaling pathway by activating the membrane bound phospholipase C-β. The phospholipase acts on an inositol lipid called phosphatidylinositol 4, 5-bisphosphate [PI-(4, 5)-P_2] present in small amounts in the inner leaflet of the plasma membrane and breaks it into two products: inositol 1, 4, 5-trisphosphate (IP_3) and diacylglycerol (DAG) (Alberts *et al.*, 2002). DAG remains embedded in the membrane where it has two potential signaling roles, the first one in the

synthesis of arachidonic acid and the second one in the activation of a Ca^{2+}- dependent serine/threonine protein kinase (PKC).

1.1.1 Lipid kinases

The expression and activity of many kinases are known to be affected in a variety of diseases. Protein kinases and lipid kinases are two important classes of biomedically relevant enzymes (Noble *et al.*, 2004). One important class of lipid kinases involved in a variety of pathological processes related to cancer, inflammation, immunology, and cardiovascular disease is the phosphatidylinositol kinase (PI-K) family (Anderson *et al.*, 1999). There are three classes of PI kinases, the PI-4-kinases, the PI-phosphate kinases (PIPK), and the PI-3-kinases. The PI-4-kinases exist in multiple isoforms, three of which have been identified and they belong to type II and type III subclasses. The isoforms were named according to their molecular weight, PI4K230, PI4K92, and PI4K55. The PI-4-K phosphorylates the 4'-hydroxyl group on the inositol ring of PI producing PI-4-P (Heilmeyer *et al.*, 2003). Two isoforms of PIPK have been characterized, type I and II. They synthesize PI-(4, 5)-P_2 by phosphorylating the fifth hydroxyl of PI-4-P (Anderson *et al.*, 1999). The family of mammalian PI-3-kinases includes eight identified isoforms divided into three main classes. The members of the PI-3-kinase family phosphorylate the 3'-hydroxyl of the inositol head group of phosphoinositides forming PI-(3, 4, 5)-P_3 (Anderson and Jackson, 2003).

The 1-phosphate derivatives of sphingosine and ceramide have been recently discovered to be involved in lipid signaling. S1P acts as an extracellular mediator and as

an intracellular second messenger, while C1P is known to be involved in intracellular processes (Baumruker *et al.*, 2005). The enzymes involved in the generation of these lipid mediators are the sphingosine kinases (SPHK) and the ceramide kinases (CERK). Two functional mammalian SPHK have been identified and designated type 1 and type 2 and a number of splice variants have been identified. The product of SPHK, S-1-P, is known to be involved in diverse and fundamental processes such as cell growth and survival, calcium mobilization, and adhesion molecule expression (Baumruker *et al.*, 2005). There is only one isoform of CERK that has been characterized and a new ceramide kinase-like (CERKL) sequence was cloned recently (Baumruker *et al.*, 2005). The enzymatic activity of CERK was first described by Bajjalieh *et al.*, 1989. Recently the product of the CERK reaction, C-1-P, was determined to regulate many physiological processes related to cell proliferation, apoptosis, phagocytosis, and inflammation (Baumruker *et al.*, 2005).

Another important class of lipid kinases is the diacylglycerol kinase (DGK) family, which will be presented in detail in the section 1.2 of this manuscript.

1.1.2 Interfacial catalysis

The enzymes involved in lipid signaling pathways include lipid biosynthetic enzymes, lipid degrading enzymes, and enzymes that utilize lipid cofactors. Lipid kinases are one class of enzymes involved in lipid signaling pathways. These enzymes have hydrophobic or amphipathic lipid substrates, cofactors, inhibitors, and products that aggregate in solution. Many of these enzymes are water-insoluble integral membrane proteins.

The term interfacial catalysis refers to the enzyme catalyzed reactions that involve at least one reactant that is present at an interface. The sequestration of the substrate in the interface introduces additional factors not found in soluble kinetics. Firstly, the enzyme needs to gain access to the substrate by association with the surface; secondly, the activity of the enzyme depends on the surface concentration of the substrate; and thirdly, the nature of the interface can have various effects on enzyme activity (Deems, 2000). In the case of an integral membrane protein, the surface binding step is circumvented. In order to resolve the problem of calculating the surface concentration of the substrate a new concept was developed termed "surface dilution kinetics" (Dennis, 1973; Deems *et al.*, 1975). This model is critical for defining the kinetic parameters of lipid-dependent enzymes because it accounts for both the surface concentration of the lipid substrate expressed in mole fraction units and the bulk concentration of the substrate expressed in terms of molarity (Carman *et al.*, 1995). The third factor affecting the kinetics is that the substrate is not moving freely in solution but it is sequestered in micellar aggregates or vesicles. The substrate is hence held in a certain position, which will either hinder or facilitate the interaction with the enzyme (Dennis, 1983).

The basic goal of a kinetic analysis is to determine the model that best fits the experimental data and to obtain estimates of the appropriate parameters. The "surface dilution kinetic" model uses mixed micelles and studies initial rate based on varying ligand concentrations. This data is analyzed using nonlinear regression and is equivalent to the Michaelis-Menten analysis of soluble enzymes (Deems, 2000). To determine if an enzyme follows interfacial kinetics using the surface dilution model, the enzyme's activity must be determined over a wide range of substrate concentrations. There are a

number of caveats when dealing with interfacial catalysis: the enzyme surface binding, the quality of the substrate interface, and the heterogeneous concentration of surface substrate among aggregates (Deems, 2000).

Substrate specificity with respect to acyl chain length and degree of unsaturation is of great interest in enzymology. Acyl group composition is important for membrane structure and function and for lipid signaling. Studying the specificity of lipid-dependent enzymes can be hard due to changes in the physical characteristic of the surface brought by different lipid substrates. This problem was circumvented by the use of detergent micelles that prevent such changes (Deems, 2000).

1.2 Diacylglycerol kinases (DGK)

The hydrolysis of PI- (4, 5)-P_2 by PLC enzymes initiates numerous intracellular signaling pathways. The products of this reaction, DAG and IP_3, rise only transiently and then fall back to basal levels (Luo *et al.*, 2004). IP_3 causes calcium release from intracellular stores by binding to intracellular receptors. DAG is a membrane lipid that recruits and often activates signaling proteins that contain Cys-rich domains (C1) (Luo *et al.*, 2004). A well-known DAG binding protein is PKC. However, other DAG targets exist such as the family of four RasGRP nucleotide exchange factors, the chimaerins-RacGTPase activating proteins, PKD, and the Munc13 proteins (Topham and Prescott, 2002). Because DAG can regulate so many different signaling proteins, its intracellular levels have to be tightly regulated. Excessive and/or prolonged DAG signaling, seen in

tumours and transformed cell lines, are equivalent to the effects of the tumour-promoting phorbol esters (Luo *et al.*, 2004).

DAG can be metabolized in three ways: hydrolysis by DAG lipase to generate monoacylglycerol (MAG) and a free fatty acid; addition of CDP-choline or CDP-ethanolamine to form phosphatidyl choline (PC) or phosphatidyl ethanolamine (PE); or by phosphorylating the free hydroxyl group to form phosphatidic acid (PA). The major route of DAG metabolism is considered to be its conversion to PA mediated by DGKs (Topham, 2006).

1.2.1 DGK gene family-mammalian isoforms

The mammalian DGK family comprises of ten isoforms, of which nine have been identified and studied extensively, while the tenth one, DGKκ, has been identified recently (Imai *et al.*, 2005). Moreover, the occurrence of alternative splicing was recently detected in five mammalian DGK genes (β, γ, δ, ζ, η) (Luo *et al.*, 2004), and probably in other isotypes as well. Based on shared structural motifs, the DGK isoforms are classified into five classes (Fig. 1). The DGK isoforms differ from each other with respect to their structure, tissue expression, and enzyme properties. The heterogeneity of this family of enzymes is similar to PKC and PLC suggesting that the DGKs are not simply lipid biosynthetic enzymes, but have more complex roles in signaling (Topham and Prescott, 2002).

In contrast to mammals, only a few DGK isozymes have been identified in *C. elegans*, *D. melanogaster*, and *A. thaliana* while no DGK has been identified in yeast.

The structural diversity of DGKs in mammals and the absence of DGK gene in yeast may suggest that the mammalian DGK isozymes have roles in biological processes specific to higher vertebrates, such as development and differentiation, neural networking, the immune system, and organogenesis (Topham, 2006). It is interesting to note that several

DGKs belonging to different DGK subtypes can be expressed in the same tissue and the same cell, suggesting that each DGK subfamily has a specific function (Topham, 2006).

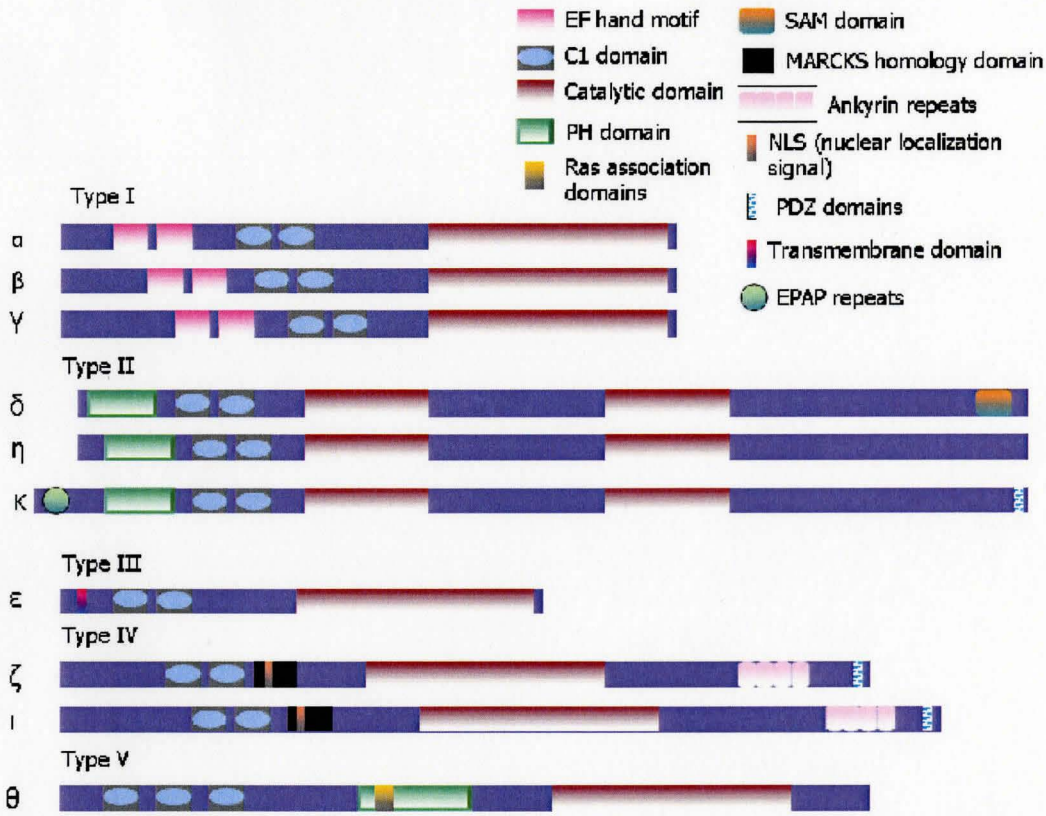

Fig. 1 The five classes of mammalian DGK isoforms. The ten mammalian isoforms are organized in five classes based on shared structural features. The Type I DGKs share an N-terminus EF hand motif. The Type II DGKs share an N-terminus PH domain. The Type III DGK has only one isoform with an N-terminus putative transmembrane domain. The Type IV DGKs share C-terminus ankyrin repeats and PDZ domains and a MARCKS homology domain with a nuclear localization signal. The Type V has only one isoform with a PH domain and a nuclear localization signal.

1.2.1.1 Mammalian isoforms- primary structure

All DGK isoforms identified to date are similar in having a catalytic domain necessary for kinase activity. The catalytic domain has an ATP-binding site similar to a protein kinase catalytic domain with the consensus sequence GXGXXG (G= Glycine and X= any amino acid) (Goto and Kondo, 2004). However, structural differences between the DGK and protein kinases catalytic domains suggest that DGK catalytic domains may have access to DAG in lipid bilayers, whereas protein kinases do not require such access (Luo *et al.*, 2004).

All DGKs have at least a pair of Cys-rich motifs (CRDs or Zinc fingers) (DGKθ has 3). The CRDs in DGK, especially CRD1, are similar to the C1 domains of Ser/Thr PKCs but lack certain consensus residues that might be involved in binding to phorbol esters (PDBu) (Luo *et al.*, 2004). Van Blitterswijk and Houssa, 1999, mentioned that in DGKs the CRD closest to the catalytic domain has an extended motif of 15 amino acids that is highly conserved between DGKs and not present in other C1 domains. The conserved residues in this motif are critical for DGK activity (Topham, 2006), suggesting that this extended C1 domain might have a critical function in binding DAG. The C1 domains of DGKs α, β, γ, δ, η, and θ have been tested for their ability to bind PDBu, but only C1A domains of DGKβ and DGKγ could bind successfully (Topham and Prescott, 2002). Therefore, the fact that phorbol esters fail to bind certain DGK-CRDs, does not rule out the binding of DAG to DGK-CRDs. Perhaps the inability of the DGK C1 to bind PDBu is due to the structural differences between PDBu and DAG, reflecting the selectivity of DGK C1 for authentic DAG, unlike other C1 domains (Topham, 2006).

Alternatively, there is the possibility that the CRDs in DGK serve other functions such as interaction with PS or other proteins (Van Blitterswijk and Houssa, 1999).

In addition to the C1 and the catalytic domains, most DGKs have other structural domains that appear to have regulatory roles and that are used to divide them into subfamilies. Type I DGKs have calcium-binding EF hand motifs, making these isoforms more active in the presence of calcium (Yamada *et al.*, 1997). Type II DGKs have a pleckstrin homology domain (PH) domain at their amino termini. Though no specific function has been identified for these domains, the PH of DGKδ was shown to bind PI weakly and non-selectively (Takeuchi *et al.*, 1997) or the PH domain is a potential site for protein-protein interactions (Van Blitterswijk and Houssa, 1999). DGKδ and η also have an SAM (sterile alpha motif) domain that is necessary to localize DGKδ to the ER where it participates in vesicular trafficking (Nagaya *et al.*, 2002). The SAM also mediates oligomerization of Type II DGKs (Murakami *et al.*, 2003). In some cases oligomerization may suppress DGK activity (Murakami *et al.*, 2003) or may coordinate enzyme translocation to the membrane (Imai *et al.*, 2002). The only type III DGK is the DGKε, a unique isoform in that it has an unusual specificity toward acyl chains of DAG, strongly preferring a fatty acid with an arachidonate at the sn-2 position (Tang *et al.*, 1996). This preference may suggest that this enzyme is involved in the PI turnover, being a component of the pathway that enriches PI with arachidonate (Fig. 2) (Prescott and Majerus, 1981).

Type IV DGKs have domains similar to the phosphorylation site domain of the MARCKS protein. This domain functions as a nuclear localization signal and it is phosphorylated by PKC (Topham *et al.*, 1998; Ding *et al.*, 1998). The phosphorylation of

DGKζ reduces nuclear localization (Topham *et al.*, 1998) and suppresses DGK activity (Luo *et al.*, 2003). Type IV DGKs also have four ankyrin repeats and PDZ-binding domains at their C-terminal ends (Hogan *et al.*, 2001). The type V DGK, DGKθ, has three C1 domains, a putative PH domain, and a Ras association domain (Houssa *et al.*, 1997).

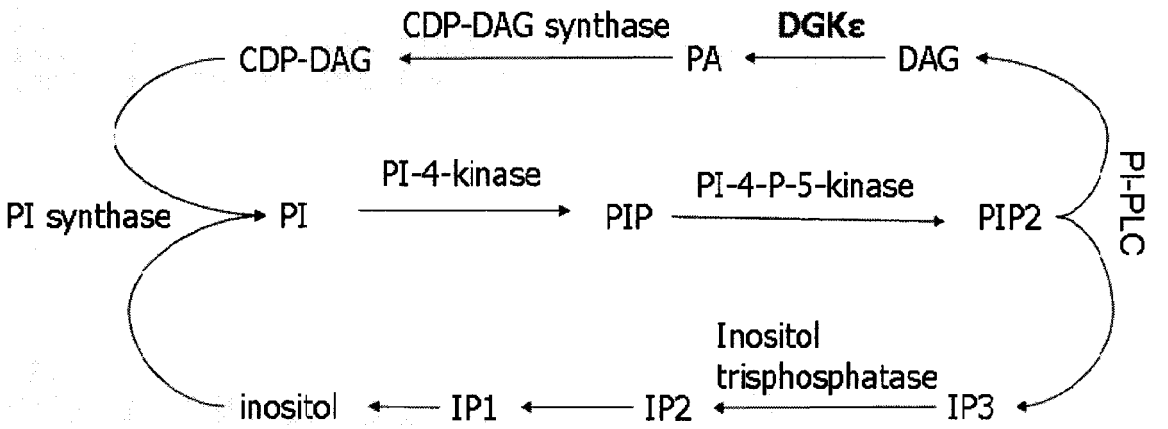

Fig. 2 Phosphatidylinositol turnover pathway. The PI-PLC enzyme breaks down PI-(4, 5)-P_2 to DAG and IP_3. Upon increased levels of DAG, DGKε gets activated and phosphorylates DAG to PA. Upon the action of cytidyl diphosphate-diacylglycerol (CDP-DAG) synthase, CDP-DAG is formed from PA and cytidyl trisphosphate (CTP). CDP-DAG reacts with the inositol formed from repeated dephosphorylation of IP_3 and upon the action of PI synthase forms PI. PI is then phosphorylated to PI- (4, 5)-P_2 by several PI-kinases. The cycle continues with the break down of PI- (4, 5)-P_2 by PI-PLC.

1.2.1.2 Mammalian isoforms- regulation of DGK activity

The complex family of DGK enzymes suggests complicated regulatory mechanisms specific for each DGK isotype. In most cases, the DGKs must translocate to a membrane to access the substrate, but translocation does not always activate the enzyme (Van Blitterswijk and Houssa, 2000). DGK activity can be modified by various cofactors such as calcium and lipids, and by post-translational modifications (Luo *et al.*, 2004). Also, alternative splicing regulates the activity of various DGKs (Luo *et al.*, 2004). The type IV and V DGK enzymes are regulated through associations and/or phosphorylation by different protein kinases such as PKC and Src kinase (Luo *et al.*, 2004). DGKs can be differentially regulated depending on the availability of cofactors and the activation state of protein kinases.

DGK activity is mainly restricted to membrane DAG pools generated after receptor activation. DGKs appear to be active in a number of cell compartments such as the endoplasmic reticulum, the neuromuscular junction, the cytoskeleton, and the nucleus (Luo *et al.*, 2004). The nucleus has a PI cycle that is separately regulated from its plasma membrane counterpart. Several DGKs have been detected in the nucleus (Luo *et al.*, 2004) and their presence is related to regulation of distinct pools of DAG at this intracellular site.

Another level of specificity is achieved during DGK enzyme regulation by associations with protein binding partners and regulation of enzyme activity. The best example of this kind of regulation is the DGKζ, which binds and regulates at least three proteins, Ras GRP1, RasGRP3, and PKCα (Luo *et al.*, 2004).

1.2.2 Diacylglycerol epsilon

One distinct class of mammalian DGKs, the type III, seems to have no other regulatory domains but the Cys-rich regions (C1 domains) and the catalytic domain. DGKε is the only isoform in this class and it is a 64kDa protein that has a strong preference for DAG substrates with an arachidonate moiety at the sn-2 position of the glycerol backbone. Since a large fraction of the DAG in cells that contain an arachidonate moiety arises from phospholipase C-catalyzed hydrolysis of PI- (4, 5)-P_2, it suggests that the unusual substrate specificity of DGKε is related to its involvement in the PI turnover cycle and accounts for the enrichment of PI with arachidonate (Topham and Prescott, 2002). It is important that PI maintain a proper fatty acid composition since some targets of DAG signaling, including PKCs, are specifically activated by DAG-containing unsaturated fatty acids like arachidonate (Topham and Prescott, 2002). Inositol lipid signaling is an important component of neuronal transmission. Rodriguez de Turco *et al.*, 2001 created null mice with a targeted deletion of the DGKε gene, and examined the mice susceptibility to seizures and the composition of their brain lipids. The null mice had shorter seizures and recovered much faster than wild type mice, and the brain lipids had reduced levels of arachidonate in both PI- (4, 5)-P_2 and DAG, compared to wild type (Rodriguez de Turco *et al.*, 2001).

DGKε is also unique in being the only DGK isoform with a predicted transmembrane helix (Thirugnanam *et al.*, 2001; Epand *et al.*, 2004). This putative transmembrane helix comprises approximately residues 20-40. The presence of a hydrophobic domain in the primary structure of the protein is suggestive of DGKε being

a putative integral membrane protein. This feature is unique among the DGK isoforms since the other isoforms require translocation to the membrane to come in closer proximity to the substrate. Therefore, DGKε should have different regulatory mechanisms compared to the other DGK isoforms.

Since 1988 to date several papers have mentioned the presence of a membrane bound mammalian DGK with an unique substrate specificity for unsaturated acyl chains. MacDonald *et al.*, 1988 have characterized a membrane- bound DGK from Swiss 3T3 cells and compared its enzymatic properties with the cytosolic DGK from 3T3 cells and with the bacterial membrane bound DGK. Walsh *et al.*, 1994 have purified arachidonoyl-DGK from bovine testis and studied the properties of this enzyme in mixed micelles. Ohanian and Heagerty, 1994 have demonstrated that the rat small arteries contain a membrane-associated DGK, which metabolizes arachidonoyl-containing substrates. Vasoconstrictor hormones differentially regulated the activity of this enzyme. Tang *et al.*, 1996 have cloned the human DGKε gene from a human endothelial cell library. They have shown that DGKε protein metabolized arachidonoyl-containing substrates. Kohyama-Koganeya *et al.*, 1997 have cloned a DGK predominantly expressed in rat retina that showed high homology to human DGKε and had a predicted mass of 64 kDa. The expression pattern of the rat DGKε was different from the human DGKε. Tang *et al.* 1999 investigated the presence of the human DGKε in the retina and its involvement as a regulator of the phototransduction pathway. The investigators generated a mouse strain with disrupted DGKε alleles by gene targeting and the mice showed no histological abnormality compared to wild type mice. These results indicate that it is unlikely that DGKε is a specific regulator of vertebrate phototransduction (Tang *et al.* 1999). Pettitt

and Wakelam, 1999 showed for the first time that DGKε phosphorylated DAG *in vivo* and that in doing so it regulated PKC localization and activity. This study provided evidence for DGKε being the physiological terminator of DAG signaling *in vivo*.

A very important finding in the function of DGKε was published in 2001 by Rodriguez de Turco *et al.* DGKε was shown to regulate seizure susceptibility and long-term potentiation through arachidonoyl-inositol lipid signaling. Following this study, Musto and Bazan, 2006 showed that DGKε modulated rapid kindling epileptogenesis through arachidonoyl-inositol lipid signaling. They postulated that the shortage of inositol lipids and second messengers rich in arachidonate is a key signaling event in epileptogenesis.

1.3 Objectives

Diacylglycerol kinases (DGKs) are a class of enzymes that influence many signaling pathways because both the substrate and the product of their reaction, DAG and PA, have signaling properties; therefore, their concentration in the cell must be tightly regulated. One class of DGKs, the type III, is known to be distinct since the isoform belonging to this type has an N-terminus hydrophobic domain and it possesses an unusual specificity for substrates containing an arachidonate moiety at the *sn*-2 position.

This present study investigated the importance of the putative transmembrane domain for DGKε activity and substrate specificity. We designed a truncated form of DGKε lacking aminoacid residues 1-41 (position 1 being Met) and we attached an N-terminus 3XFLAG tag both to the full-length and the truncated enzyme. The objective of

this work was to compare the two 3XFLAG-tagged constructs by determining their kinetic parameters. In addition, we compared the N-terminal 3XFLAG tag DGKε with a DGKε containing a C-terminal His tag to determine how the nature and position of the tag may affect the kinetic behaviour of the recombinant enzymes.

Since the results of the above mentioned kinetic study revealed that the truncated DGKε maintained enzyme activity and specificity for DAGs with arachidonic acid, the next step was to investigate other possible roles of the putative transmembrane domain. It is known that one regulatory mechanism of integral membrane enzymes is oligomerization. Therefore, the possible involvement of the transmembrane domain in oligomerization was investigated. To answer this question, various electrophoresis methods and co-immunoprecipitation techniques were employed.

Furthermore, proteins containing hydrophobic domains are interesting to study in the membrane since their transmembrane segment orientation could give information about possible functional roles. Therefore, the membrane topology of the hydrophobic domain of DGKε was investigated with the use of indirect immunofluorescence microscopy.

Chapter 2. Experimental procedures

2.1 Materials

Lipids used in the enzyme activity assay, including the DAG substrates, were purchased from Avanti Polar Lipids (Alabaster, AL). ATP was the disodium salt, Sigma Ultra grade (Sigma-Aldrich) and [γ-^{32}P] ATP was from Perkin-Elmer (Boston, MA). Other chemical reagents used were purchased from Sigma-Aldrich or Invitrogen/Gibco Life Sciences unless otherwise specified.

2.2. Experimental procedures

2.2.1 Construction of 3XFLAG Epitope-tagged DGKε Expression Vectors

A human DGKε PCR fragment was amplified from an N-terminus HA tagged DGKε vector supplied by Dr. M. K. Topham (Huntsman Cancer Institute, University of Utah, Utah, USA) by 25 cycles of PCR using Pfu DNA polymerase (Stratagene) and "polished" with Taq DNA polymerase (Stratagene). The following primers were used: forward, 5'-GATCTGGAAGCGGAGAGGCGG-3' (this primer contained a *Bgl*II site and corresponded to amino acids EAERR of human DGKε (Tang *et al.*, 1996); reverse, 5'-GTCGACTATTCAGTCGCCTTTATATC-3' (this primer contained a *Sal*I site and corresponded to amino acids DIKATE of human DGKε (Tang *et al.*, 1996). An N-terminally truncated human DGKε [DGKΔε (1-41)] PCR fragment was amplified as

described above for the full length construct, except that the following primers were used: forward, 5'-AGATCTCCAGCGGTCGCGCC-3' (this primer contained a *Bgl*II site and corresponded to amino acids LQRSR of human DGKε (Tang *et al.*, 1996); reverse, 5'-GTCGACTATTCAGTCGCCTTTATATC-3' (this primer contained a *Sal*I site and corresponded to amino acids DIKATE of human DGKε (Tang *et al.*, 1996).

The resulting PCR fragments were gel-purified using the QIAquick Gel Extraction Kit from QIAGEN and cloned into a TOPO-TA cloning vector (Invitrogen) following the manufacturer's protocol. The TOPO-TA vector containing the insert was extracted and purified using the QIAprep Spin Miniprep Kit from QIAGEN and following the manufacturer's protocol. The identity of the DNA was verified by DNA sequencing at the McMaster sequencing facility, MOBIX. The DNA fragments of interest were excised from the TOPO-TA vector using *Bgl*II and *Sal*I restriction enzymes by following standard protocols from Fermentas and gel-purified using the QIAquick Gel Extraction Kit from QIAGEN and following the manufacturer's protocol. The fragments of interest were subcloned by ligation into the corresponding site of a p3XFLAG-CMV-7.1 mammalian vector (Sigma-Aldrich), which attaches a 3XFLAG epitope at the N-terminus of the protein. The ligation was performed at 15°C overnight and XL1-Blue competent cells prepared after a protocol supplied by Dr. M. K. Topham's lab at Huntsman Cancer Institute (Utah, USA) were transformed by heat-shock transformation with the ligation mixture. 70µl XL1-Blue competent cells were mixed with 10µl of the ligation mixture and left 30min on ice. The cells were then placed in a 42°C water-bath for 30sec-1min and then put on ice for 5min. 1ml LB growth media was added to the cells and they were grown at 37°C for an hour with shaking. The cells were then placed

on antibiotic media plates and incubated overnight at 37°C. The plasmid DNA was extracted and purified using either QIAprep Spin Miniprep Kit or QIAfilter Plasmid Midi Kit from QIAGEN.

2.2.2 Cell Culture and Transfection of DGKε in COS-7 Cells

COS-7 cells were maintained in Dulbecco's modified Eagle's medium (DMEM, GIBCO/Invitrogen) containing 10% fetal bovine serum (FBS, GIBCO/Invitrogen) and 1% penicillin/streptomycin (GIBCO/Invitrogen) at 37°C in an atmosphere of 5% CO_2. The p3XFLAG constructs were transiently transfected into COS-7 cells using Lipofectamine 2000 according to the manufacturer's instructions (Invitrogen). Cells were transfected in parallel with the p3XFLAG-CMV-7.1 vector as a control. The lipofectamine reagent is a liposome formulation of polycationic and neutral lipid that forms complexes with the nucleic acid and cells then take up the complexes by endocytosis (Invitrogen). Transient transfections were performed on COS-7 cells for protein expression and on NIH3T3 cells for microscopy experiments. The cells were grown to about 70%-80% confluency in DMEM with 10%FBS and 1%Pen/Strep and then the plates were washed with DMEM one time and the DNA-lipofectamine complexes diluted in DMEM were overlayed on top of the cells. The plates were kept in the 37°C incubator under an atmosphere of CO_2 for 5-6 hours, and then the media was replaced with DMEM containing 10%FBS. The cells were harvested after 18-24 hours by scraping them off the plate in 1X PBS containing 1:100 protease inhibitor cocktail (Sigma-Aldrich). The cells were kept at -70°C until further use.

2.2.3 Enzyme Preparations

The transfected cells were harvested after 24-48 hours in ice-cold cell lysis buffer (20mM Tris-HCl, pH 7.5, 150 mM NaCl, 1 mM EDTA, and Protease Inhibitor Cocktail (1X) (Sigma-Aldrich)). The cells were pelleted at low speed (6,000g) and the pellets were kept at -70°C until further use. Prior to the assay cell pellets were resuspended in cell lysis buffer containing 30 mM OG or other detergents such as Triton X-100, Triton X-114, digitonin, or high salts such as 2M KCl and allowed to lyse for 10-30 minutes on ice. DNase I (1u/µl) was added to the samples that were used for electrophoresis. The samples were centrifuged at 100,000 g, for 30min at 20°C. The supernatants were used in the DGK activity assay and in protein electrophoresis followed by western blotting. Full length human DGKε was also prepared from SF1 insect cell pellets. The pellets were prepared in Utah. Insect cells were infected with baculovirus stocks containing DGKε cloned into BacPAK6 (Clontech) and carrying a C-terminus 6XHis epitope. The pelleted cells were shipped on dry ice and kept at -70°C freezer until further use.

2.2.4 DGK Activity Assay

The assay was adapted from the method described by Walsh *et al.*, 1994. For each assay DAG stock solutions (DOG, SAG, or SLG, in 1:1 $CHCl_3/CH_3OH$) together with any other lipid component used in the assay were dried under a stream of N_2 gas in a glass test tube and evaporated under vacuum for 2 hours to remove any traces of the solvent. The lipid was hydrated with 50µl of 4X assay buffer (300 mM OG, 200 mM

MOPS, pH7.2, 400 mM NaCl, 20 mM $MgCl_2$, 4 mM EGTA), 20 µl of 100 mM $CaCl_2$, 20 µl of 10 mM DTT, 10-20 µl of cell lysate either from cells transfected with one of the DGKε preparations or with an extract from mock-transfected cells. The final volume was 180 µl. The reaction was initiated by adding 20 µl of 5.0 mM [γ-^{32}P] ATP (50 µCi/ml). The final assay mixture contained 75 mM OG, 50 mM MOPS, pH 7.2, 100 mM NaCl, 5 mM $MgCl_2$, 1 mM EGTA, 10 mM $CaCl_2$, 1 mM DTT, the enzyme preparation, a range of substrate concentrations from 0.12 mM to 0.96 mM, and 3.5 mM phospholipids (unless otherwise noted) and 0.5 mM ATP. The reaction was carried out for 10 min at 25°C and was terminated by extraction of the lipid with the addition of 2 ml $CHCl_3/CH_3OH$ (1:1 v/v) containing 0.25 mg/ml dihexadecyl phosphate. The organic phase was washed three times with 2 ml each of 1% $HClO_4$, 0.1% H_3PO_4 in H_2O/CH_3OH (7:1 v/v). The volume of the final $CHCl_3$ phase was 0.80ml. A 0.40ml aliquot of the organic phase was dried at 50°C for 2 hours, and the incorporation of ^{32}P into PA was determined by scintillation counting. Controls were run with the addition of mock-transfected (empty-vector) cell lysates or without the addition of protein lysates. In both cases, the counts remaining in the organic phase were only slightly above background. The DGK activity measured with mock-transfected cells was subtracted from the values obtained using cells overexpressing one of the DGKε constructs. The production of PA was linear with time over 10 min (data not shown). The assays were done in triplicate and the results presented with errors showing the standard deviation of the mean for one particular experiment. Each experiment was independently repeated at least two times. The day to day variations using the same enzyme preparation and the same lipids were not much greater than those for an individual experiment.

2.2.5 Kinetic Analysis of the Micelle-Based Assay of DGK Activity

A kinetic analysis was performed on the two different DGKε full-length constructs and on the DGKΔε (1-41) truncated construct for each of the lipid substrates. The Michaelis-Menten constants, V_{max} and K_m, were evaluated using two-parameter hyperbolic plots (initial velocity (v_0) *versus* substrate concentration ([S])) and using Hanes plots ([S]/v_0 *versus* [S]). Total protein content was determined using the BCA kit (Pierce). The content of 3XFLAG-DGKε and 3XFLAG-DGKΔε (1-41) protein was determined as described below. Microcal Origin software was used to analyze the two plots, and the corresponding errors of k_{cat} and K_m were obtained using the data analysis function.

2.2.6 Estimation of the Amounts of 3XFLAG-tagged Recombinant DGKε and 3XFLAG-tagged Recombinant DGKΔε (1-41) Proteins

Amounts of 3XFLAG-DGKε and 3XFLAG-DGKΔε (1-41) proteins in the membrane fractions of DGK transfectants were estimated by immunoblotting with a mouse anti-FLAG peptide M2 primary antibody (Sigma-Aldrich). A 3XFLAG-tagged bacterial alkaline phosphatase (3XFLAG-BAP) (Sigma-Aldrich) with a molecular mass of 49.9kDa was used as a standard in different lanes of the same blot. The 3XFLAG-BAP used as a standard is of similar size and contains a similar epitope to the 3XFLAG-DGKε constructs. Proteins in the membrane fractions were solubilized with 30 mM OG, separated by SDS-PAGE (7.5% gel), and then transferred onto Immobilon-P

polyvinylidene fluoride (PVDF) membranes (Millipore). Blotting was performed according to the manufacturer's instructions (Amersham Biosciences, GE Healthcare, USA), using mouse anti-FLAG antibody (Sigma-Aldrich) followed by anti-mouse IgG secondary antibody conjugated with horse-radish peroxidase (HRP) (Pierce Biotechnology). Immune complexes were detected using ECL solution detection system (Amersham Biosciences, GE Healthcare, and USA) and visualized using a Typhoon scanner (Amersham Biosciences, GE Healthcare, USA). The DGKε, DGKΔε (1-41), and BAP protein bands were quantitated by densitometric scanning of the digitized image (tiff file) using Scion image software (Scion Image Corp.). The software measures the volume intensity of each band in a designated area in pixels. Boxes of equal size were constructed around each band. Background readings were calculated using the average per pixel intensity of the area surrounding each band measured. A standard curve was created by blotting on the membrane increasing amounts of the 3XFLAG-BAP protein. The amounts of recombinant 3XFLAG-DGKε and 3XFLAG-DGKΔε (1-41) proteins were estimated from the sigmoidal curve of 3XFLAG-BAP protein using the sigmoidal (Boltzman) fit of the data.

2.2.7 Protein Electrophoresis and Western Blotting

The enzyme lysates obtained following the protocol outlined above were run on various polyacrylamide-gel electrophoresis (PAGE) systems depending on the purpose of the experiment. To analyse the level of the protein of interest in the lysates, SDS-PAGE on 7.5% Tris/HCl pre-made gels (Bio-Rad) was used. The sample buffer, 2X Laemmli

buffer (62.5 mM Tris/HCl, pH 6.8, 2% SDS, 25% glycerol, 0.01% Bromophenol Blue) was purchased from Bio-Rad. To analyse the state of oligomerization of the enzyme in the lysates, PFO-PAGE on 7.5% Tris/HCl pre-made gels (Bio-Rad) was used. The protocol was adapted from Ramjeesingh *et al.*, 1999 and modified according to Yang *et al.*, 2002. The 2X sample buffer contained 100 mM Tris/HCl, pH 8.0, 0.2% NaPFO (Sigma-Aldrich), 20% glycerol, 0.005% Bromophenol Blue and the running buffer had 25 mM Tris/HCl, pH 8.5 192 mM glycine, and 0.1% NaPFO. To analyse the state of oligomerization of the enzyme in the lysates BN-PAGE was used. The protocol was adapted from the method of Schagger *et al.*, 1994. The samples were run on the freshly prepared Bis-Tris /ACA native gels by adding to the cell lysates 300mM ACA with or without Coomassie Blue G250. The method was later modified according to Camacho-Carvajal *et al.*, 2004.

The proteins separated by PAGE were then transferred to PVDF membranes by using the blotting sandwiches supplied by Bio-Rad. The transfer protocol followed is outlined in the Bio-Rad manual. Blotting was performed according to the manufacturer's instructions as outlined above.

2.2.8 Cross- linking studies

To analyze the state of oligomerization of the 3XFLAG-DGKε and 3XFLAG-DGKΔε (1-41) enzymes at the membrane, disuccinimidyl suberate (DSS) (Sigma-Aldrich) cross-linking reagent was used. DSS is a homobifunctional, water-insoluble, lipophilic, and membrane permeable cross-linking reagent. The experimental method

followed was adapted from the manufacturer's protocol. Cross-linking was performed in solution (A) after the protein was extracted from the membrane with 30mM OG or 1% Triton X-100 or in the membrane (B) before protein extraction. For method A, the protein was extracted with detergent as outlined above and then the lysate was incubated with DSS in 1X PBS buffer, pH 7.4. The reaction was incubated 2 hours on ice and then quenched with 1M Tris/HCl, pH 7.5, by incubation for 15 min at room temperature. The samples were run on an SDS-PAGE gel. For method B, the whole cells were incubated with DSS in PBS, pH 7.4 for 2 hours on ice. Then the reaction was quenched by incubating it with 1M Tris/HCl for 15 min at room temperature. The samples were run on an SDS-PAGE gel. The gels were then transferred to PVDF membrane and the proteins were detected by Western blotting according to the protocol outlined above.

2.2.9 Immunoprecipitation

The immunoprecipitation protocol was adapted from Sigma-Aldrich where the anti-FLAG M2 affinity gel freezer-safe beads were purchased. One confluent 10cm dish of COS-7 cells transfected with the corresponding plasmid vector DNA were scraped into 1X PBS containing 1:100 protease inhibitor cocktail and centrifuged 5min at 6,000g. Cells were resuspended in CS lysis buffer containing 30mM OG and incubated on ice for 30min. The cells were then centrifuged at 13,000rpm for 10min at 4°C. The supernatant was then mixed with 50µl of bead slush (glycerol removed and equilibrated with buffer) and the mixture was incubated on a rotary shaker for minimum 3 hours to maximum overnight. The mixture was then centrifuged at 3,000 rpm for 5 min and the flow-through

collected. The beads were then washed three times with 500 µl TBS (50mM Tris/HCl, pH 7.4, 150mM NaCl). The mix was spun in between washes at 3,000 rpm for 5min. The pellet was either run directly on the gel by elution with the SDS sample buffer or the protein was first eluted from the beads with 150 µl 3XFLAG-peptide in TBS with/without 30mM OG and then run on the gel. The presence of the protein was detected either by Coomassie Blue staining (Bio-Rad) or by western blotting.

2.2.10 Preparation of subcellular fractions

The method was adapted from Wang *et al.*, 2005. Three confluent 10cm dishes of COS-7 cells transfected with 3XFLAG-DGKε and 3XFLAG-DGKΔε (1-41) were scraped into 1X PBS containing 1:100 protease inhibitor cocktail and centrifuged 5min at 6,000g. Cells were resuspended in 2ml of buffer A (5mM sodium phosphate (Na_2HPO_4X $7H_2O$) pH 7.5, 250 mM sucrose), incubated on ice for 15 min and homogenized through a bent 22-gauge needle attached to a 5 ml syringe. The lysate was mixed with 4 ml of CS lysis buffer supplemented with 62% sucrose, overlaid with a 6 ml linear sucrose gradient of 15-35% sucrose in CS lysis buffer and centrifuged at 40,000rpm for 3.5 hours at 4°C in a Beckman SW40Ti rotor. One ml samples were collected from the top to bottom. The concentration of sucrose in each fraction was measured by refractometry. The presence of 3XFLAG-DGKε and 3XFLAG-DGKΔε (1-41) proteins in each fraction was detected by Western blotting using mouse anti-FLAG M2 antibody (Sigma-Aldrich). In addition, the presence of plasma membrane in each fraction was detected by checking the 5'-nucleotidase activity. The method was adapted from Liscum *et al.*, 1989. The buffer used

contained 50 mM Tris-HCl pH 8.5, 5 mM 5'-AMP, and 8 mM $MgCl_2$ and 0.1% (v/v) Triton X-100. 100µl of cell homogenate (each collected fraction) was added to 900 µl of buffer described above. We left the mixture for 1 hour at 37°C. Then 200 µl of 30% TCA solution was added and the mixture centrifuged 5 min at 13,000 rpm. To 400 µl of the supernatant we added 700 µl of Ames reagent (100 µl of 10% Ascorbic acid, and 600 µl of 0.42% Ammonium molybdate dissolved in 1N H_2SO_4. We left the mixture at 60°C for 10min and read the absorbance at 820 nm after cooling the samples down.

2.2.11 Indirect immunofluorescence

The protocol was adapted from Sigma-Aldrich where the mouse monoclonal anti-FLAG M2 antibody was purchased. The NIH3T3 cells were grown on poly-L-lysine coated coverslips in a six well plate. The cells were grown to around 50-70% confluency in DMEM with 10% Calf Serum (CS) and 1% Pen/Strep. The cells were then transiently transfected with Lipofectamine 2000 reagent from Invitrogen. The media was replaced after 5 hours and the cells were left in the incubator for 16-18 hours. Next day, the cells were fixed with 4% paraformaldehyde (PFA) in 1XPBS, pH 7.4 and after several washes the cells were either blocked in 5% BSA in PBS for 1.5 hours or the cells were treated with 0.1% TritonX-100 in PBS for 10min, washed a few times and then blocked in 5% BSA in PBS for 1.5 hours. The cells were rinsed with PBS and then incubated with the mouse monoclonal anti-FLAG antibody (Sigma-Aldrich) in PBS (1:200) for 1.5 hours at 37°C in 5% CO_2. After rinsing 3 times with PBS, the cells were incubated with Alexa-Fluor 488 labeled goat anti-mouse IgG (Molecular Probes/ Invitrogen) in PBS (1: 500, or

1:1,000) for 1 hour at 37°C in 5% CO_2. After washing five times with PBS, the glass coverslips were mounted onto the glass slides and left to dry at room temperature in the dark. Next morning the slides were sealed with nail polish and left to dry. The slides were visualized using the inverted wide-field fluorescent microscope in Dr. Ray Truant's lab with assistance from Rhandi Singh.

Chapter 3. Results

3.1 DGKε has an N-terminus hydrophobic domain

3.1.1 Transmembrane prediction software analysis

As previously mentioned in the literature, experimental studies found that the DGKε enzyme could not be extracted from insect cell membranes with high salt solutions (2M KCl) (Epand *et al.*, 2004) and a combination of salt and detergent or detergent alone was needed to solubilize this enzyme from the membrane (Walsh *et al.*, 1994). In addition, transmembrane prediction software showed the possibility that the mammalian DGKε has a putative transmembrane domain at the N-terminus of the protein. Therefore, researchers speculated that mammalian DGK ε is an integral membrane protein (Thirugnanam *et al.*, 2001).

The present study used one type of transmembrane prediction software, the dense alignment surface (DAS) method (Cserzo *et al.*, 1997), to support the previous results. The DAS method was introduced in an attempt to improve sequence alignments in the G-protein coupled receptor family of transmembrane proteins, but it has been generalized to predict segments in any integral membrane protein. DAS is based on low-stringency dot-plots of the query sequence against a collection of non-homologous membrane proteins using a special scoring matrix (Cserzo *et al.*, 1997). These curves are obtained by pairwise comparison of the proteins. There are two cutoffs indicated on the plots: a "strict" one at 2.2 DAS score, and a "loose" one at 1.7. The hit at 2.2 is informative in

terms of the number of matching segments, while a hit at 1.7 gives the actual location of the transmembrane segment (Cserzo *et al.*, 1997).

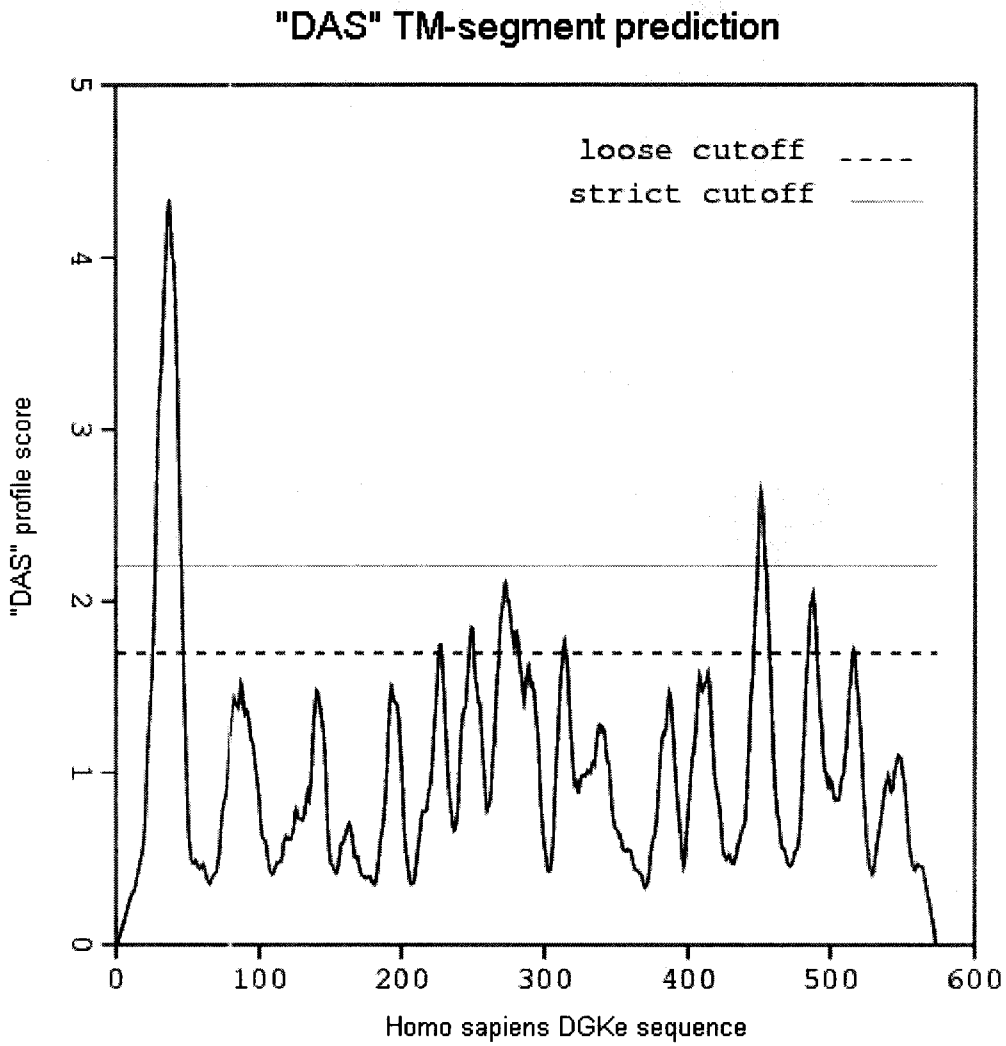

Fig. 3 DAS transmembrane domain prediction profile of *Homo sapiens* DGKε. The profile shows the presence of an N-terminus putative transmembrane segment between amino acids 20 and 40 since the peak is well above the strict cutoff point and it contains around 20 aminoacids. There is another hydrophobic segment between amino acids 450 and 460 but the peak is short and the length of the segment is not indicative of a transmembrane segment (less than 20 amino acids in length).

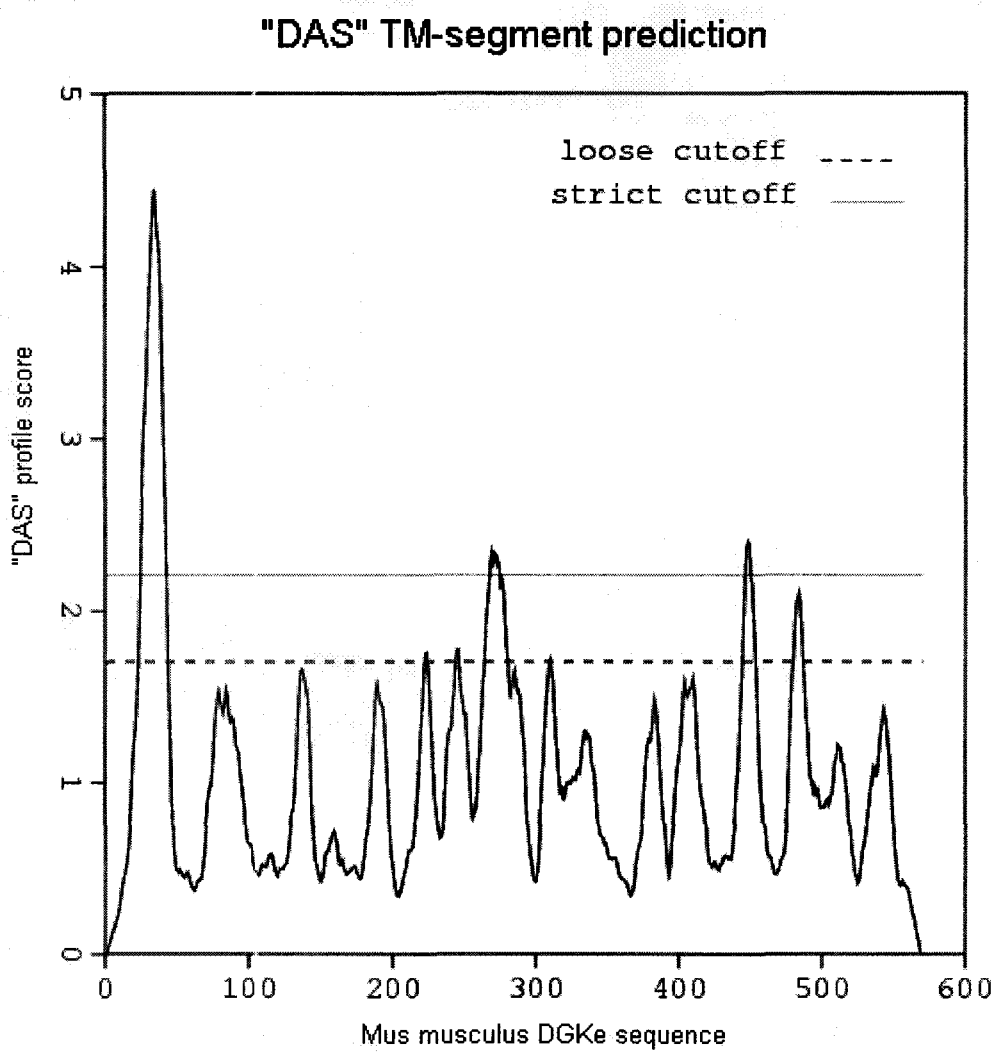

Fig. 4 DAS transmembrane domain prediction profile of *Mus musculus* DGKε. The profile shows the presence of an N-terminus putative transmembrane segment between amino acids 20 and 40 since the peak is well above the strict cutoff point and it contains around 20 aminoacids. There are two other hydrophobic segments between amino acids 270 and 285 and between amino acids 450 and 460, but the peaks are short and the length of the segments is not indicative of a transmembrane segment (less than 20 amino acids in length).

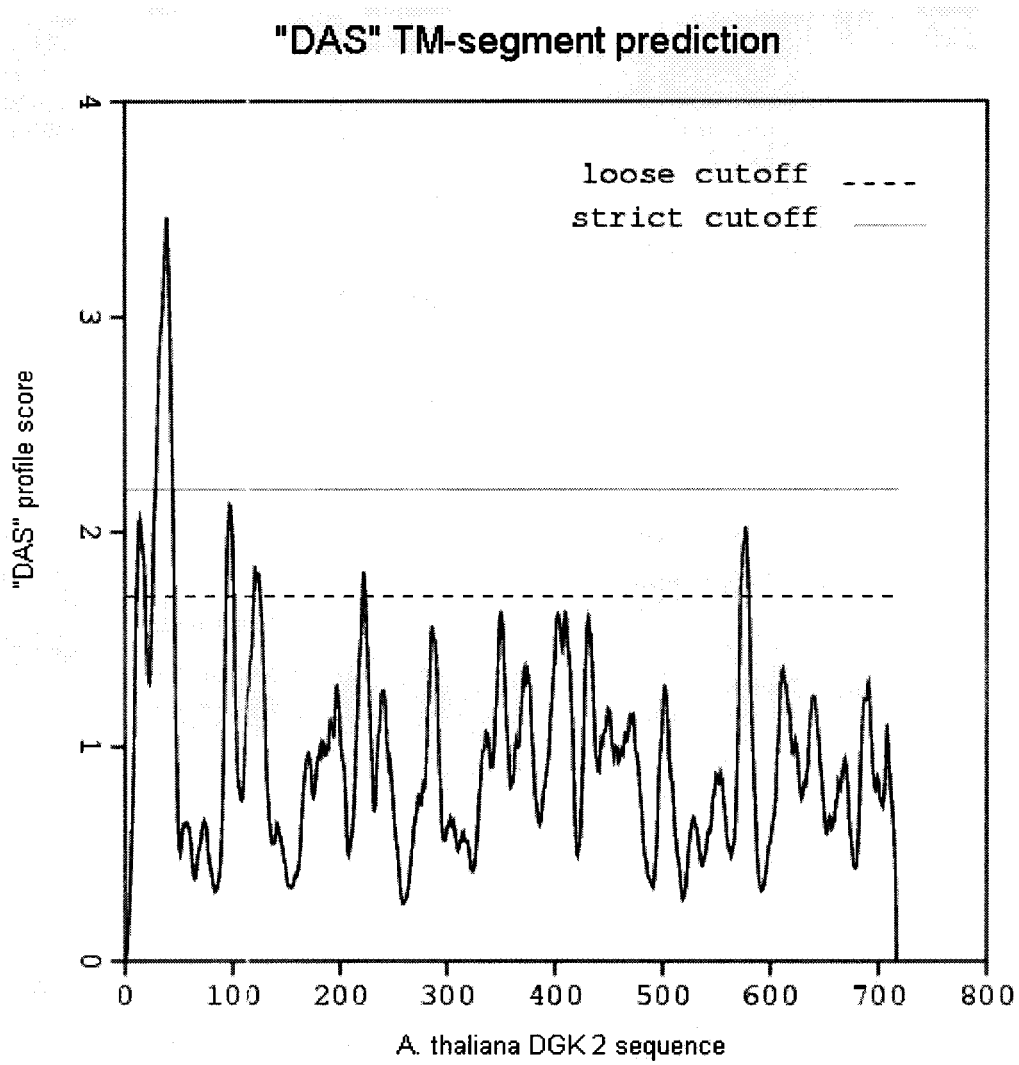

Fig. 5 DAS transmembrane domain prediction profile of *Arabidopsis thaliana* DGK2. The profile shows the presence of an N-terminus putative transmembrane segment between amino acids 20 and 40 since the peak is well above the strict cutoff point and it contains around 20 aminoacids. There are no other segments above the strict cutoff point present in this isoform.

As noted above, the hydrophobic domains of the mammalian DGKε are located at the N-terminus of the protein and they are 18 amino acids long (the human hydrophobic domain sequence is: LILWTLCSVLLPVFITFW and the mouse hydrophobic domain sequence is: LVLWTLCSVLLPVFITLW) as counted at the "strict" cutoff point of 2.2 of

the DAS program (Fig. 3 and Fig. 4). Also, the mammalian DGKε is not the only DGK to present an N-terminus hydrophobic segment. Interestingly, the plant DGK2 also has an N-terminal hydrophobic segment of 16 amino acids long (the plant hydrophobic domain sequence is: GWLVTGSVGLLAVIYT) (Fig. 5) as counted at the "strict" cutoff point of 2.2 of the DAS program. The plant DGK2 also possesses the same substrate specificity for substrates with an unsaturated acyl chain at the sn-2 position as do the mammalian DGKε (Gomez-Merino *et al.*, 2004).

To verify the efficiency of the prediction we used a known integral membrane protein, the influenza A virus hemagglutinin, and obtained a DAS curve which shows the C-terminus transmembrane domain (29 aminoacids) of influenza and the N-terminus signal peptide (only 9 aminoacids) as above the "strict" 2.2 restriction line (Fig. 6).

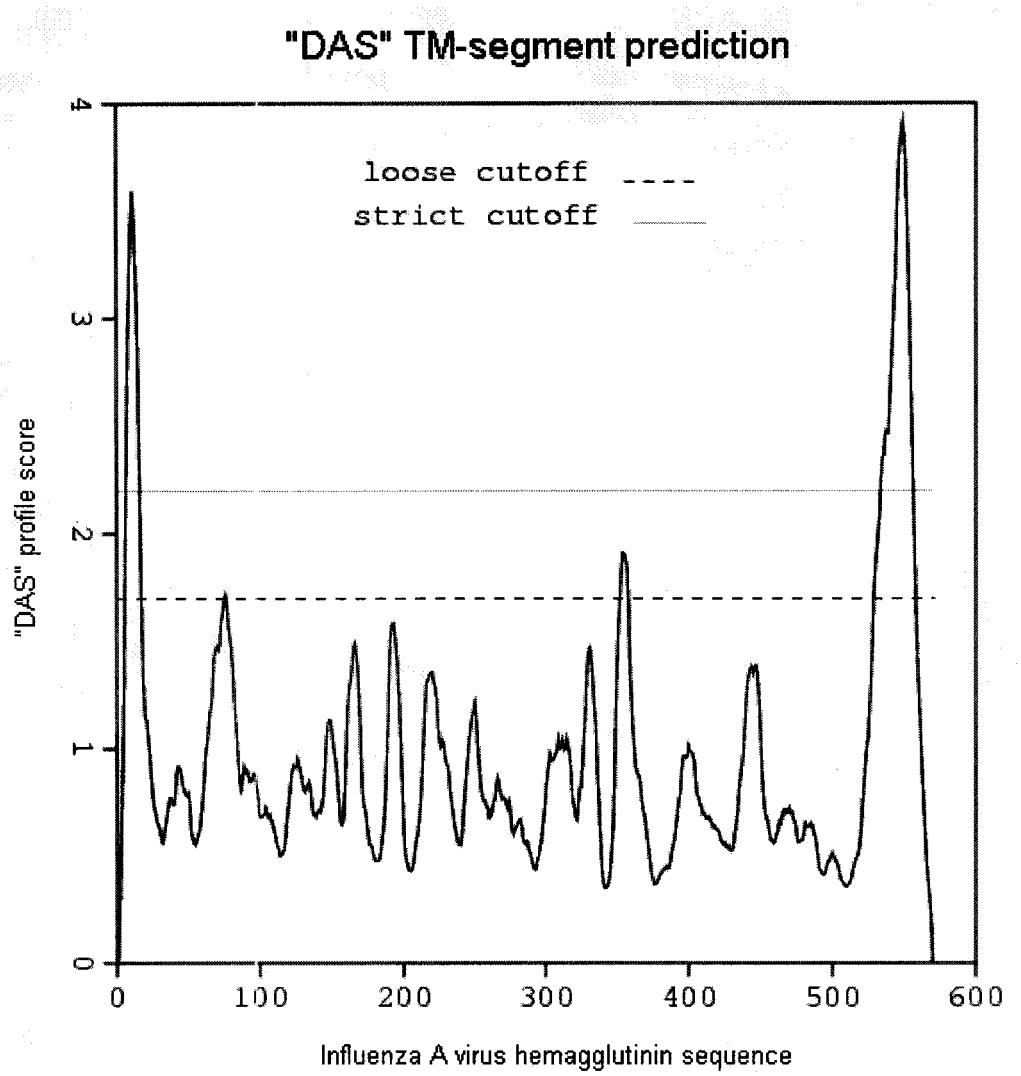

Fig. 6 DAS transmembrane domain prediction profile of Influenza A virus hemagglutinin. The profile shows the presence of the N-terminus signal peptide of influenza A hemagglutinin between amino acids 5 and 14. The peak is short and contains around 10 aminoacids. There is another segment at the C-terminus of influenza A hemagglutinin, which is a transmembrane segment. This peak is well above the strict cutoff point and it is 29 amino acids in length.

Thus, DGKε has a segment that is of comparable hydrophobicity to a transmembrane segment of a known integral membrane protein, Influenza A virus hemagglutinin.

3.1.2 Construction of 3XFLAG Epitope-tagged DGKε Expression Vectors

The design of the 3XFLAG Epitope-tagged DGKε [3XFLAG-DGKε] and the 3XFLAG Epitope-tagged truncated DGKε [3XFLAG-DGKΔε (1-41)] was accomplished with help from Dr. Mathew K. Topham at Huntsman Cancer Institute, Utah. All of the DGKε- related constructs referred to in this thesis correspond to the human form of the protein. The protocol was outlined in the experimental methods section. The constructs used in this study are drawn below (Fig. 7 and Fig. 8). The drawings are not to scale.

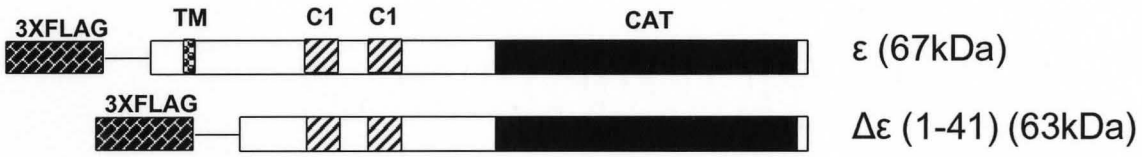

Fig. 7 Structures of DGKε constructs designed and used in this study. Diagrams of the full-length DGKε construct and truncated DGKε mutant are shown. The putative transmembrane domain (TM), the two cysteine-rich domains (C1), and the catalytic domain (CAT) are indicated on the figure, together with the appropriate epitope tag for easier detection and quantification on immunoblots.

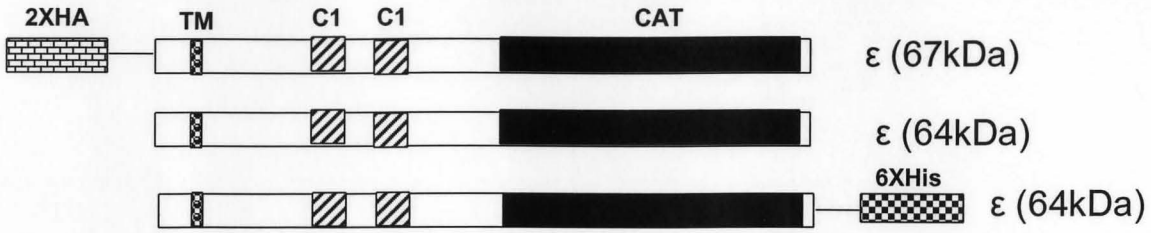

Fig. 8 Other constructs mentioned or used in this study. The N-terminus HA tagged construct was designed by Dr. M.K. Topham and the DGKε gene was cloned into the pCMV-HA vector from Clontech. The DGK construct devoid of a tag was also designed by Dr. M. K. Topham and the DGKε gene was cloned into the pcDNA3 vector from Invitrogen. The N-terminus HA tagged DGKε and the no tag DGKε vector DNA were a kind gift from Dr. M.K. Topham. The DGKε constructs mentioned above were transiently transfected into COS-7 mammalian cells using the protocol outlined in the methods section. The C-terminus His tagged full-length construct is described in the methods section and the insect cell pellets containing the recombinant protein were a kind gift from Dr. M.K. Topham. Insect cells were infected with the baculovirus stocks carrying the C-terminus His tagged DGKε gene and the insect cell pellets were used in further experiments.

3.1.3. 3XFLAG-DGKε or 3XFLAG-DGKΔε (1-41) proteins associate with the plasma membrane of COS-7 cells

Subcellular localization of the full-length, 3XFLAG-DGKε, and truncated, 3XFLAG-DGKΔε (1-41), enzyme was studied in order to detect the similarities and differences between the localization of the two proteins. The protocol followed was outlined in the experimental procedure section. We collected 1ml samples from top to bottom of the gradient, subsequent to centrifugation and checked for the presence of 3XFLAG-tagged proteins by Western blot. To identify the plasma membrane fraction, we performed a 5'nucleotidase activity assay. The protocol is outlined in the methods section.

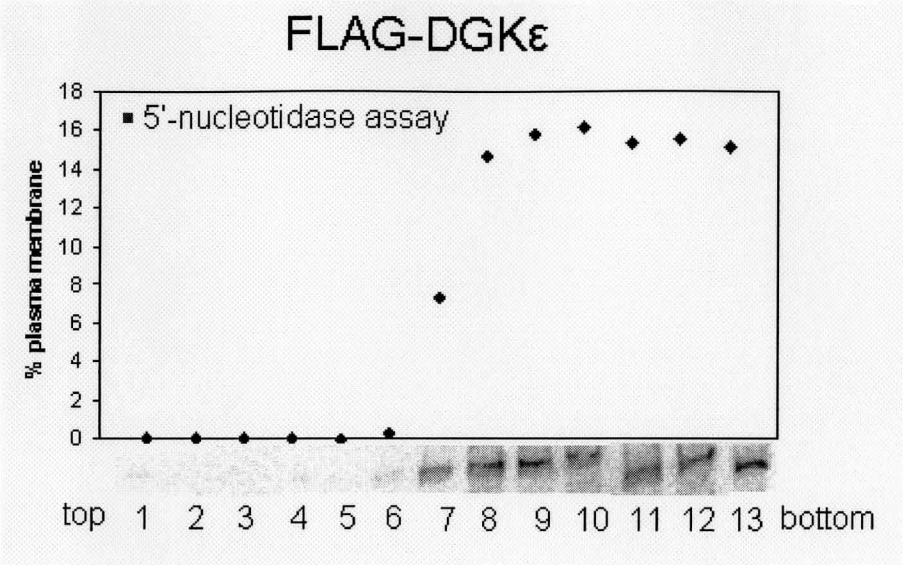

Fig. 9 Subcellular fractionation of 3XFLAG-DGKε. A linear sucrose gradient was implemented on top of the sample cell lysate and the tubes were centrifuged at 40,000rpm for 3.5 hours in a swinging bucket rotor. One ml samples were collected from the top to bottom. The presence of the 3XFLAG-DGKε was detected by western blotting using the anti-FLAG antibody and HRP linked anti-IgG. The presence of plasma membrane in each fraction was determined by checking the activity of a 5'-nucleotidase in each fraction. 5'-AMP was used as a substrate and the relative amount of phosphate released was determined.

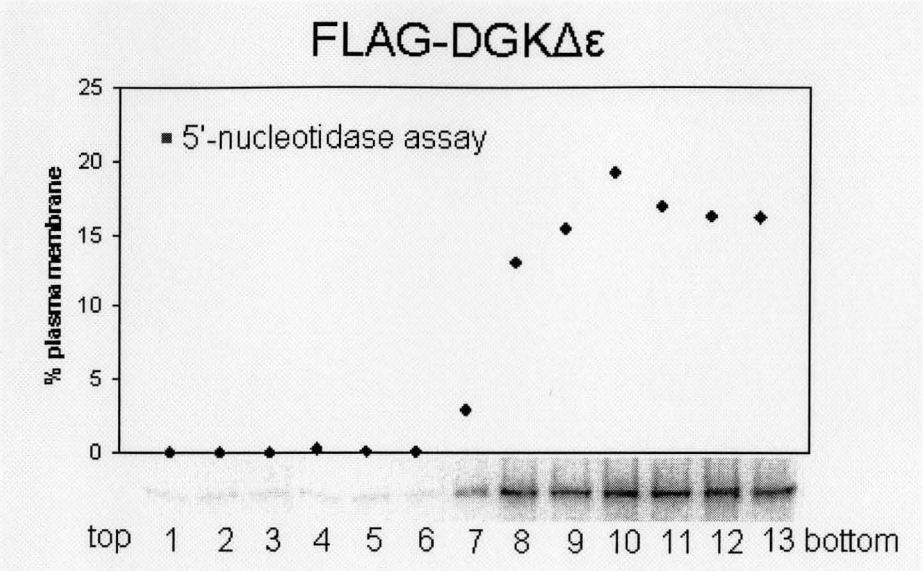

Fig. 10 Subcellular fractionation of 3XFLAG-DGKΔε (1-41). A linear sucrose gradient was implemented on top of the sample cell lysate and the tubes were centrifuged at 40,000rpm for 3.5 hours in a swinging bucket rotor. One ml samples were collected from the top to bottom. The presence of the 3XFLAG-DGKΔε (1-41) was detected by western blotting using the anti-FLAG antibody and HRP linked anti-IgG. The presence of plasma membrane in each fraction was determined by checking the activity of a 5'-nucleotidase in each fraction. 5'-AMP was used as a substrate and the relative amount of phosphate released was determined.

Both proteins were found in the bottom fractions 7-13 which corresponded to the fractions containing plasma membrane as verified by the 5'-nucleotidase assay. Therefore, it appears that both proteins are associated with the plasma membrane in transfected COS-7 cells.

3.1.4 The relationship between the presence of a hydrophobic domain in mammalian DGKε and the speculation that DGKε is an integral membrane protein

Singer and Nicolson, 1972 proposed the terms integral and peripheral membrane proteins based on the proteins' tightness in membrane binding. An integral membrane protein requires disruption of the lipid bilayer in order to be released, while a peripheral membrane protein can be released from the membrane without disturbing the lipid bilayer (Jennings, 1989). Experimentally, integral membrane proteins are defined by their resistance to extractions with high salt reagents and alkali, and by their partitioning into the detergent-rich phase of a Triton X-114 phase partitioning (Zhu *et al.*, 2005). A fourth year student's project, Lindsay Ottaway, supports the previous data found in the literature (Thirugnanam *et al.*, 2001; Epand *et al.*, 2004) in that the DGKε constructs used in the present study are hard to extract from membranes with high salt (Fig. 11).

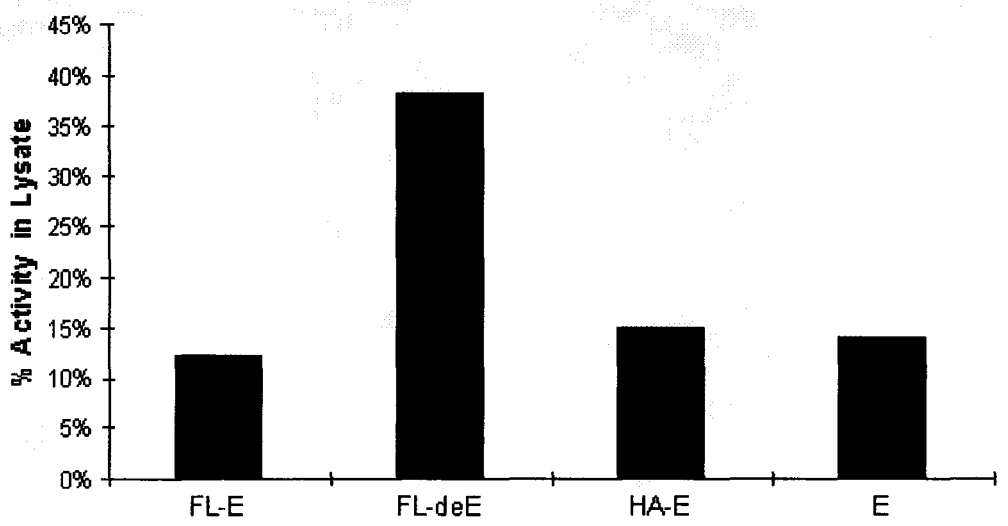

Fig. 11 Percent activity found in the salt extracted lysate. Total cell lysates of each DGK isoform (3XFLAG-DGKε, 3XFLAG-DGKΔε, 2XHA-DGKε, and DGKε) were extracted with 2M KCl by centrifugation at 73,000rpm at 20°C. Activity was measured for the extracted lysates and compared to the activity of the starting cell pellet. Activity in the salt extracted lysate was computed as a percentage of the activity of the starting cell pellet. The truncated form of the enzyme showed higher percent activity than the full-length enzyme; in addition, the type of epitope tag did not make a difference for extraction. Figure adapted from Lindsay Ottaway's fourth year project thesis (Ottaway, 2006).

The results of the Triton X-114 phase partitioning performed by a summer student in the lab show contradictory results (data not shown) in that the enzymes 3XFLAG-DGKε and 3XFLAG-DGKΔε (1-41) partition in both, the aqueous phase and the detergent phase. Therefore, it is still an open question whether the mammalian DGKε is an integral membrane protein regardless of the presence of the hydrophobic N-terminus domain.

3.1.5 Biophysical studies of the hydrophobic domain peptide show favourable insertion in membrane mimetic environments by circular dichroism

Our collaborators from Toronto, Glukhov, E. and Deber, C., have studied the peptide corresponding to the human DGKε transmembrane domain. According to the hydrophobicity scale rules proposed by Liu and Deber, 1998, nine Lys residues were attached to the sequence to get a water soluble and a symmetrically charged peptide (four to the N-terminal and five to the C-terminal). The peptide used in the study was: KKKKLILWTLCSVLLPVFITFWKKKKK.

One biophysical study performed on the peptide was circular dichroism (CD). CD measures differences in the absorption of left-handed versus right-handed circularly polarized light, which arise due to structural asymmetry caused by the chiral environment of a chromaphore. The absence of a regular structure results in a CD spectrum in the far UV that is different from that of an ordered structure (Fig. 12).

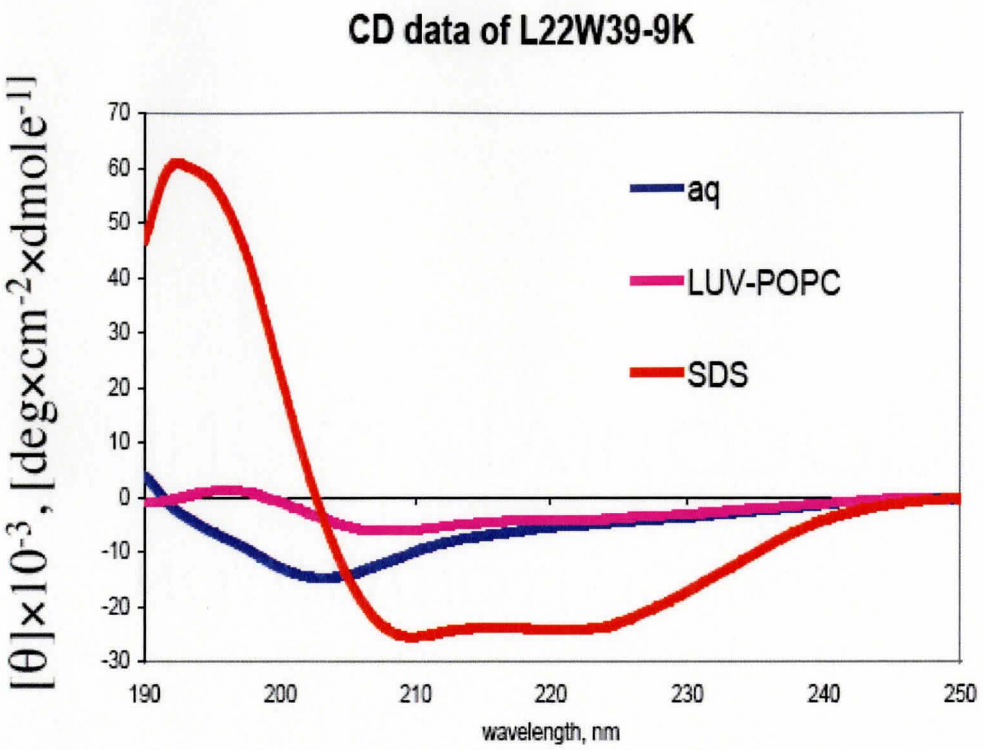

Fig. 12 CD spectra of human DGKε hydrophobic peptide, KKKKLILWTLCSVLLPVFITFWKKKKK, in aqueous buffer (blue curve), zwitterionic vesicles (pink curve) and SDS micelles (red curve). The peptide was synthesized with 9 lysine residues attached to each end. The CD spectrum was measured in different media, aqueous, zwitterionic POPC large unilamellar vesicles, and SDS micelles. The peptide showed clear helical structure in SDS micelles and a compressed pattern similar to a helical structure in LUV-POPC. The peptide showed random coil structure in aqueous buffer.

Human DGKε transmembrane peptide was used for CD in different media (Fig. 12). The peptide was mostly random coil in aqueous buffer, largely helical in SDS micelles, and slightly helical in zwitterionic large unilamellar vesicles (LUV) of POPC.

3.1.6 Modeling studies of the hydrophobic domain peptide show favourable membrane insertion

Ducarme *et al.*, 1998 have developed a simple restraint field to simulate the association of peptides with the membrane, named IMPALA for internal membrane proteins (IMP) and lipid association. The method is based on calculation of restraints and uses a full atomic description of the molecule. The IMPALA uses a Monte Carlo minimization procedure to calculate the depth and the angle of insertion of membrane-interacting peptides taking into account the restraints conferred by the lipid bilayer. The purpose of this approach is not to determine the precise interactions that occur during IMP folding, but to obtain more realistic models to support the experimentally known features of IMP structures.

Our collaborators from Belgium, Decaffmeyer M. and Brasseur R., have modeled the peptide corresponding to the human DGKε in a membrane environment. First, they modeled the peptide in a dimer form and then they studied the dimers in a membrane environment. The dimer with the greatest stability is shown in Fig. 13.

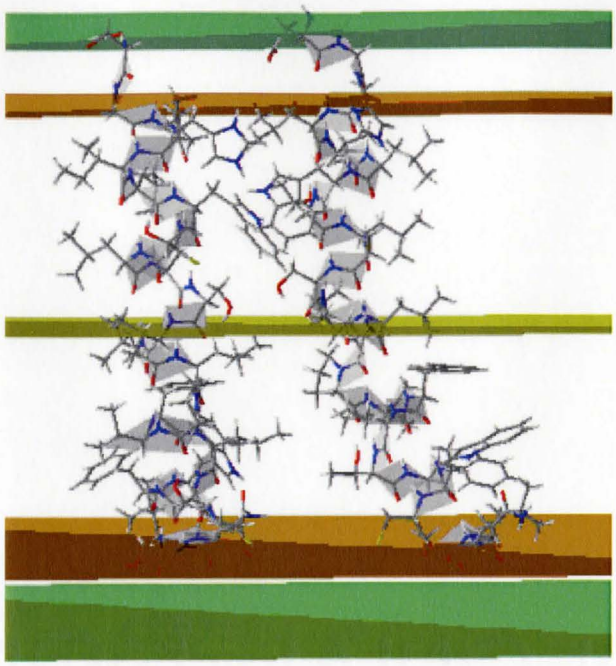

Fig. 13 Human DGKε dimer inserted in a lipid bilayer. The interaction between two peptides corresponding to the hydrophobic segment of the full-length DGKε was studied. First, the energy of interaction between the peptides was calculated and the complex with the lowest energy was kept. Second, the peptide dimer was inserted in a membrane model. The view was perpendicular to the membrane section. The biological membrane effect was mimicked by accounting for the water-lipid interfaces and describes the membrane as an apolar layer with water content varying from 1.0 (water phase) to 0.0 (the lipid acyl chains) (Basyn *et al.*, 2001).

3.2 Deletion of the N-terminus hydrophobic domain of DGKε appears to have no effect on the enzyme's substrate specificity in a detergent-micelle system

The kinetic behaviour of an enzyme offers great insight into its regulation and physiological role. To evaluate the essential kinetic parameters of the DGKε constructs we performed kinetic experiments in an octyl-β-glucoside/phosphatidylcholine (OG/PC) mixed micellar assay using several DAG substrates. Our results revealed that the

truncated 3XFLAG-DGKΔε (1-41) maintained enzyme activity and specificity for DAGs with arachidonic acid.

3.2.1 Determination of the level of protein expression

The concentration of 3XFLAG-DGKε or 3XFLAG-DGKΔε (1-41) in extracts from COS7 cells, prepared as described in the experimental procedure section, was determined using Western blotting with an anti-FLAG antibody. The correspondence between the intensity of the band in Western blots and the amount of protein was determined using 3XFLAG-tagged BAP protein as standard (Fig. 14). For quantification of DGK, we used only bands of intensity lower than 25 units. The standard curves for both 3XFLAG-DGKε and 3XFLAG-DGKΔε (1-41) showed good linearity with regression coefficients of 0.97 and 0.99, respectively (Fig. 15). Attempts to do a similar analysis with DGKε-His using anti-His tag antibody (Amersham Biosciences) or anti-DGKε antibody (Santa Cruz Biotech) did not yield a reliable standard curve for quantitation (data not shown). The enzyme activity for this construct is presented only in relative terms for different substrates.

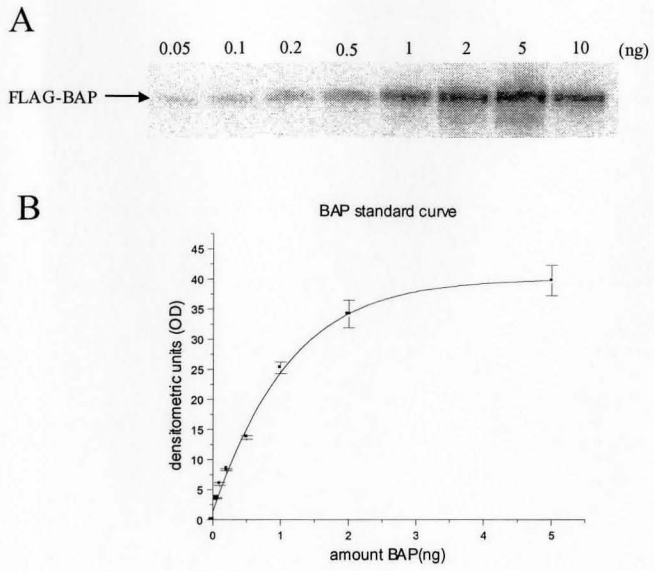

Fig. 14 Calibration curve for the intensity of bands in Western blots. (**A**) Western blotting analysis of serial dilutions of 3XFLAG-tagged BAP protein. The intensity of the 49.9kDa (BAP protein) bands increased with increasing content of 3XFLAG-tagged BAP protein (**B**) Depiction of the relationship between the content of BAP protein and the band density; a sigmoidal (Boltzman) fit was obtained using Microcal Origin.

A. **B.**

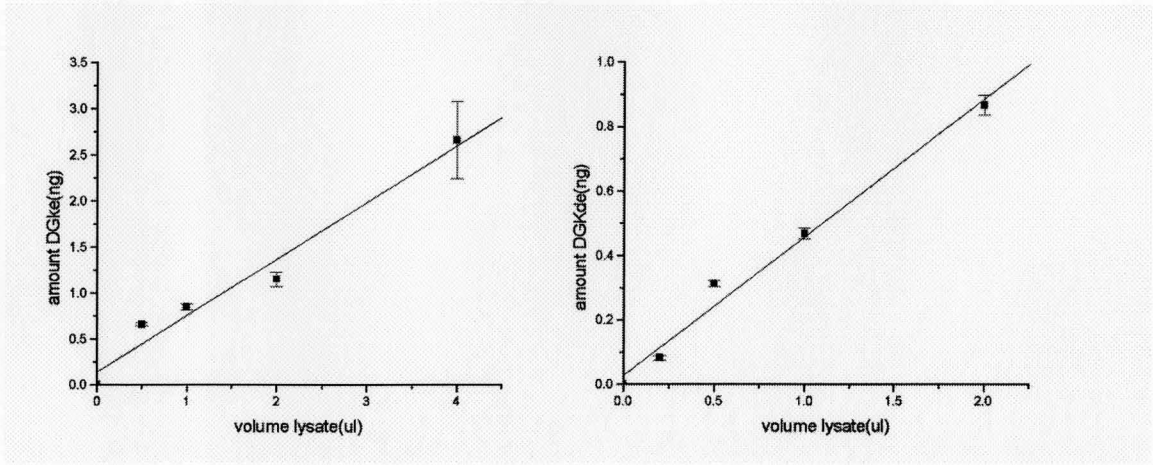

Fig. 15 Relationship between the volume of the membrane protein lysate and the content of 3XFLAG-DGKε and 3XFLAG-DGKΔε (1-41) protein A. Curve depicting the relationship between the volume of the membrane protein lysate and the content of 3XFLAG-DGKε protein estimated from the BAP standard curve. **B**. Curve depicting the relationship between the volume of the membrane protein lysate and the content of 3XFLAG-DGKΔε (1-41) protein estimated from the BAP standard curve. Estimation of the amount of each enzyme was calculated using directly the sigmoidal (Boltzman) formula in the linear range of the curve.

3.2.2 Kinetic analysis of ATP as substrate

In the process of phosphorylation of DAG, DGKε utilizes two substrates, a water-soluble substrate, ATP, and a water-insoluble substrate, DAG. Each of these substrates binds to the enzyme at different sites. There are also different consequences to the kinetics because one of the substrates is water soluble, while the other is not. The binding of ATP to the enzyme is determined by its concentration in the total volume of the solution, as is common for other enzyme catalysis. To determine the apparent disassociation constant (K_m) for ATP from the enzyme, we varied the ATP concentration at a constant high concentration of SAG (1.5 mol %) and examined the effect on the

catalytic activity (Fig. 16). The values of the $K_{m\,(ATP)}$ are 0.13 mM for both 3XFLAG-DGKε and 3XFLAG-DGKΔε (1-41) (Table 1).

Table 1

Apparent kinetic constants of ATP

isoform	substrate	K_m (mM)	k_{cat} (s^{-1})	kcat/K_m ($s^{-1}mM^{-1}$)
3XFLAG-DGKε	ATP	0.13 ± 0.03	8.2 ± 0.8	63
3XFLAG-DGKΔε (1-41)	ATP	0.135 ± 0.06	23 ± 5	169
DGKε-His	ATP	0.2 ± 0.15	0.010 ± 0.0011*	0.05

Activity represents the average of at least two independent experiments performed in three replicates. Errors represent the standard deviation for two experiments under each condition. * The values for DGKε-His are in nmolePA/min since the amount of protein in the lysates was not determined.

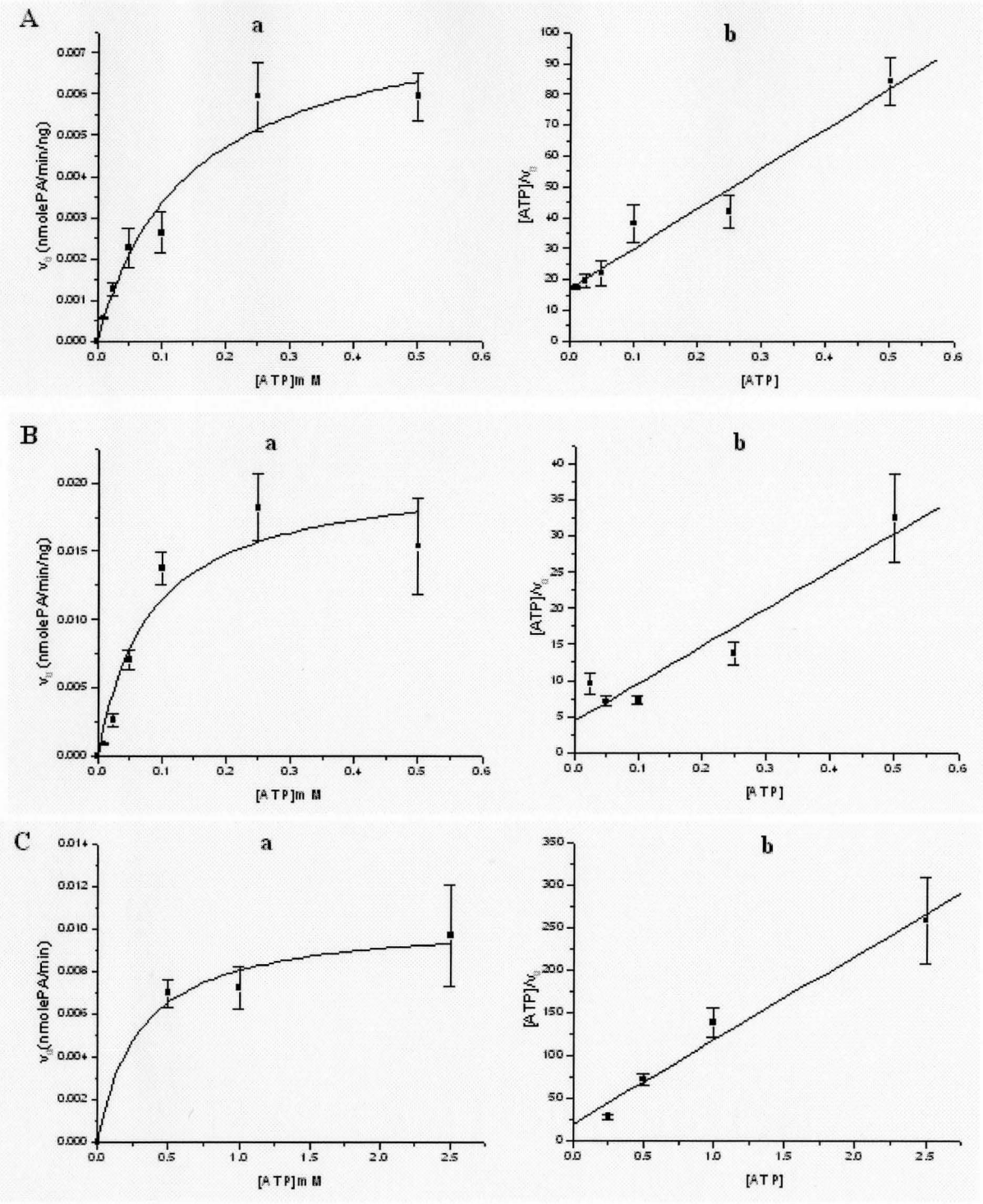

Fig. 16 Dependence of the initial velocity (v_o) of DGK-catalyzed phosphorylation of SAG based on varying ATP concentration. a. Two-parameter hyperbolic plots of initial velocity (v_o) versus ATP substrate concentration. **b**. Hanes plots were used to determine the Michaelis-Menten constants. **A**. 3XFLAG-DGKε. **B**. 3XFLAG-DGKΔε (1-41). **C**. DGKε-His. The data reported are an average of two experiments performed in triplicates. Error bars indicate the standard error of the mean.

A summary of 3XFLAG-DGKε and 3XFLAG-DGKΔε (1-41) kinetic constants for ATP substrate is included below. The purpose of the summary is for easier comparison of the kinetic constants for the two constructs designed and used in this study.

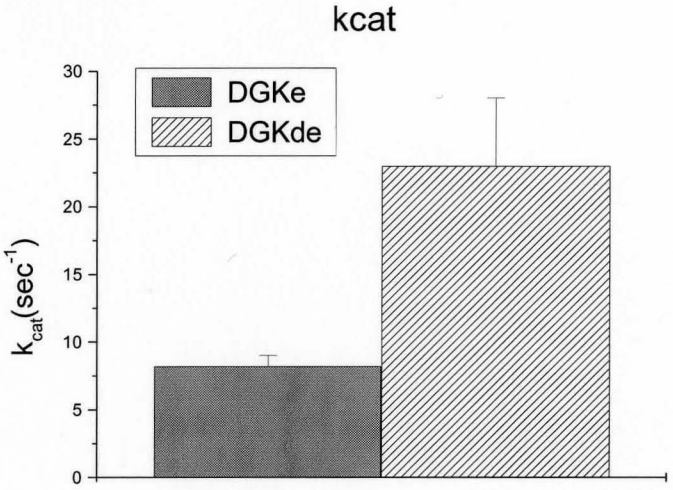

Fig. 17 Summary of kcat for ATP of the 3XFLAG-DGKε and 3XFLAG-DGKΔε (1-41) proteins. The k_{cat} determined previously and tabulated in Table 1 was used to construct the bar graph. The substrates used were ATP (varying concentrations) and SAG (0.8mM, maximum concentration). The k_{cat} for ATP of the full-length DGKε was about 3X lower than the k_{cat} for ATP of the truncated DGKε.

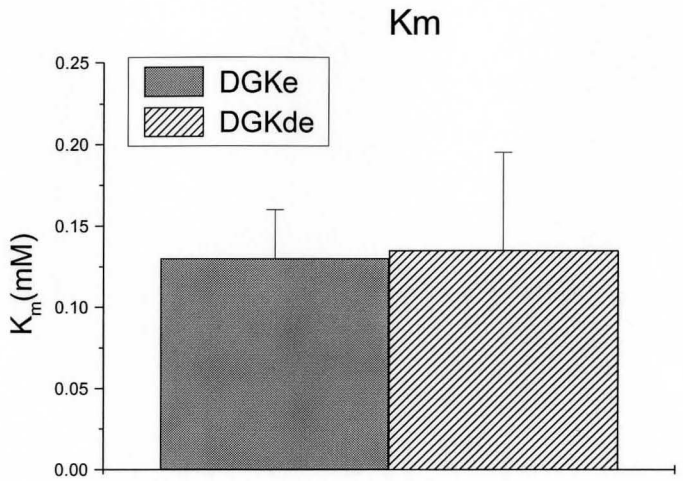

Fig. 18 Summary of Km for ATP of the 3XFLAG-DGKε and 3XFLAG-DGKΔε (1-41) proteins. The Km determined previously and tabulated in Table 1 was used to construct the bar graph. The substrates used were ATP (varying concentrations) and SAG (0.8mM, maximum concentration). The Km for ATP of the full-length DGKε was almost the same as the Km for ATP of the truncated DGKε.

3.2.3 Kinetic analysis of DAG as substrate

The kinetic assays were done in a DAG-detergent-phospholipid mixed micellar system using a high concentration of ATP (0.5 mM). The presence of the phospholipid was required since at higher substrate concentrations aggregation of the lipid substrate was noticed in its absence. The concentration of DAG substrate is expressed as its mole fraction in the lipid-detergent mixture. The binding of the lipid substrate to the catalytic site is determined, not by its bulk concentration but by its concentration within the water-insoluble phase of micelles or liposomes (Carman *et al.*, 1995). The initial rate of the enzyme-catalyzed reaction was determined as a function of the concentration of SAG (Fig. 19), SLG (Fig. 20) or DOG (Fig. 21) in the micellar phase. Kinetic properties of DGKε phosphorylating three different lipid substrates were determined (Table 2).

Table 2

Apparent kinetic constants of SAG, SLG, and DOG

Isoform[a]	Substrate	K_m (mol %)	k_{cat} (s^{-1})	k_{cat}/K_m ($s^{-1}mol\%^{-1}$)
3XFLAG-DGKε	SAG	0.54 ± 0.13	1.7 ± 0.9	3.1
3XFLAG-DGKε	SLG	0.65 ± 0.08	1.23 ± 0.02	1.9
3XFLAG-DGKε	DOG	2.5 ± 2.2	1.2 ± 0.2	0.48
3XFLAG-DGKΔε (1-41)	SAG	0.97 ± 0.11	5.7 ± 0.38*	5.9
3XFLAG-DGKΔε (1-41)	SLG	0.8 ± 0.1	2.8± 0.99*	3.5
3XFLAG-DGKΔε (1-41)	DOG	1.2 ± 0.3	2.43 ± 0.09	2.0
DGKε-His	SAG	0.85 ± 0.04	0.162 ± 0.005[b]	0.191[b]
DGKε-His	SLG	0.51 ± 0.04	0.087 ± 0.011[b**]	0.171[b]
DGKε-His	DOG	2.7 ± 0.2	0.032 ± 0.001[b]	0.0119[b]

[a]Nature of the epitope tag included to distinguish between the two forms of DGKε used. .
[b]Values of k_{cat} are relative values since the amount of enzyme in the cell preparations is not known.
* The kcat values were calculated using direct linear plots (Cornish-Bowden, 2004) and Hanes plots
** The kcat value for SLG is calculated relative to the k_{cat} for SAG at the same enzyme concentration and at maximal substrate concentration.
Activity represents the average of at least two independent experiments performed in three replicates. Errors represent the standard deviation for two experiments under each condition.

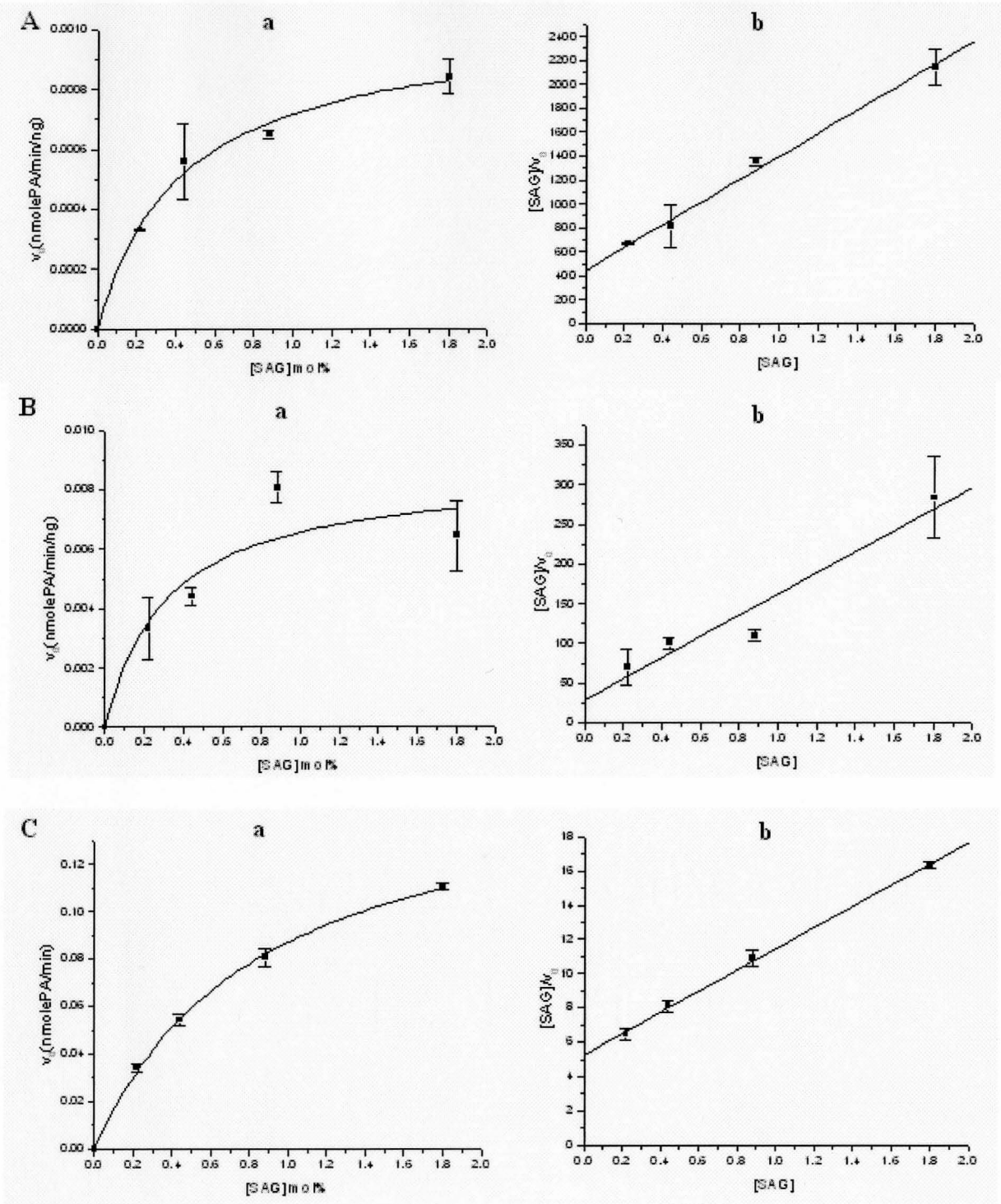

Fig. 19 Dependence of the initial velocity (v_o) of DGK-catalyzed phosphorylation of SAG. a. Two-parameter hyperbolic plots of initial velocity (v_o) versus SAG substrate concentration. **b**. Hanes plots were used to determine the Michaelis-Menten constants. **A**. 3XFLAG-DGKε. **B**. 3XFLAG-DGKΔε (1-41). **C**. DGKε-His. The data reported are an average of two experiment performed in triplicates. Error bars indicate the standard error of the mean.

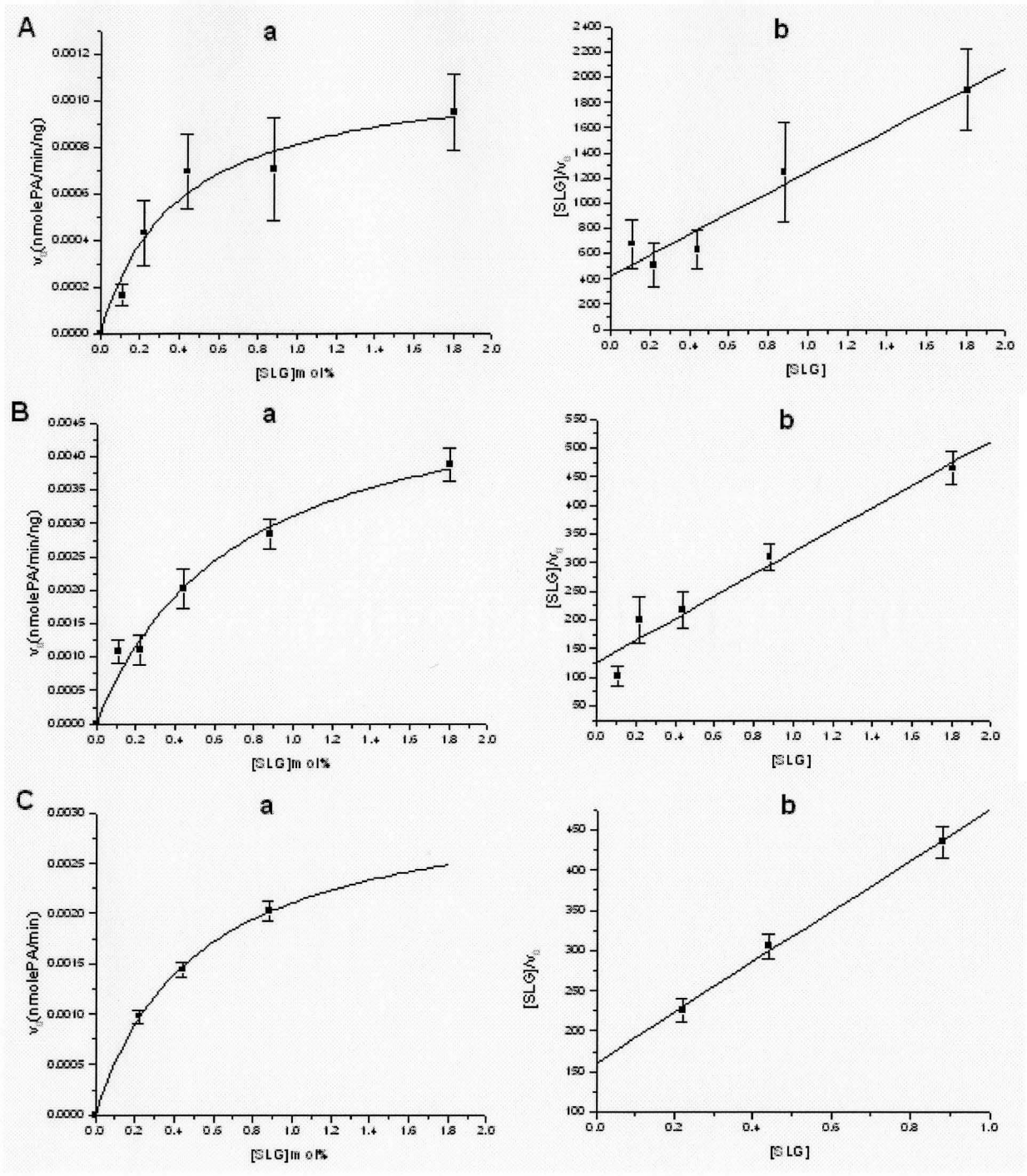

Fig. 20 Dependence of the initial velocity (v_o) of DGK-catalyzed phosphorylation of SLG. a. Two-parameter hyperbolic plots of initial velocity (v_o) versus SLG substrate concentration. **b**. Hanes plots were used to determine the Michaelis-Menten constants. **A.** 3XFLAG-DGKε. **B**. 3XFLAG-DGKΔε (1-41). C. DGKε-His. The data reported are an average of two experiment performed in triplicates. Error bars indicate the standard error of the mean.

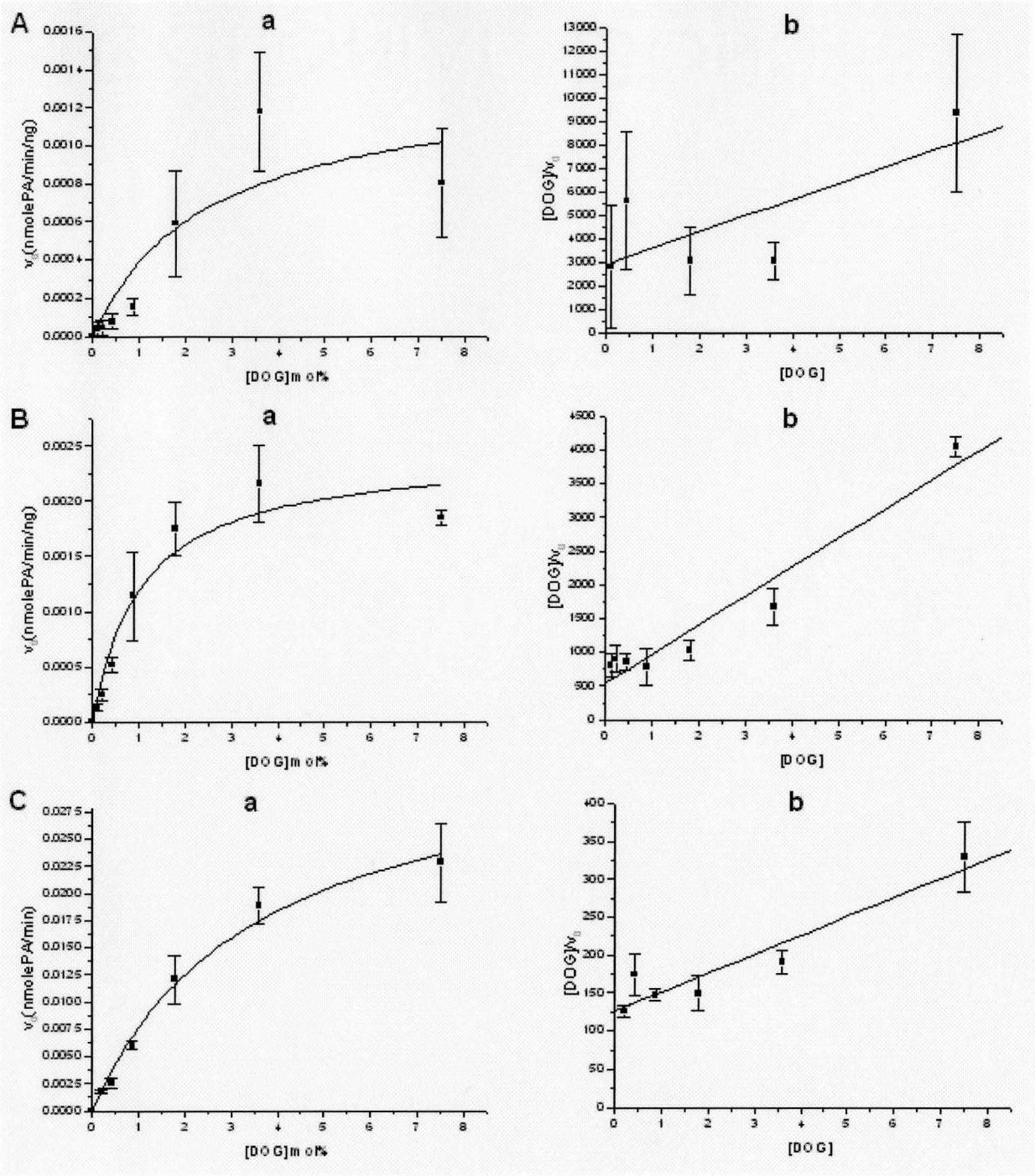

Fig. 21 Dependence of the initial velocity (v_o) of DGK-catalyzed phosphorylation of DOG. a. Two-parameter hyperbolic plots of initial velocity (v_o) versus DOG substrate concentration. **b**. Hanes plots were used to determine the Michaelis-Menten constants. **A**. 3XFLAG-DGKε. **B**. 3XFLAG-DGKΔε (1-41). **C**. DGKε-His. The data reported are an average of two experiment performed in triplicates. Error bars indicate the standard error of the mean.

A summary of 3XFLAG-DGKε and 3XFLAG-DGKΔε (1-41) kinetic constants for DAG substrates (SAG, SLG, and DOG) is included below. The purpose of the summary is for easier comparison of the kinetic constants for the two constructs designed and used in this study.

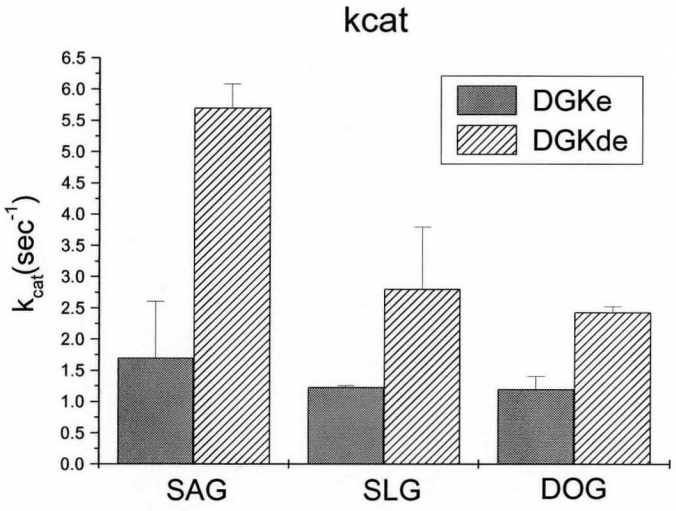

Fig. 22 Summary of kcat for the lipid substrates of the 3XFLAG-DGKε and 3XFLAG-DGKΔε proteins. The k_{cat} determined previously and tabulated in Table 2 was used to construct the bar graph. The substrates used were SAG, SLG, and DOG (varying concentrations) and ATP (5mM, maximum concentration). The k_{cat} for SAG of the full-length DGKε was about 4X lower than the k_{cat} for SAG of the truncated DGKε, the k_{cat} for SLG of the full-length DGKε was about 2X lower than the k_{cat} for SLG of the truncated DGKε, and the k_{cat} for DOG of the full-length DGKε was less than 2X lower than the k_{cat} for DOG of the truncated DGKε.

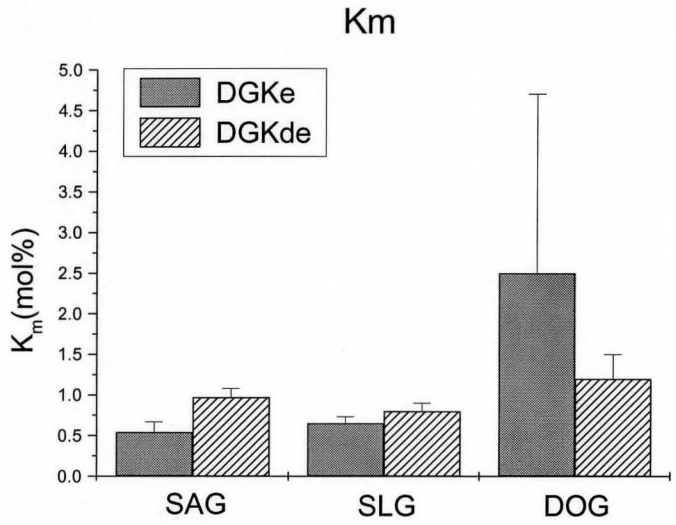

Fig. 23 Summary of Km for the lipid substrate of the 3XFLAG-DGKε and 3XFLAG-DGKΔε (1-41) proteins. The Km determined previously and tabulated in Table 2 was used to construct the bar graph. The substrates used were SAG, SLG, and DOG (varying concentrations) and ATP (5mM, maximum concentration). The Km for SAG of the full-length DGKε was about 2X lower than the Km for SAG of the truncated DGKε, the Km for SLG of the full-length DGKε was about the same as the Km for SLG of the truncated DGKε, and the Km for DOG of the full-length DGKε was about 2.5X higher than the Km for DOG of the truncated DGKε.

3.3 Oligomerization studies of 3XFLAG-DGKε and 3XFLAG-DGKΔε (1-41) proteins

The quaternary structure or the state of oligomerization of membrane proteins may be important for the function of the protein in biological membranes (Yeagle, 1993). It is hard to determine the molecular weight of functional membrane proteins since they require solubilization with detergents that can interfere with the hydrodynamic properties of the proteins. The present study shows various approaches taken into solving the state of oligomerization of 3XFLAG-DGKε protein and the role of the N-terminus hydrophobic domain of DGKε by investigating the truncated 3XFLAG-DGKΔε (1-41) protein.

3.3.1 PFO electrophoresis

Assessment of the quaternary structure of membrane proteins by PAGE has been problematic due to the relatively poor solubility of membrane proteins in non-dissociative detergents. A novel method for evaluating the oligomeric structure of membrane proteins uses the perfluoro-octanoic acid (PFO) detergent, which is less denaturing than SDS and allows assessment of multimeric protein complexes in the gel (Ramjeesingh *et al.*, 1999). The protocol was modified according toYang *et al.*, 2002 and is outlined in the methods section.

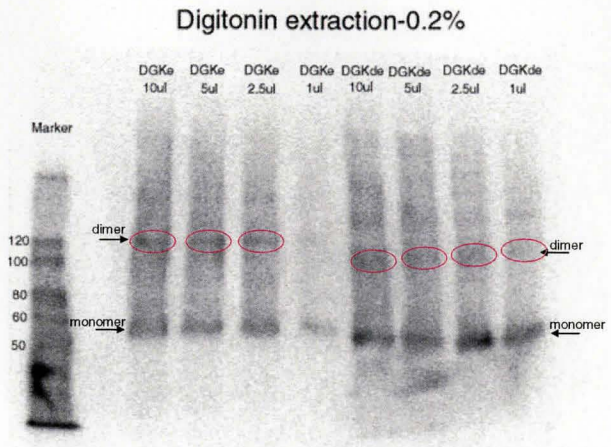

Fig. 24 PFO –PAGE of 3XFLAG-DGKε and 3XFLAG-DGKΔε (1-41) lysates after digitonin extraction. Whole cell lysates of 3XFLAG-DGKε and 3XFLAG-DGKΔε (1-41) extracted with 0.2% digitonin were loaded on a PFO gel. The sample buffer and the running buffer contained 0.1% PFO. Four different dilutions (10 µl, 5 µl, 2 µl, and 1 µl) of the two proteins were loaded on the gel and the presence of the protein was detected by western blotting using primary mouse anti-FLAG antibody and HRP linked anti-mouse secondary antibody.

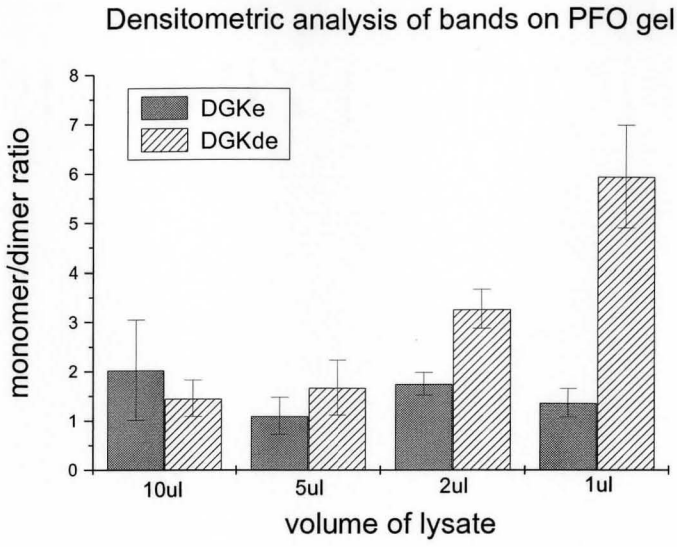

Fig. 25 Ratio between the band intensity for the 3XFLAG-DGKε and the band intensity for the 3XFLAG-DGKΔε (1-41). The intensity of the bands was determined with the Scion Image software. The mean intensity of five readings for each of the bands was calculated and the background intensity was subtracted. The ratio was calculated by dividing the average density of the monomer band to the average density of the dimer band.

The ratio of monomer/dimer increases as the dilution of the protein increases. The result is more noticeable for the 3XFLAG-DGKΔε (1-41) construct. Also, the ratio monomer/dimer is higher for the 3XFLAG-DGKΔε (1-41) construct versus the 3XFLAG-DGKε construct.

3.3.2 Cross-linking studies using DSS

The use of cross-linking reagents in studies of multisubunit enzymes and protein complexes is pretty common. Chemical cross-linking introduces covalent bonds within a protein complex or between proteins; therefore proteins that are in close proximity can be connected stably (Pierce Biotech Inc).

A limitation of this method is the dependence of the coupling on the specific side-chains of amino-acids in the proteins. These side-chains need to be in a certain distance and orientation to allow cross-linking. On the other hand, there could be unspecific cross-linking of proteins that happen to be within the distance required for the cross-linker to react. There are different compounds used for cross-linking studies and usually the cross-linker is chosen to be efficient for the system one is working with (Pierce Biotech Inc). The present study used the water-insoluble, homobifunctional N-hydroxysuccinimide ester (NHS ester), non-charged, lipophilic and membrane permeable DSS (disuccinimidyl suberate). NHS esters react with primary amino-groups in pH 7-9 buffers to form stable amide bonds. The membrane-permeability feature of DSS makes it a good candidate for intracellular and intramembrane conjugations. After the cross-linking reaction is stopped the samples can be run on an SDS-PAGE gel since the covalent bonds formed are quite stable under denaturing conditions. The protocol used was adapted from Sigma-Aldrich protocol that came with the product.

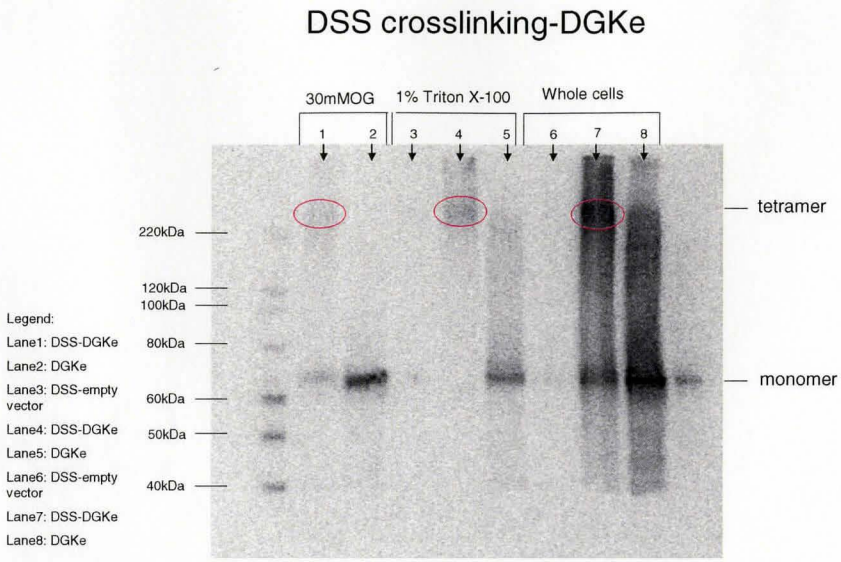

Fig. 26 The effect of DSS cross-linking on 3XFLAG-DGKε. Protein cross-linking was done in solution (OG and Triton X-100 lysates) and in the membrane (whole cells). Cross-linking in solution was performed by adding the cross-linking reagent (DSS) to the detergent extracted whole cell lysates of 3XFLAG-DGKε. The reaction was stopped by adding 1M Tris/HCl, pH 7.5, and incubating the mixture for 15 min at room temperature. Cross-linking in the membrane was performed by incubating whole cells expressing the 3XFLAG-DGKε protein with the cross-linking reagent. The reaction was quenched with 1M Tris/HCl, pH 7.5 as previously mentioned, and proteins were extracted with the SDS sample buffer and run on the gel. Reducing agent was present in the sample buffer.

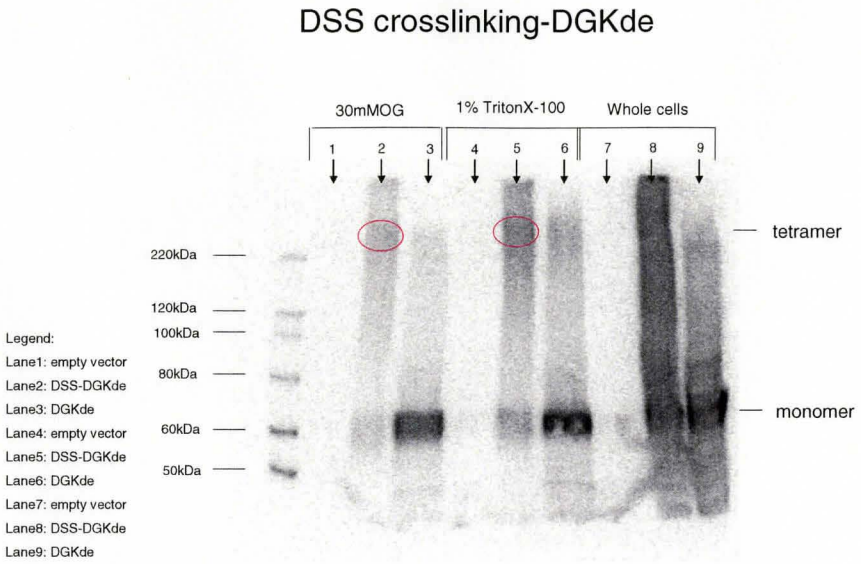

Fig. 27 The effect of DSS cross-linking on 3XFLAG-DGKΔε (1-41). Protein cross-linking was done in solution (OG and Triton X-100 lysates) and in the membrane (whole cells). Cross-linking in solution was performed by adding the cross-linking reagent (DSS) to the detergent extracted whole cell lysates of 3XFLAG-DGKΔε (1-41). The reaction was stopped by adding 1M Tris/HCl, pH 7.5, and incubating the mixture for 15 min at room temperature. Cross-linking in the membrane was performed by incubating whole cells expressing the 3XFLAG-DGKΔε (1-41) protein with the cross-linking reagent. The reaction was quenched with 1M Tris/HCl, pH 7.5 as previously mentioned, and proteins were extracted with the SDS sample buffer and run on the gel. Reducing agent was present in the sample buffer.

The results of the DSS cross-linking study of 3XFLAG-DGKε and 3XFLAG-DGKΔε (1-41) are hard to interpret since the western blots of the SDS-PAGE gels show low intensity bands for a tetrameric form of both proteins. The presence of a tetrameric band for the3XFLAG-DGKΔε (1-41) protein suggests that oligomerization may be a process rendered by a different segment from the transmembrane segment of the full length DGKε.

3.3.3 Blue-native electrophoresis

Electrophoretic techniques separating native proteins are rare because of the tendency for aggregation of the membrane proteins. In Blue-native PAGE (BN-PAGE) the aggregation problem is reduced by adding the negatively charged dye Coomassie blue G-250. This dye is not a detergent but it keeps membrane proteins solubilized in the absence of detergent. Coomassie binds to the hydrophobic domains on the surface of the proteins reducing the problem of aggregation (Shagger *et al.*, 1994).

For mammalian whole cell lysates the problem of aggregation was not solved until 2004, when Camacho-Carvajal *et al.* published a paper, which shows a method of BN-PAGE applicable to whole cellular lysates. The researchers identified an unknown cytosolic component smaller than 3.5kDa which was the probable cause for protein aggregation and which could be eliminated by dialysis/ filtration before the samples were loaded on the gel. Recently, a review paper by Eubel *et al.*, 2005 gathered data from the literature on the detergent solubilization of various membrane protein complexes and the importance of the type of detergent used in maintaining the stability of these complexes. The protocol used in this study is summarized in the experimental procedure section and is adapted from the methods outlined in the papers mentioned above.

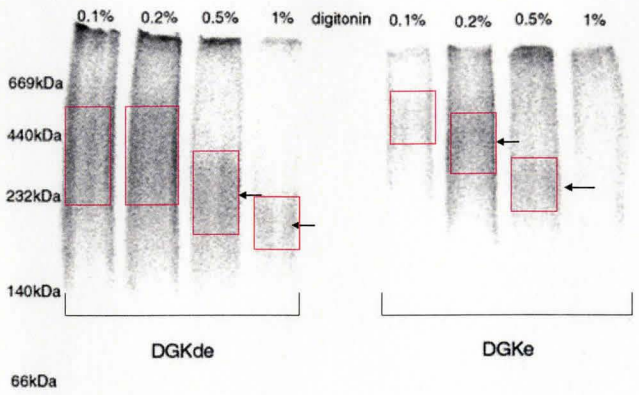

Fig. 28 BN-PAGE of digitonin extracted lysates. Coomassie Blue was not added to the sample buffer since it promoted precipitation of the protein in the wells. Whole cell lysates of 3XFLAG-DGKε and 3XFLAG-DGKΔε (1-41) were prepared by extracting the proteins with various digitonin concentrations (0.1%, 0.2%, 0.5%, and 1%). The ratio of detergent to Coomassie Blue was kept constant for the loaded samples and the run was performed on a polyacrylamide gradient gel (4-15%). The proteins were detected by western blotting with mouse anti-FLAG primary antibody and HRP linked goat anti-mouse secondary antibody.

Although in the absence of Coomassie the protein travels through the gel, it was hard to determine the molecular weights of the darker regions of the gel since the bands were not well defined.

3.3.4 Co-immunoprecipitation studies of 3XFLAG-DGKε

Co-immunoprecipitation is one of the most commonly used methods to determine whether two proteins can interact. This method was adapted in the present study to determine whether the target protein oligomerizes. For this purpose, mammalian cells were transfected with two constructs of the same protein carrying different tags. The proteins in the 30mM OG detergent extracted lysate were immunoprecipitated with antibody bound agarose beads. The antibody was raised against one of the tags and the protein was called bait. The presence of the other tagged protein, the target, was detected by western blotting of the immunoprecipitated complex.

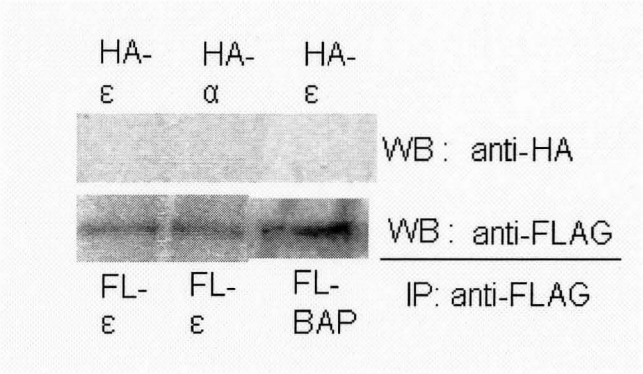

Fig. 29 Co-immunoprecipitation studies of 3xFLAG-DGKε. 3XFLAG-DGKε was co-transfected with 2XHA-DGKε at a 1:1 ratio of plasmid DNA. Two controls were used, one where 3XFLAG-DGKε was co-transfected with 2XHA-DGKα and the other one where 3XFLAG-BAP was co-transfected with 2XHA-DGKε. The proteins were extracted from the cell membranes with 30mM OG for 30min on ice. The lysates were centrifuged at 16,000g for 10min to clear up the supernatants. The clear supernatants were then mixed with anti-FLAG antibody bound agarose beads for 3 hours at 4°C. The mixture was centrifuged for 30sec at 16,000g and the flow through was aspirated and saved for later. The beads were washed three times with TBS wash buffer and then they were used for running on an SDS-PAGE gel. The proteins were detected by western blotting using mouse anti-HA primary antibody and mouse anti-FLAG primary antibody.

The results show that the target protein, 2XHA-DGKε, was not detected in the immunoprecipitated complex. The presence of the 3XFLAG-DGKε on the beads was detected with mouse anti-FLAG primary antibody. These results show that the 2XHA-DGKε and the 3XFLAG-DGKε proteins do not interact with each other as showed by the co-immunoprecipitation studies. Because of the biochemical diversity of protein-protein interactions optimization is often necessary.

3.3.5 Modeling studies of the hydrophobic domain peptide show favourable dimerization positions and amino acid interactions

Our collaborators from Belgium have modeled the peptide corresponding to the human DGKε hydrophobic domain. They modeled the peptide in a dimer form and then they studied the interaction between the peptides. They maintained one helix fixed while the other helix was moved around. For each position, the energy of interaction was calculated as the sum of Coulomb, van der Waals, and solvation energies and the complex with the lowest energy was kept. The researchers found several possibilities for dimerization. The complex presented in Fig. 30 is interesting since the packing in the center is not very good but the packing at the ends is stabilized by aromatic interactions between the His and Trp at the N-terminus and Phe, Phe and Trp at the C-terminus.

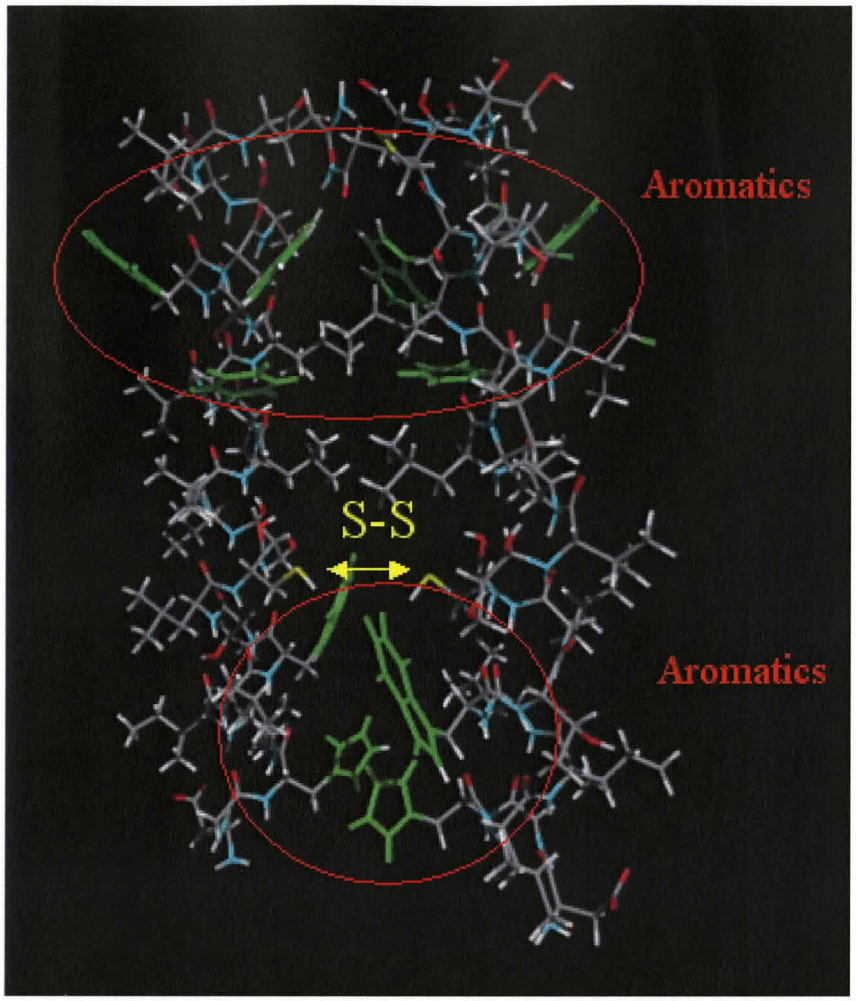

Fig. 30 Model of 3XFLAG-DGKε transmembrane peptide in parallel orientation dimeric form. The transmembrane peptide of full length DGKε was used for modeling the association into dimers. The researchers maintained one helix fixed while the other helix was moved around. For each position, the energy of interaction was calculated as the sum of Coulomb, van der Waals, and solvation energies and the complex with the lowest energy was kept. The packing of the helices was better at the ends due to stabilization by aromatic residues while the packing in the center was not ideal. There was also an S-S bridge in the center.

The study of peptide interaction in antiparallel orientation (Fig. 31) gave surprising results since the packing was very good all along the helices compared to the parallel orientation. It appeared as if the interaction could continue with another partner and lead to the formation of a barrel with alternating up-down peptides. This model does not appear to hold a true biological role for the full-length enzyme.

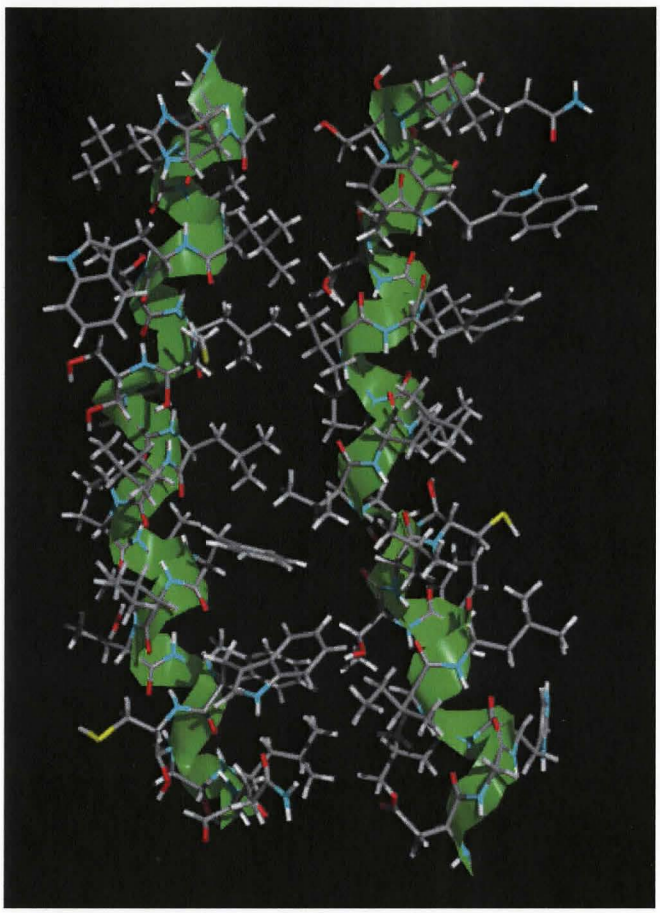

Fig. 31 Model of DGKε transmembrane peptide in antiparallel orientation dimeric form. The transmembrane peptide of full length DGKε was used for modeling the association into dimers. The researchers maintained one helix fixed while the other helix was moved around. For each position, the energy of interaction was calculated as the sum of Coulomb, van der Waals, and solvation energies and the complex with the lowest energy was kept. The packing of the helices was good all along the helices. It appeared as if the interaction could continue with another partner and form a barrel.

3.3.6 Biophysical studies of the hydrophobic domain peptide show dimerization by electrophoresis and FRET analysis

Our collaborators from Toronto have studied the peptide corresponding to the human DGKε transmembrane domain. As mentioned above, the peptide used in the study was: KKKKLILWTLCSVLLPVFITFWKKKKK. As a first step in studying oligomerization of the peptide, SDS-PAGE was performed in reducing (β-mercaptoethanol present) and non-reducing conditions (data not shown).

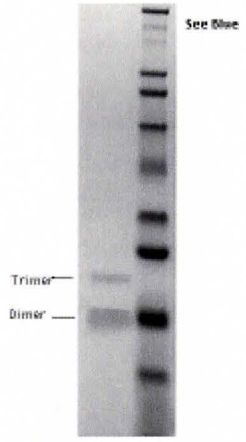

Fig. 32 Nu-PAGE of DGKε transmembrane peptide in reducing conditions. Our collaborators synthesized the peptide corresponding to the transmembrane domain of full length DGKε. 52μM of peptide was run on a Nu-PAGE gel in the presence of β-mercaptoethanol. The gel presented was done at 52μM of peptide and the dominant oligomer was the dimer. The ratio of dimer to trimer depended on the concentration of peptide used (data not shown).

In order to confirm the oligomerization of the peptide, FRET experiments were done in non-reducing conditions in zwitterionic large unilamellar vesicles of POPC and in reduced conditions in SDS micelles.

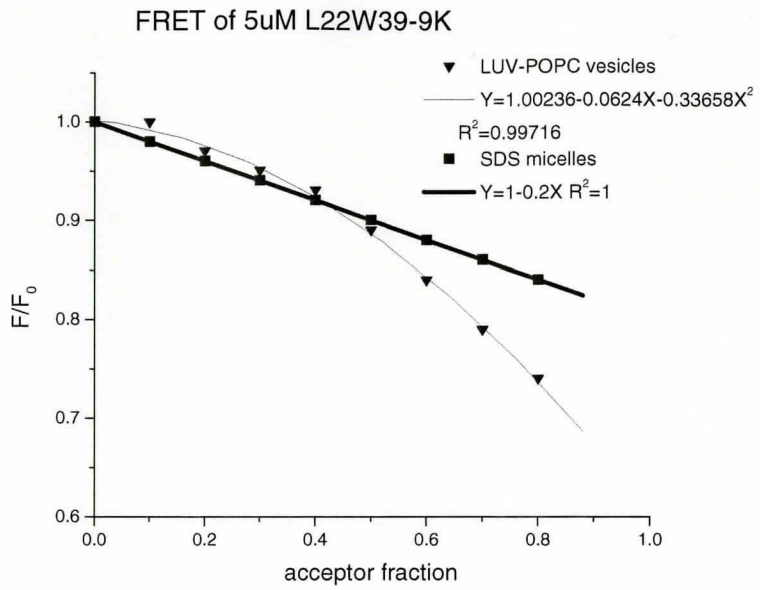

Fig. 33 FRET analysis of the DGKε transmembrane peptide, KKKKLILWTLCSVLLPVFITFWKKKKK, in SDS micelles and LUV-POPC vesicles. The peptide corresponding to the transmembrane domain of full length DGKε was labeled at the N-terminal Lys residue with dansyl or dabcyl chloride by synthesis. The peptides were purified and there association was studied by FRET. The amount of donor (dansyl peptide) fluorescence quenching was calculated as a function of the acceptor (dabcyl peptide) fraction. In SDS micelles the relative quantum yield of the donor decreases linearly with increasing acceptor fraction while in POPC large unilamellar vesicles the relative quantum yield of the donor decreases with increasing acceptor fraction according to a second-degree polynomial curve.

FRET was used to confirm the dimerization of the peptide noticed through SDS-PAGE. Specific labeling of the peptide was achieved during synthesis by attaching either dansyl or dabcyl chloride to the N-terminal Lys residue (Glukhov *et al.*, 2005). Labeled peptides were cleaved from the resin and purified. The stoichiometry of association in a peptide oligomer was analyzed by calculating the amount of donor (N-terminal dansyl-labeled peptide) fluorescence quenching as a function of the acceptor (N-terminal dabcyl-labeled peptide) fraction (Glukhov *et al.*, 2005). In the case of monomers, no quenching

should be observed while in the case of oligomerization, the relative quantum yield (F/F_o) of the donor decreases linearly with increasing acceptor fraction in case of dimerization and according to a more complex function for higher order oligomers (Glukhov *et al.*, 2005). FRET experiments of the DGKε transmembrane peptide confirmed the tendency of the peptide to dimerize.

3.4 Membrane topology of 3XFLAG-DGKε

An interesting topic in membrane protein research is the study of membrane protein orientation or topology. The reason to study membrane protein topology is to provide some insight into the function of the protein. The transmembrane segments of membrane proteins are very important in functions such as active transport, transmembrane signaling, and ion conduction (Jennings, 1989).

The present study allowed detection of the topology of the N-terminus of the protein. The protocol used is presented in the methods section. The results of the study show that the N-terminus FLAG tag is detected only upon cell permeabilization (Fig. 34). Non-permeabilized cells (Fig. 35) and empty vector control cells (Fig. 36) show only background fluorescence.

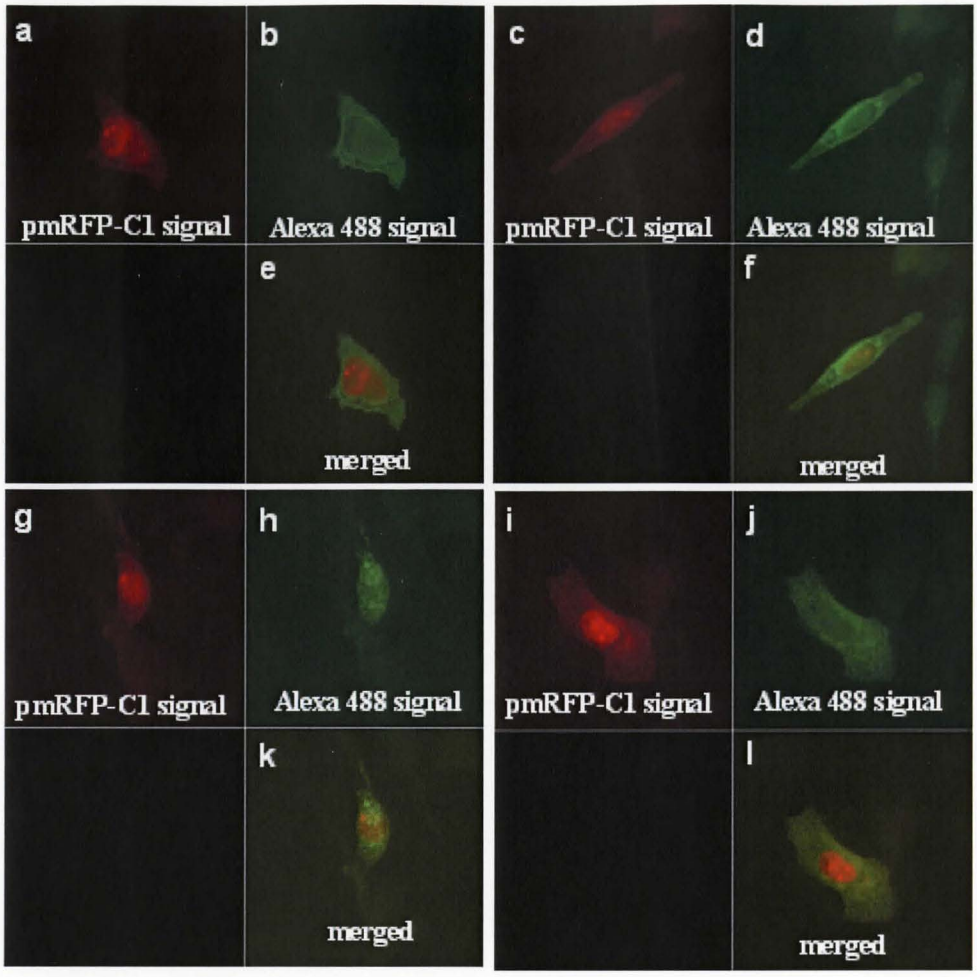

Fig. 34 Wide field fluorescence microscopy of Triton X-100 permeabilized NIH 3T3 cells co-transfected with pmRFP-C1 vector and p3XFLAG-DGKε vector. COS-7 cells were co-transfected with pmRFP-C1 and p3XFLAG-DGKε vectors. The cells were fixed with paraformaldehyde and permeabilized with Triton X-100 prior to indirect immunofluorescence using an antibody directed against the FLAG tag and an Alexa 488 secondary antibody. Panels a, c, g, and i show the pmRFP-C1 signal. Panels b, d, h, and j show the 3XFLAG-DGKε signal. Panels e, f, k, and l show the merged images.

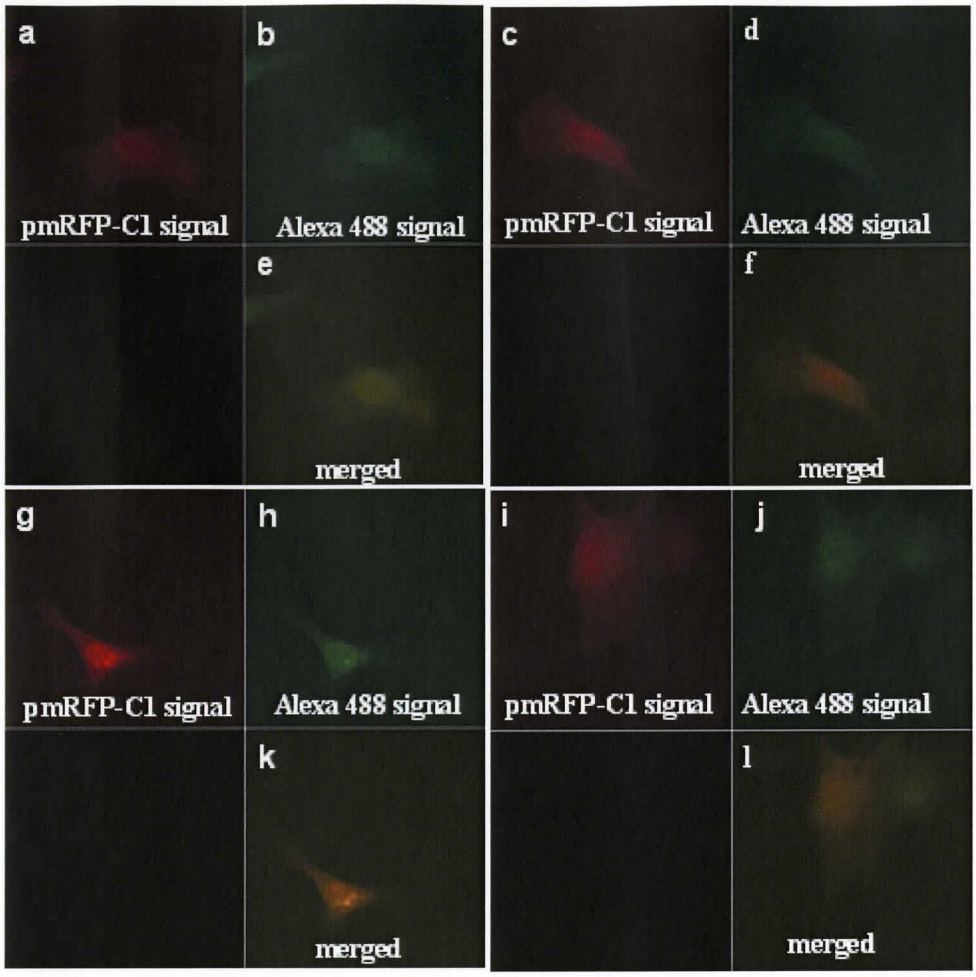

Fig. 35 Wide field fluorescence microscopy of non-permeabilized NIH 3T3 cells co-transfected with pmRFP-C1 vector and p3XFLAG-DGKε vector. COS-7 cells were co-transfected with pmRFP-C1 and p3XFLAG-DGKε vectors. The cells were fixed with paraformaldehyde and left non-permeabilized prior to indirect immunofluorescence using an antibody directed against the FLAG tag and an Alexa 488 secondary antibody. Panels a, c, g, and i show the pmRFP-C1 signal. Panels b, d, h, and j show the 3XFLAG-DGKε signal. Panels e, f, k, and l show the merged images.

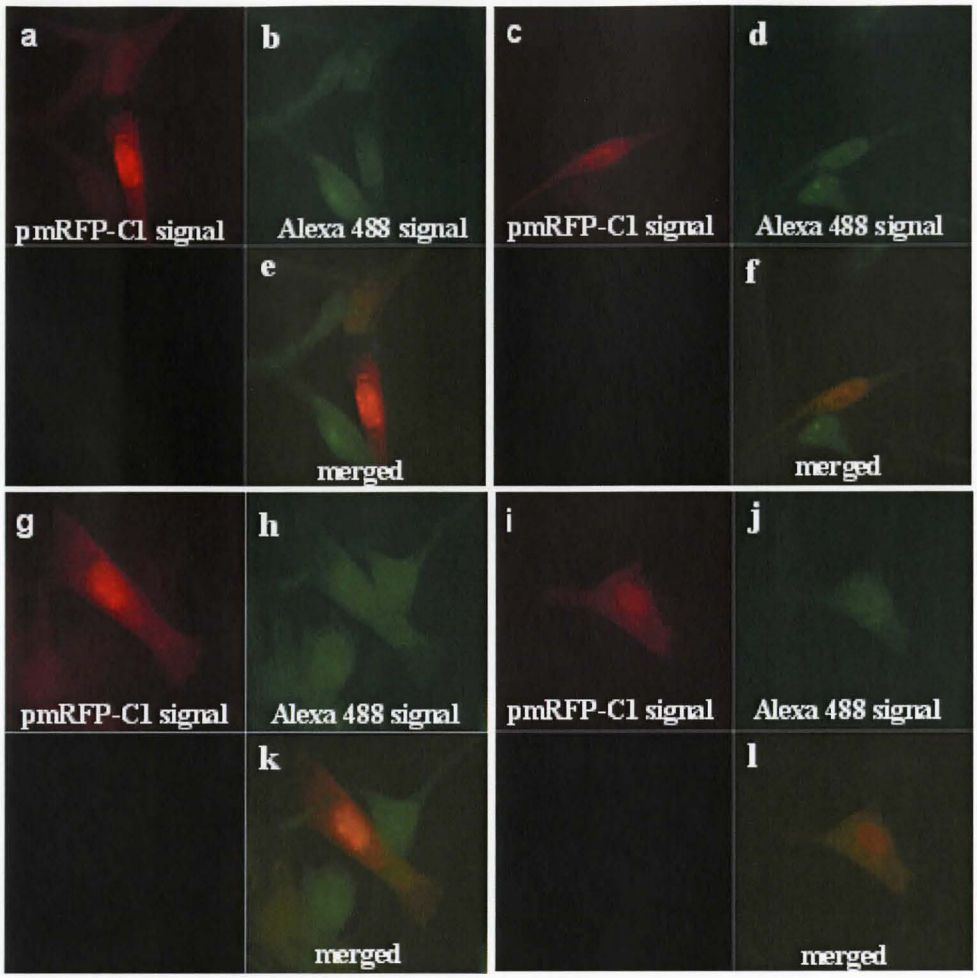

Fig. 36 Wide field fluorescence microscopy of Triton X-100 permeabilized NIH 3T3 cells (A and B) and non-permeabilized NIH 3T3 cells (C and D) co-transfected with pmRFP-C1 vector and p3XFLAG empty vector. COS-7 cells were co-transfected with pmRFP-C1 and p3XFLAG empty vectors. The cells were fixed with paraformaldehyde and permeabilized with Triton X-100 (panels a, b, c, d, e, and f) or non-permeabilized (panels g, h, i, j, k, and l) prior to indirect immunofluorescence. Indirect immunofluorescence was performed using an antibody directed against the FLAG tag and an Alexa 488 secondary antibody. Panels a, c, g, and i show the pmRFP-C1 signal. Panels b, d, h, and j show the Alexa 488 background signal. Panels e, f, k, and l show the merged images.

3.5 Construction of two new mutants of DGKε

Two new constructs of truncated DGKε have been designed as presented in the experimental methods section. The constructs were designed in pcDNA3.1 vector. The vector was graciously donated by Dr. Nohturfft's lab at Harvard University. Thirugnanam *et al.,* 2001 have mentioned the presence of a cationic cluster near the putative transmembrane domain of DGKε. Therefore, the two constructs designed are truncation 1-41 (cationic cluster still present) and truncation 1-59 (cationic cluster removed) (Fig. 37).

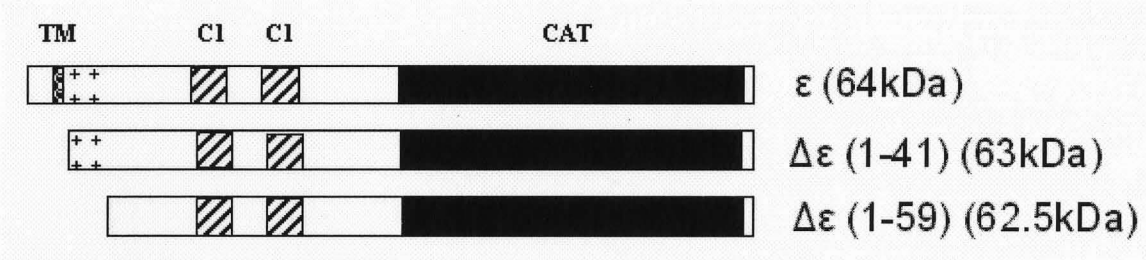

Fig. 37 Structures of DGKε constructs designed for further investigations. Diagrams of the one full-length DGKε construct and two truncated DGKε mutants are shown. The drawings are not at scale. The putative transmembrane domain (TM), the two cysteine-rich domains (C1), and the catalytic domain (CAT) are indicated on the figure. Dr. Matthew K. Topham designed the full-length construct and the DGKε gene was cloned into the pcDNA 3 vector from Invitrogen. The plasmid was a kind gift from Dr. Topham. The two truncated mutants of DGKε were designed by cloning into the pcDNA3.1 vector as mentioned above.

Chapter 4. Discussion

4.1 DGKε has an N-terminus hydrophobic domain

Although transmembrane prediction software programs such as DAS calculated that the probability of having a transmembrane domain at the N-terminus of DGKε is quite high, the experimental data on the full-length protein did not resolve the question whether DGKε is an integral membrane protein or not. Studies on the peptide corresponding to the hydrophobic domain of DGKε showed that the peptide inserted spontaneously into the micellar amphiphiles (SDS micelles), and even into zwitterionic bilayers (LUV of POPC) (Fig. 12). Therefore, the 20 amino acid hydrophobic segment could insert itself in the membrane. In addition to the biophysical studies, the modeling of the peptide corresponding to the hydrophobic domain of DGKε with the IMPALA simulations showed that the peptide inserted easily in the membrane and more so, the dimerized peptide inserted easily as well (Fig. 13).

Therefore, the studies on the hydrophobic peptide support the hypothesis that DGKε is an integral membrane protein. However, studies on the full-length enzyme have proven more challenging. A truncated form of the enzyme lacking the N-terminus hydrophobic domain was constructed (Fig. 7) in order to determine the effect of the domain on the protein function. The full-length enzyme and the truncated mutant were both treated with high salt. As expected, the full-length enzyme was less extractable from the membrane than the truncated enzyme (Fig. 11). In addition to the high salt extractions, Triton X-114 experiments were performed on the two forms of the enzyme

(data not shown), but the results were not as clear. Both the full-length and the truncated enzyme were present in both phases, aqueous and detergent phase. The question whether DGKε is an integral membrane protein remains open.

From subcellular localization experiments there is evidence that both the full-length and the truncated enzyme associate with the plasma membrane (Fig. 9 and Fig. 10). This result was expected since both the full-length and truncated enzyme showed activity, which means they both associate with the membrane where their lipid substrate is found. In addition, the wide field fluorescence microscopy of Triton X-100 permeabilized NIH 3T3 cells (Fig. 34) showed a scattered fluorescence pattern, typical of a membrane protein, at the periphery of the cell of transiently transfected cells with 3XFLAG-DGKε. On the contrary to the findings of this study, Fukunaga-Takenaka et al., 2005 used an N-terminus GFP-DGKε construct in confocal laser fluorescence scanning microscopy and determined the presence of that construct in the cytoplasm of DDT1-MF2 cells (Fukunaga- Takenaka et al, 2005). These findings prove the importance of the type of tag attached to certain proteins. The paper does not give details about the activity of the GFP-DGKε construct but it is expected that the enzyme activity is affected due to cytoplasmic localization of this previously determined membrane associated protein (Walsh et al., 1994). In addition, information provided by Dr. Kaoru Goto, who originally designed the plasmid with the GFP tag at the N-terminus, suggests that the N-terminus GFP-DGKε has sufficient activity, but the same tag attached at the C-terminus might abolish the enzyme activity as it happened with the other isoforms such as DGKζ (unpublished data). Therefore, great care has to be taken when choosing a tag for

detection of a recombinant protein. The FLAG tag proved to be small enough to maintain enzyme activity and subcellular localization similar to the endogenous enzyme. Additional experiments have to be done on the full-length and truncated forms of DGKε in order to answer the question whether the enzyme is an integral membrane protein. It has proven to be a difficult task due to the unclear and contradictory results obtained from different experiments.

Additional results of membrane protein topology determination bring some clarification onto why it is possible that a protein with a hydrophobic domain be extractable from the membrane with high salt concentrations and reside in both the aqueous and detergent phases of Triton X-114 phase partitioning.

If the findings of this study hold true in that the N-terminus and C-terminus of the protein both reside on the cytoplasmic side of the plasma membrane, the transmembrane domain should insert itself only in the inner leaflet of the membrane bilayer or attach itself to the membrane superficially as a planar amphipathic helix. Moreover, a fraction of the protein can be removed from the membrane without destroying the membrane structure, indicating that the protein may have properties intermediate between that of an integral membrane protein and peripheral protein. Thus, DGKε behaves largely like a monotopic membrane protein (see section 4.4 and Fig. 38).

4.2 Deletion of the N-terminus hydrophobic domain of DGKε appears to have no effect on the enzyme's substrate specificity in a detergent-micelle system.

Although DGKε is unique among isoforms of this enzyme, both in possessing a putative transmembrane domain and exhibiting specificity for substrates containing an arachidonoyl group, deletion of the N-terminal segment of the enzyme that contains the hydrophobic stretch of amino acid residues has no effect on the substrate specificity. This is indicated by the comparison of k_{cat}. The k_{cat} for 3XFLAG-DGKΔε (1-41) agrees reasonably well when determined using a high concentration of SAG (Table 2) or a high concentration of ATP (Table 1) and the value is about 2-fold larger than that for SLG, but 4.5-fold larger than for DOG, demonstrating a high specificity for substrates containing polyunsaturated acyl chains. The substrate selectivity for the two full-length constructs appears somewhat less than for the truncated form, but k_{cat} for SAG is still the largest among the three substrates used (Table 2). It is interesting that the removal of a large segment of the protein appears to have no deleterious effect on the activity and may even result in an enhanced catalytic rate. This situation has precedent with DGKα that has higher activity after truncation of the amino terminus (Abe *et al.*, 2003). All values are apparent since the dissociation constant of the enzyme from the micelles was not determined. The kinetic values may be dependent on the type of detergent used in the micelle assay since different detergents produce different sized micelles and the exchange rate between micelles is different for each detergent. The above is the reason why we kept the composition of micelles constant throughout the experiments. Although the assay conditions are not identical, our values are similar to other values found in the

literature. For example, the Km for SAG phosphorylation reported here, 0.30 mM-0.53 mM, is in good agreement with the reported values of 0.56 mM for the purified arachidonoyl specific DAG kinase from pig testes (Hodgkin *et al.*, 1997), and 0.35mM for the arachidonoyl-selective DAG kinase from bovine testes (Walsh *et al.*, 1994), and 0.25mM for the baculovirus expressed recombinant DGK ε (Epand *et al.*, 2004).

It appears *a priori* unlikely that the transmembrane domain, a segment unique to DGKε, has no functional role. It is possible that this domain facilitates targeting DGKε to the plasma membrane or even to a specific domain in the membrane. Alternatively, the hydrophobic segment may play a role in protein-protein interactions. However, the results of the present study show that this domain does not enhance substrate specificity and it does not have a direct and drastic effect on the catalytic activity of the enzyme.

4.3 Oligomerization studies of 3XFLAG-DGKε and 3XFLAG-DGKΔε (1-41) proteins.

Since the N-terminal hydrophobic domain appears to have no apparent effect on the enzyme's substrate specificity and no deleterious effect on the enzyme's activity but its removal may even result in an enhanced enzyme activity, the next step is to investigate the involvement of this unique segment in protein-protein interactions. Since most membrane proteins have a tendency to oligomerize in the membrane and this oligomerization plays a functional role in enzyme regulation, one can assume that the role of the N-terminus hydrophobic domain is to regulate the enzyme's activity through oligomerization or localization to specific domains in the membrane.

The present study investigated the presence of oligomers in solution for 3XFLAG-DGKε and 3XFLAG-DGKΔε (1-41) proteins by various electrophoretic methods. The clearest results were obtained when the proteins were extracted from the membrane with digitonin, a very mild detergent known to be the best at maintaining weak protein-protein interactions. The lysates were then run on PFO-PAGE, a milder detergent replacing SDS, and the results presented in Fig. 24 clearly showed the presence of a dimeric form of the enzyme, for both the 3XFLAG-DGKε and 3XFLAG-DGKΔε (1-41) proteins. The only difference between the two was the ratio of monomer to dimer, which was higher for the truncated enzyme (Fig. 25). Also to note was the increase in monomer to dimer ratio upon increasing protein dilution. The presence of dimers in the truncated enzyme together with the increase in monomer/dimer ratio upon dilution increase, points to the possibility that there might be another domain besides the transmembrane segment, which may play a role in oligomerization.

Besides studies on the full-length protein, the interactions between the transmembrane peptides were studied by molecular modeling (Fig. 30 and Fig. 31) and by biophysical methods (Fig. 32 and Fig. 33) by our collaborators and the results are presented in this thesis. The transmembrane peptides appear to associate well at the ends of the helices due to aromatic interactions, whereas the packing in the centre of the helices is not as good. Also, the antiparallel orientation of the two peptides shows good packing all along the helices. Therefore, it appears that the antiparallel orientation is favoured even if this interaction might not be biologically relevant. The biophysical studies on the transmembrane peptide show a tendency for aggregation into dimers, or

trimers, depending on the concentration of peptide used. Therefore, these additional studies on the hydrophobic peptide support the results of the PFO-PAGE of the full-length DGKε protein. The conclusion drawn from this gel method is that the transmembrane domain seems to play a role in oligomerization but this domain may not be the only segment of the protein involved in oligomerization.

Additional studies on the full-length and truncated enzyme have given less clear-cut or even contradictory results to the data obtained through PFO-PAGE. For example, the results from DSS cross-linking (Fig. 26 and Fig. 27) show higher molecular weight forms of the enzyme of the size of a tetramer. These results could be due to the tendency of cross-linking reagents to link other proteins found in the vicinity of the enzyme or to link two dimers. Another possibility is the stabilization effect of cross-linking reagents, which might be lost after detergent extraction and electrophoresis. Maybe the interaction between two monomers is stronger than between two dimers since only dimers are detected by PFO-PAGE, but the tetrameric form cannot be ruled out.

Ideally, the presence of oligomeric forms of a protein should be studied in the absence of detergents. This condition is hard to meet in the case of membrane proteins. Electrophoretic techniques separating native proteins are rare because of the tendency for aggregation of the membrane proteins. In Blue-native PAGE (BN-PAGE) the aggregation problem is reduced by adding the negatively charged dye Coomassie blue G-250. This dye is not a detergent but it keeps membrane proteins solubilized in the absence of detergent. Coomassie binds to the hydrophobic domains on the surface of the proteins

reducing the problem of aggregation (Shagger *et al.*, 1994). However, for mammalian whole cell lysates, the problem of aggregation was not solved.

Camacho-Carvajal *et al.*, 2004 showed a method of BN-PAGE applicable to whole cellular lysates. The researchers identified an unknown cytosolic component smaller than 3.5kDa which was the probable cause for protein aggregation and which could be eliminated by dialysis/ filtration before the samples were loaded on the gel. Even after several optimization protocols, the results of BN-PAGE for 3XFLAG-DGKε and 3XFLAG-DGKΔε (1-41) (Fig. 28) showed unclear results of the molecular weight of the enzyme.

In addition, co-immunoprecipitation studies (Fig. 29) have brought contradictory results to the electrophoretic findings. Proteins are heterogeneous in nature and a myriad of factors affect their structure and interaction with other proteins. Therefore, a potential problem is determining the effective conditions for co-immunoprecipitation such as cell lines, buffer components, extracting detergents, etc. (Masters, 2004). In the present study the proteins were extracted with 30mM OG prior to immunoprecipitation. OG is a pretty mild detergent, but it may still break the weak interactions between the DGKε monomers. Previous electrophoretic studies (data not shown) have not shown the presence of higher molecular weight forms of the enzyme when extracted with other detergents (30mM OG, 1% TritonX-100) than digitonin. Therefore, the next step would be to perform immunoprecipitation studies on digitonin extracted lysates.

In conclusion, the oligomerization data of the full-length enzyme from PFO-PAGE supports the transmembrane peptide studies. The N-terminus hydrophobic domain may be involved in oligomerization but it may not be the only domain contributing to the interaction. Also, since the co-immunoprecipitation data shows no interaction between the monomers, optimization of the protocol is needed in the future.

4.4 Membrane topology of 3XFLAG-DGKε

Membrane proteins have been classified by Blobel, 1980 on the basis of the number of times their hydrophobic domains span the membrane. Therefore, monotopic proteins are hydrophobically associated with the membrane but do not pass across the bilayer, bitopic proteins cross the membrane only once, and polytopic proteins cross the membrane more than once (Jennings, 1989). Monotopic proteins are rare. The monotopic proteins are in contact with only one side of the membrane bilayer. Their segments can associate with the membrane in different ways.

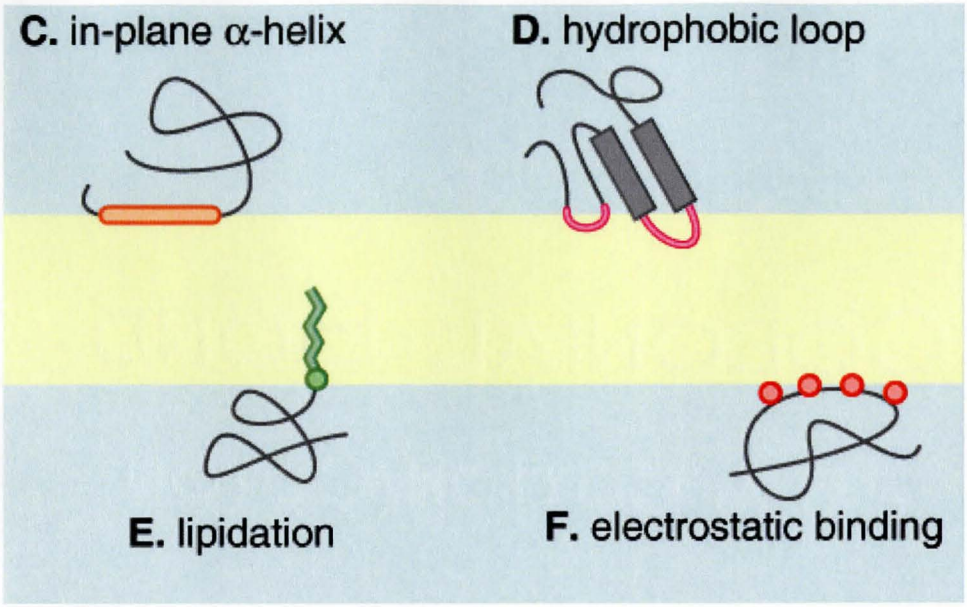

Fig. 38 Classes of monotopic proteins presented by Sapay, 2006. The classes of monotopic proteins are heterogeneous in their structure and distribution at the membrane. Some are planar α- helices (C); others form hydrophobic loops (D), while others interact with the membrane through covalent links (E) or electrostatic bonds (F) (Sapay, 2006). Bitopic membrane proteins are quite common and the class of polytopic membrane proteins is quite large (Jennings, 1989).

Since 3XFLAG-DGKε has only one hydrophobic segment, it is suspected that the protein is either monotopic or bitopic. To differentiate between monotopic and bitopic membrane proteins, the topology of the protein at the membrane has to be studied. The N-terminus hydrophobic peptide of 3XFLAG-DGKε protein has the sequence: **LILWTLCSVLLPVFITFWC** and as highlighted, it has a proline residue around the middle of the sequence. This proline residue could promote a kink formation and the transmembrane domain could form a hydrophobic loop (Fig.38D). However, since the residues around the Pro are not Gly, it may be hard to accommodate a very sharp kink with an angle smaller than 90°. Another possibility is the presence of the transmembrane domain as a planar helix (Fig.38C). As per Fig. 39, the helical wheel given by the SOSUI

program shows the presence of polar residues on one side of the helix. The orientation of the residues is a clue into the orientation of an amphipathic helix at the membrane.

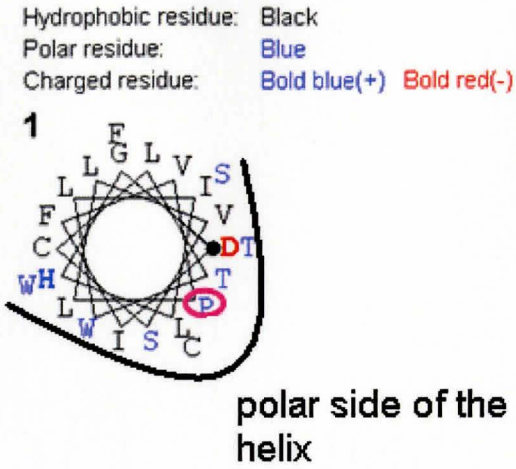

Fig. 39 Helical wheel of the hydrophobic domain of DGKε. The peptide corresponding to the transmembrane domain of full-length DGKε was run through the SOSUI software, which is a transmembrane and topology prediction program. One output of the program is the helical wheel corresponding to the transmembrane helix of the protein. The program also highlights the hydrophobic residues in black, the polar residues in blue, and the charged residues in bold blue (+) and bold red (-). For the peptide corresponding to the hydrophobic domain of DGKε there seems to be a more polar side of the transmembrane helix.

The presence of an amphipathic helix does not necessarily indicate the presence of an in-plane membrane anchor (IPM anchor). Sapay *et al.*, 2006 describe the first attempt to develop a prediction method for in-plane membrane anchors. The method called "AmphipaSeeK" was implemented on the NSP@ server. However, the method is based on only 21 sequences of monotopic proteins reported as IPM anchored. The 21 sequences were determined experimentally to have an IPM anchor (Sapay *et al.*, 2006).

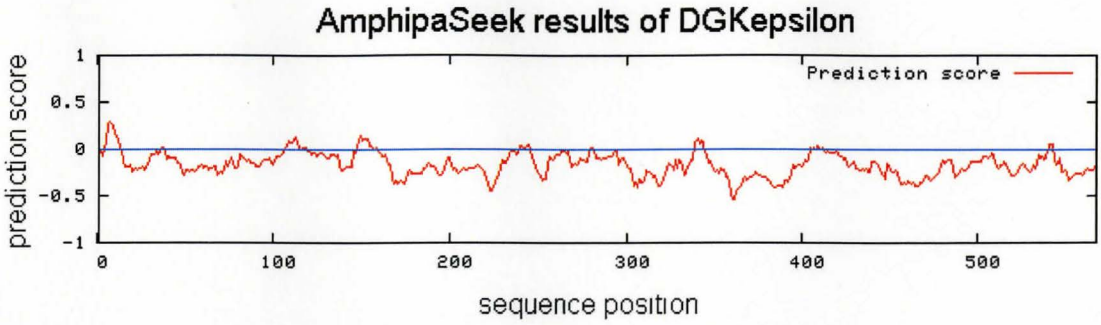

Fig. 40 AmphipaSeek results of the full-length DGKε protein. AmphipaSeek was developed as a method to predict in-plane membrane anchors. The full-length DGKε protein does not seem to have an in-plane membrane anchor between amino acids 19 and 40, which would correspond to the hydrophobic domain of the protein. A prediction score close to 0.5 would suggest the presence of an IPM anchor.

Based on the AmphipaSeek prediction, it appears that the transmembrane domain (residues 20-40) of DGKε may not be a planar helix.

Transmembrane prediction and topology prediction software, SOSUI, was run using the DGKε sequence. SOSUI is a system that bases its prediction not on sequence alignment but on the physicochemical properties of amino acid sequences (Hirokawa *et al.*, 1998). There are two basic assumptions in the SOSUI system, first, membrane proteins are characterized by at least one hydrophobic helix and second, the primary transmembrane helices are stabilized by amphiphilic side chains at the helix ends and high hydrophobicity in the center (Hirokawa *et al.*, 1998). The SOSUI system is a web-based tool. Two predictions and two graphs are presented in the output page. Included are the helical wheel diagrams and the topology of the DGKε protein (Fig. 40).

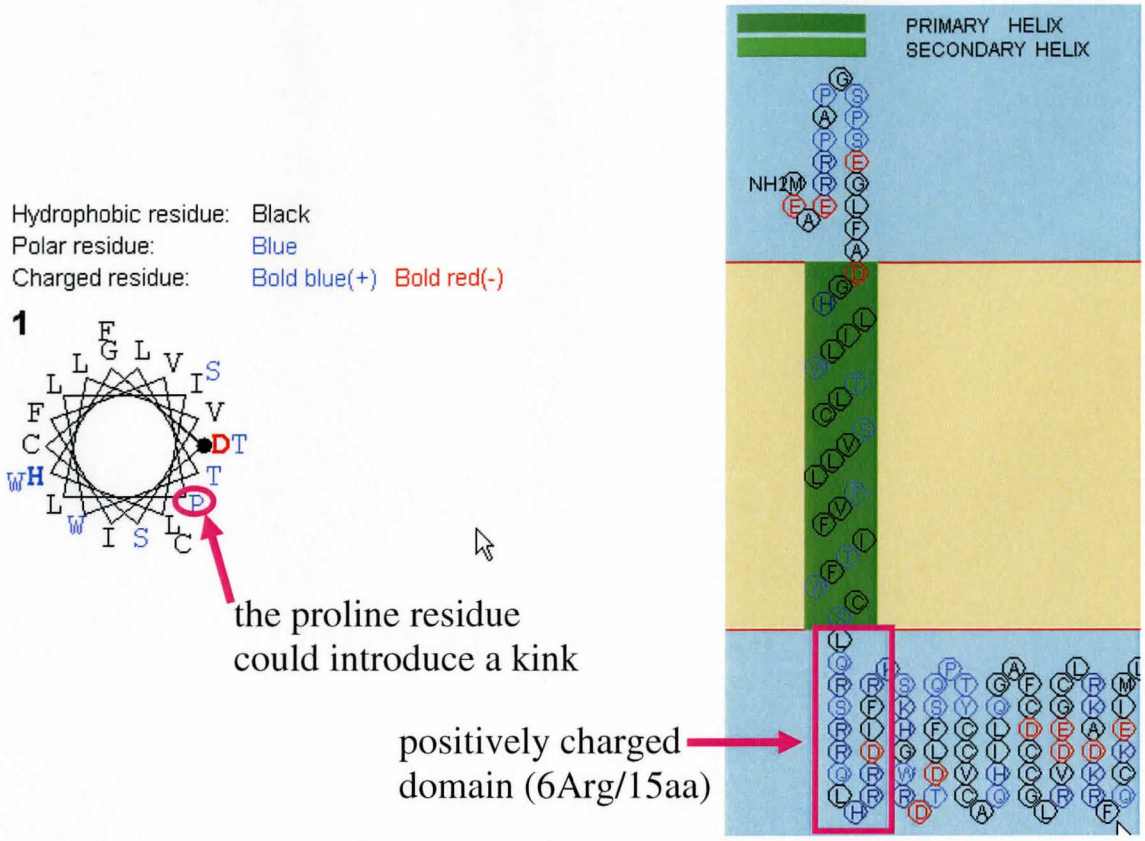

Fig. 41 SOSUI prediction results of full-length **DGKε protein.** The peptide corresponding to the transmembrane domain of full-length DGKε was run through the SOSUI software, which is a transmembrane and topology prediction program. One output of the program is the helical wheel corresponding to the transmembrane helix of the protein and the other output is the predicted topology of the transmembrane helix. For the peptide corresponding to the hydrophobic domain of DGKε there seems to be a proline residue in the middle of the transmembrane peptide sequence. Also, the sequence following the transmembrane peptide has a positively charged domain rich in Arg residues. As predicted by SOSUI, the protein has the N-terminus on the outside of the membrane.

The SOSUI prediction software shows that the DGKε has a bitopic topology with the transmembrane domain crossing the membrane once. The results of the prediction software have to be followed by experimental studies. The experimental results are more biologically relevant.

The present study attempted to solve the orientation of the N-terminus portion of 3XFLAG-DGKε. Since only the permeabilized cells showed increased green fluorescence compared to the background, it can be concluded that the N-terminus of the protein is found on the cytoplasmic side of the membrane. Since the method used in this study did not give information about the orientation of the C-terminus of the protein, the differentiation between monotopic or bitopic protein was not fully solved. Due to assumptions linked to the structure and function of the protein, one can presume that the C-terminus would be found on the cytoplasmic side of the membrane. The catalytic domain of DGKε is expected to be on the cytoplasmic side of the plasma membrane where its substrates reside. However, the possibility of having the catalytic domain extracellularly increases with the findings that show the existence of an ecto-PLC enzyme that would produce DAG in the outer leaflet of the plasma membrane (Birrel *et al.*, 1993). Therefore, from the experimental findings of this study the 3XFLAG-DGKε protein seems to be a monotopic protein but additional experiments to detect the position of the C-terminus of the protein will clarify the hypothesis presented above.

The finding that the N-terminus and C-terminus of the protein reside on the same cytoplasmic side of the plasma membrane implies that the transmembrane domain has either a kink in the middle and that it penetrates only one of the two lipid monolayers of the membrane or that the hydrophobic domain is a planar helix attached superficially to the membrane.

There are few examples of monotopic proteins in the literature. One example is the caveolin-1 protein (Spisni *et al.*, 2005; Schlegel *et al.*, 2000) that presents its hydrophobic domain at the membrane in the form of a hydrophobic loop. Caveolins are a

family of proteins that coat the cytoplasmic side of caveolae, vesicular invaginations of plasma membranes. Caveolin proteins have various functions in organelle biogenesis, in cellular transport, and in the cell signaling machinery (Schlegel *et al.*, 2000). The primary sequence of caveolin 1 contains a central hydrophobic domain (102-134) that is believed to anchor the protein to membranes. The sequence of this domain is **LFGIPMALIWGIYFAIL** and is mainly organized in an α-helix with a kink in the middle (Spisni *et al.*, 2005; Schlegel *et al.*, 2000).

Since caveolin 1 is known to be tightly associated with the membrane but also to have only a single hydrophobic domain, a major focus was the study of this protein's topology.

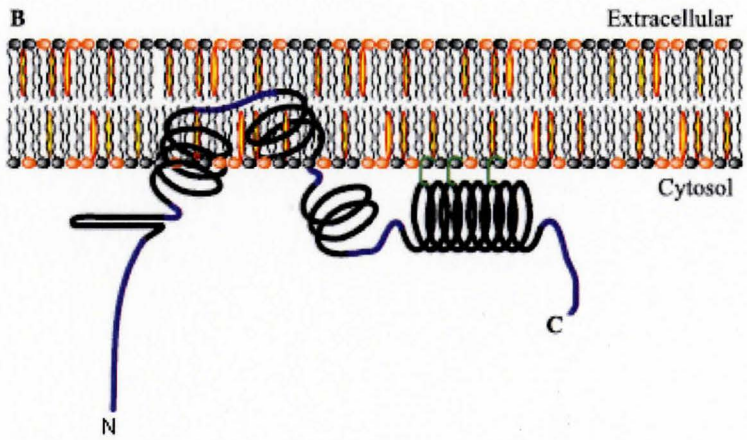

Fig. 42 A view of caveolin 1 topology (Spisni *et al.*, 2005). The α-helices and β strands are positioned according to prediction analysis or mutation analysis studies. The blue regions are unstructured and the black regions are structured.

As noted above, the similarities between caveolin 1 and DGKε primary sequence in having a single hydrophobic domain and the similarities in experimental evidence of

N-terminus detection through indirect immunofluorescence microscopy provide initial evidence upon the structure of diacylglycerol kinase epsilon at the membrane.

Based on the caveolin 1 topology and caveolin 1 sequence similarity to the DGKε we propose the following model for the structure of 3XFLAG-DGKε and its association with the plasma membrane.

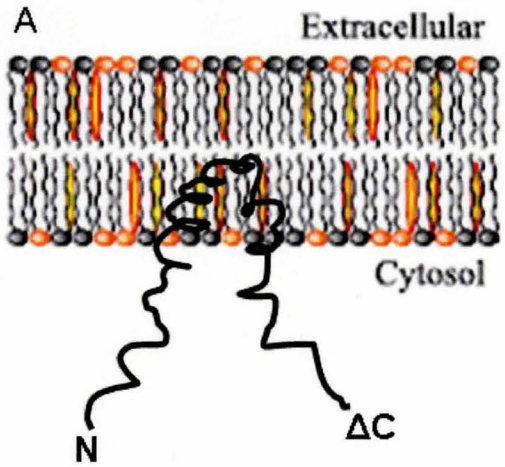

Fig. 43 Proposed model of 3XFLAG-DGKε association with the plasma membrane. The hydrophobic domain is represented as a hydrophobic loop with a kink in the middle. The protein is not drawn at scale. Only the sequence corresponding to the first 100 amino acids is indicated in the figure. The purpose of the scheme is only to show the nature of the membrane insertion.

Even though the sequence similarities between the caveolin 1 TM domain and DGKε TM segment point to the model of hydrophobic loop isertion as presented in Fig. 42, there could still be the possibility that the DGKε TM segment inserts in the membrane as a planar amphipathic helix (Fig. 44). There are several examples in the literature of proteins that associate with the membrane through a planar amphipathic helix. A list of 21 proteins experimentally determined to bind to a membrane through an IPM anchor are listed on the amphipaSeek server help website

(http://npsa-pbil.ibcp.fr/cgi-bin/npsa_automat.pl?page=/NPSAHLP/npsahlp_primanalamphipaseek.html).

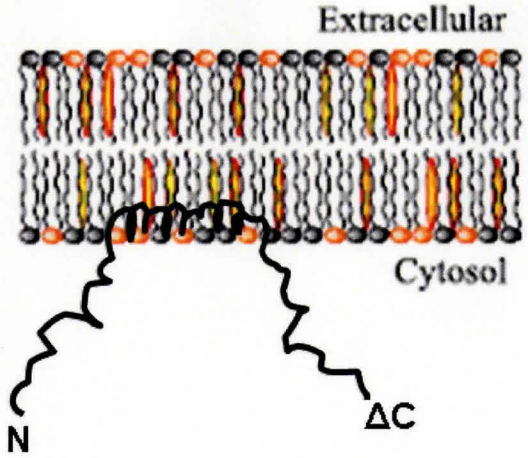

Fig. 44 Proposed model of 3XFLAG-DGKε association with the plasma membrane. The hydrophobic domain is represented as a planar helix. The protein is not drawn at scale. Only the sequence corresponding to the first 100 amino acids is indicated in the figure. The purpose of the scheme is only to show the nature of the membrane insertion.

4.5 Proposed models for DGKε regulatory mechanisms

Membrane proteins can have several regulatory mechanisms. The primary regulatory mechanism could be through their hydrophobic transmembrane domain. In the case of DGKε the catalytic domain is known not to include the putative transmembrane region (Tang *et al.*, 1996). This study has shown that the transmembrane domain of DGKε is not a required segment for enzyme activity or substrate specificity. The transmembrane domain of integral membrane proteins is known to anchor the protein to the membrane. In the case of DGKε it was thought that this domain could bring the enzyme closer to the lipid substrate pool located in the membrane.

The transmembrane domain of enzymes could be involved in regulation through association of the monomeric form of the enzyme in higher molecular weight oligomers. Oligomerization is known to result in the activation of several enzymes such as glyceraldehyde 3-phosphate dehydrogenase, phosphoglycerate mutase, and enolase (Torshin, 1999).

The oligomerization of DGKε could play a role in this enzyme's regulation. It is know that upon receptor activation, the PI-PLC is activated and more DAG is formed at the membrane. Increased levels of DAG in the membrane activate the DAG dependent protein kinases such as protein kinase C. To maintain low levels of DAG in the membrane, diacylglycerol kinases are activated and they phosphorylate DAG to PA, therefore, playing a role in controlling the activation of PKC. The results of the activity assays showed increased activity for the truncated enzyme. Therefore, our hypothesis was that the truncated enzyme was not aggregating into higher molecular structures and it presented higher activity. In the case of DGKε, oligomerization could be inhibitory. The dissociation of the oligomeric structures could be caused by increased levels of DAG in the membrane. There is precedence with inhibitory oligomerization in the literature. For example, DGKδ forms oligomers through its SAM domain (Imai *et al.*, 2002). In stimulated cells, the oligomers are dissociated by phorbol esters (TPA) and the enzyme is translocated to the membrane in a monomeric form. The dissociation of the DGKδ oligomers is mediated by PKC-catalyzed phosphorylation. No significant changes in enzyme activity were detected upon cell stimulation; therefore, the relevance of oligomer dissociation for enzyme catalytic activity is unknown (Imai *et al.*, 2002). Another relevant example of enzyme regulation by oligomerization is DGKη (Murakami *et al.*,

2003). Investigations on DGKη showed that the oligomer formation through the SAM domain resulted in the inhibition of catalytic activity of this enzyme. Also oligomerization was responsible for the sustained enzyme stabilization at the membrane (Murakami *et al.*, 2003).

Besides the natural tendency of DGKε to form oligomers in quiescent cells, oligomerization could also be initiated by incorporation of the protein in lipid rafts. Lipid rafts are membrane microdomains that are enriched in cholesterol and glycosphingolipids. Their roles are quite complex from signal transduction, endocytosis, to cholesterol trafficking. The rafts appear to be heterogeneous in their lipid and protein composition and this is indicative of a cross-talk between the raft components (Pike, 2004).

DGKε has the N-terminus transmembrane domain, which may target the protein to rafts. Raft association of DGKε has been studied by an undergraduate student in the lab, Craig Aarts. His results (data not shown) presented in his fourth year project thesis (Aarts, 2006) indicated that the protein does not appear to associate with lipid rafts in the membranes of COS-7 cells. However, the lipid raft association could be stimulated by other unknown factors, which still need to be discovered.

The results of the oligomerization studies of DGKε point to the possibility that the transmembrane domain may not be the only domain involved in oligomerization. It is also known from the literature that caveolin 1 forms homo-oligomers and homo-oligomerization is mediated by domains outside the transmembrane domain. One such

domain is found at the N-terminus and the other one at the C-terminus. Below is a diagram of a proposed model for caveolin 1 oligomerization as presented by Spisni *et al.*, 2005.

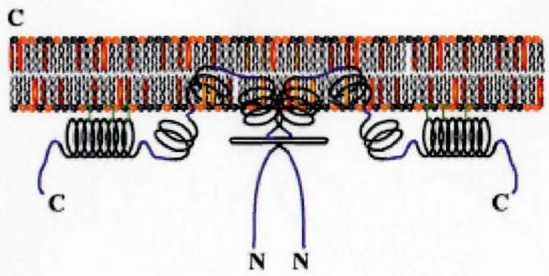

Fig. 45 Proposed model for caveolin 1 oligomerization (Spisni *et al.*, 2005). The oligomerization domain (61-101) comprises the β strand and the α-helix within the caveolin scaffolding domain

Since the experimental evidence from immunofluorescence microscopy came late in the project, the modeling studies of the oligomerization of the transmembrane peptide did not take into account the possibility of a hydrophobic loop in the peptide or the association of an amphipathic helix with the membrane. More modeling studies may be necessary to investigate these new findings.

Another possible regulatory mechanism for DGKε enzyme activation is the phosphorylation by various protein kinases. Protein kinases such as protein kinase C could phosphorylate DGKε and activate it. For example, DGKδ1 was shown to be phosphorylated by multiple protein kinases, cPKC phosphorylated amino acids in the PH domain, while another site of phosphorylation was predicted to be present at the C-terminus (Imai *et al.*, 2004). Phosphorylation of DGKδ1 negatively and critically regulated the translocation of this enzyme to the plasma membrane. In addition, Luo *et*

al., 2003, reported that PKCα interacted and phosphorylated DGKζ. The activated enzyme would then phosphorylate DAG to PA.

The phosphorylation of DGKε has not been studied but prediction software programs such as the NetPhos 2.0 Server (Blom *et al.*, 1999) have identified a set of sites of possible phosphorylation (Fig. 46).

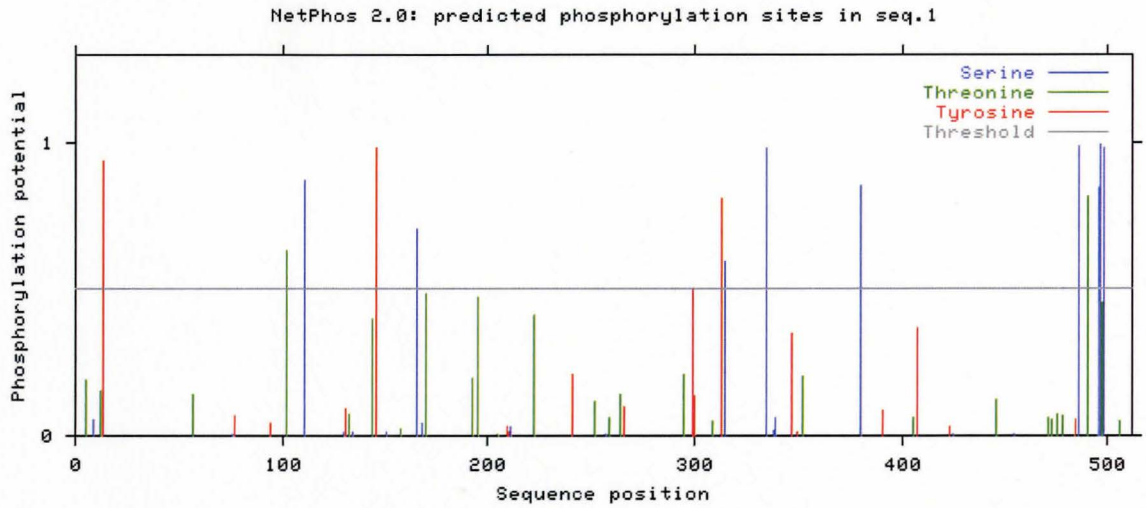

Fig. 46 Prediction of possible phosphorylation sites of human DGKε protein. The human DGKε protein sequence was run on the NetPhos 2.0 program. The program predicted 9 Ser residue sites, 3 Tyr residue sites, and 2 Thr residue sites of phosphorylation.

In addition, the NetPhosK 1.0 server program (Blom *et al.*, 2004) predicted specific kinases that would possibly phosphorylate the DGKε protein at specific sites (Table 3). Currently NetPhosK includes in the prediction the following kinases: PKA, PKC, PKG, CKII, Cdc2, CaM-II, ATM, DNA PK, Cdk5, p38 MAPK, GSK3, CKI, PKB, RSK, INSR, EGFR and Src.

Table 3

Prediction of possible kinases that would phosphorylate DGKε. The predicted kinase with the highest score was PKC at position 506.

S-11	GSK3	0.51
S-11	cdk5	0.53
T-26	PKA	0.58
S-29	cdc2	0.51
S-41	DNAPK	0.51
S-58	PKC	0.51
S-69	CKI	0.53
S-69	DNAPK	0.55
S-69	ATM	0.55
S-171	PKC	0.72
S-171	PKA	0.65
T-204	CKII	0.58
T-204	PKG	0.60
Y-206	INSR	0.57
S-211	PKC	0.69
S-211	cdc2	0.52
T-255	p38MAPK	0.55
S-317	PKA	0.53
T-355	PKC	0.65
T-355	cdc2	0.50
Y-359	EGFR	0.51
S-398	PKC	0.60
S-440	CKI	0.58
T-466	CKII	0.53
S-485	PKC	0.66
T-506	**PKC**	**0.80**
T-550	CKII	0.65
S-555	CKII	0.52
S-556	CKII	0.62
S-556	CKI	0.51
T-557	CKII	0.69
S-558	CKII	0.72

Based on previous experimental findings of phosphorylation being a regulatory mechanism for other human DGKs, it can be predicted that it may play a role in DGKε regulation since there is a pool of PKCs found to be tightly membrane-bound (Zhu *et al.*, 2005). Therefore, access to DGKε would not require PKC translocation to the membrane. It is unknown whether DGKε is interacting with other proteins involved in cell signaling. This protein-protein interaction may play a role in enzyme activation and further investigations are needed.

4.6 Summary and future directions

Extensive research has been done on the mammalian DGK family of enzymes in the last decade or so. The focus was partly due to the fact that DGKs influence many signaling pathways because both the substrate and the product of these kinases, DAG and PA, have signaling properties and their concentration in the cell must be tightly regulated. Being such key factors in maintaining constant levels of second messengers such as DAG, DGKs have been found to impact on many cellular functions such as growth and differentiation, gene expression, and intermediary metabolism (Topham, 2006). The class of mammalian isoforms is large; there are ten mammalian isoforms identified to date and they are divided into five classes. One distinct class of mammalian DGKs, the type III, seems to have no other regulatory domains but the Cys-rich regions (C1 domains) and the catalytic domain. DGKε is the only known type III isoform.

We decided to investigate this unique DGK isoform since progress in the area has been limited and low interest has been paid to this isoform due to its simple structure and ubiquitous localization. Researchers have mentioned the presence of an N-terminus hydrophobic segment in DGKε (Epand *et al.*, 2004) and this study investigated this unique feature of DGKε and how it relates to enzyme function. A truncated mutant of the full-length enzyme was studied in parallel with the wild-type enzyme and there were surprising results from this study.

It was interesting to note that the removal of a 40 amino acid segment of the protein appeared to have no deleterious effect on the activity and may have even resulted in an enhanced catalytic rate. This situation had precedent with DGKα that had higher

activity after truncation of its amino terminus (Abe *et al.*, 2003). It appears unlikely that the N-terminal hydrophobic domain of DGKε, a segment unique to DGKε, has no functional role. The hydrophobic segment may play a role in protein-protein interactions.

Further investigations into the involvement of the N-terminus hydrophobic domain of DGKε in oligomerization have led to surprising results. The hydrophobic domain appears to affect only the monomer to dimer ratio, the dimer still being present in the truncated enzyme. This result points towards the involvement of another segment of DGKε in oligomerization.

Thirugnanam *et al.*, 2001, have pointed the attention towards a domain juxtaposed to the hydrophobic segment towards the C-terminus of the protein. This domain was found to have a cationic cluster of six arginine (Arg) amino acids in a 15 amino acid segment (Fig. 40). This cationic cluster is hypothesized to bind to anionic lipids such as PS and PIP_2 in the membrane. We constructed two new truncated mutants of DGKε without any tag, one with truncation 1-41 amino acids and the other with truncation 1-59 amino acids (Fig. 37). Further investigations involving these new mutants will hopefully bring clarification to the results obtained with truncation 1-41. It is expected that the 1-59 truncation mutant will show more drastic changes than the 1-41 truncation mutant showed in this study since it may not associate as well with the anionic lipids in the membrane and may have a different subcellular or intramembrane localization. It is expected that the anionic cluster may have an influence on the raft localization of this enzyme, but preliminary studies of raft localization (Aarts, 2006) showed that even the full-length protein did not localize to rafts. Alternatively, the cationic cluster may have a

role in oligomerization of the enzyme at the membrane. Further investigations are needed to elucidate this hypothesis.

Since there were not drastic differences between the behavior of the full-length enzyme and the truncated mutant, we decided to investigate the topology of the protein at the membrane to give clues about possible explanations to the unusual behavior of this membrane protein enzyme. The results of this experiment were surprising since the N-terminus of the enzyme was found to be on the cytoplasmic side of the membrane. There could be two different conclusions from this and further investigations are needed to differentiate the two. One conclusion is that both the N and C terminus of this protein reside in the cytoplasm and the second one is that the C terminus of the enzyme resides on the extracellular side of the plasma membrane. In addition, if both the N and the C terminus are on the cytoplasmic side of the membrane, the putative transmembrane domain can have two different orientations: one could be a hydrophobic loop caused by the presence of the Pro in the middle of the sequence and the other one could be a planar amphipathic helix since the helical wheel shows a sidedness of the polar residues.

Chapter 5. References

Aarts, C. (2006). Raft Localization and Oligomerization of Diacylglycerol Kinase Epsilon. McMaster University.
Ref type: Thesis/ 4th year project

Abe, T., Lu, X., Jiang, Y., Boccone, C.E., Qian, S., Vattem, K.M., Wek, R.C., Walsh, J.P. (2003). Site-directed mutagenesis of the active site of diacylglycerol kinase alpha: calcium and phosphatidylserine stimulate enzyme activity via distinct mechanisms. *Biochem. J* 375: 673-680.

Alberts, B., Johnson, A., Lewis, J., Raff, M., Roberts, K., Walter, P. (2002). Molecular biology of the cell. 4th edition. Garland Science. NY. USA. : 831-870.

Anderson, R.A., Boronenkov, I.V., Doughman, S.D., Kunz, J., Loijens, J.C. (1999). Phosphatidylinositol phosphate kinases, a multifaceted family of signaling enzymes. *J. Biol. Chem.* 274 (15): 9907-9910.

Anderson, K.E. and Jackson, S.P. (2003). Class I phosphoinositide 3-kinases. *Int. J. Biochem. Cell Biol.* 35: 1028-1033.

Bajjalieh, S.M., Martin, T.F., Floor, E. (1989). Synaptic vesicle ceramide kinase. A calcium-stimulated lipid kinase that co-purifies with brain synaptic vesicles. *J.Biol.Chem.* 264: 14354-14360.

Basyn, F., Charloteaux, B., Thomas, A., Brasseur, R. (2001). Prediction of membrane protein orientation in lipid bilayers: a theoretical approach. *J. Molecular Graphics and Modelling* 20: 235-244.

Baumruker, T., Bornancin, F., Billich, A. (2005). The role of sphingosine and ceramide kinases in inflammatory responses. *Immunology Letters* 96: 175-185.

Berg, O.G., Yu, B.Z., Rogers, J., Jain, M.K. (1991). Interfacial catalysis by phospholipase A_2: determination of the interfacial kinetic rate constants. *Biochemistry* 30: 7283-7297.

Birrel, G.B., Hedberg, K.K., Volwerk, J.J., Griffith, O.H. (1993). Differential expression of phospholipase C specific for inositol phospholipids at the cell surface of rat glial cells and REF52 rat embryo fibroblasts. *J. Neurochem.* 60 (2): 620-625.

Blobel, G. (1980). Intracellular protein topogenesis. *Proc. Natl. Acad. Sci.* USA 77:1496-1500.

Blom, N., Gammeltoft, S., Brunak, S. (1999). Sequence- and structure-based prediction of eukaryotic protein phosphorylation sites. *J. Molecular Biology* 294 (5): 1351-1362.

Blom, N., Sicheritz-Ponten, T., Gupta, R., Gammeltoft, S., Brunak, S. (2004). Prediction of post-translational glycosylation and phosphorylation of proteins from the amino acid sequence. *Proteomics* 4 (6): 1633-1649.

Camacho-Carvajal, M.M., Wollscheid, B., Aebersold, R., Steimle, V., Schamel, W.W.A. (2004). Two-dimensional blue-native/SDS gel electrophoresis of multi-protein complexes from whole cellular lysates. *Molecular & Cellular Proteomics* 3.2: 176-182.

Carman, G.M., Deems, R.A., Dennis, E.A. (1995). Lipid signaling enzymes and surface dilution kinetics. *J. Biol. Chem.* 270: 18711-18714.

Cornish-Bowden, A. (2004). Fundamentals of Enzyme kinetics. 3rd edition. Portland press. : 46-48, 355-359.

Cserzo, M., Wallin, E., Simon, I., von Heijne, G., Elofsson, A. (1997). Prediction of transmembrane α-helices in prokaryotic membrane proteins: the dense alignment surface method. *Protein Engineering* 10 (6): 673-676.

Deems, R.A., Eaton, B.R., Dennis, E.A. (1975). Kinetic analysis of phospholipase A_2 activity toward mixed micelles and its implications for the study of lipolytic enzymes. *J. Biol. Chem.* 250: 9013-9020.

Deems, R.A. (2000). Interfacial enzyme kinetics at the phospholipids/water interface: practical considerations. *Anal. Biochem.* 287: 1-16.

Dennis, E.A. (1973). Kinetic dependence of phospholipase A_2 activity on the detergent Triton X-100. *J. Lipid Res.* 14: 152-159.

Dennis, E.A. (1983). Phospholipases. The enzymes (Boyer, P.). 3rd edition. Academic Press. NY 16: 307-353.

Ding, L., Traer, E., McIntyre, T.M., Zimmerman, G.A., Prescott, S.M. (1998). The cloning and characterization of a novel human diacylglycerol kinase, DGKι. *J. Biol. Chem.* 273: 32746-32752.

Ducarme, Ph., Rahman, M., Brasseur, R. (1998). IMPALA: A simple restraint field to simulate the biological membrane in molecular structure studies. *Proteins: Structure, Function, and Genetics* 30: 357-371.

Epand, R.M., Kam, A., Bridgelal, N., Saiga, A., Topham, M.K. (2004).The α isoform of diacylglycerol kinase exhibits arachidonoyl specificity with alkylacylglycerol. *Biochemistry* 43: 14778-14783.

Eubel, H., Braun, H-P., Millar, A.H. (2005). Blue-native PAGE in plants: a tool in analysis of protein-protein interactions. *Plant Methods* 1 (1): 11.

Fukunaga-Takenaka, R., Shirai, Y., Yagi, K., Adachi, N., Sakai, N., Merino, E., Merida, I., Saito, N. (2005). Importance of chroman ring and tyrosine phosphorylation in the subtype-specific translocation and activation of diacylglycerol kinase α by D-α-tocopherol. *Genes to Cells* 10: 311-319.

Glukhov, E., Stark, M., Burrows, L.L., Deber, C. M. (2005). Basis for selectivity of cationic antimicrobial peptides for bacterial versus mammalian membranes. *J. Biol Chem.* 280 (40): 33960-33967.

Gomez-Merino, F.C., Brearley, C.A., Ornatowska, M., Abdel-Haliem, M.E.F., Zanor, M.-I., Roeber, B.M. (2004). AtDGK2, a novel diacylglycerol kinase from Arabidopsis thaliana, phosphorylates 1-stearoyl-2-arachidonoyl-sn-glycerol and 1, 2-dioleoyl-sn-glycerol and exhibits cold-inducible gene expression. *J. Biol. Chem.* 279 (9): 8230-8241.

Goto, K. and Kondo, H. (2004). Functional implications of the diacylglycerol kinase family. *Advan. Enzyme Regul.* 44: 187-199.

Heilmeyer Jr., L.M.G., Vereb Jr., G., Vereb, G., Kakuk, A., Szivak, I. (2003). Mammalian phosphatidylinositol 4-kinases. *IUBMB Life* 55 (2): 59-65.

Hirokawa, T., Boon-Chieng, S., Mitaku, S. (1998). SOSUI: classification and secondary structure prediction system for membrane proteins. *Bioinformatics* 14 (4): 378-379.

Hodgkin, M.N., Gardner, S.D., Rose, S., Paterson, A., Martin, A., Wakelam, M.J.O. (1997). Purification and characterization of sn-1-stearoyl-2-arachidonoylglycerol kinase from pig testes. *Biochem J.* 322: 529-534.

Hogan, A., Shepherd, L., Chabot, J., Quenneville, S., Prescott, S.M., Topham, M.K., Gee, S.H. (2001). Interaction of γ1-syntrophin with diacylglycerol kinase ζ. *J. Biol. Chem.* 276: 26526-26533.

Houssa, B., Schaap, D., van der Wal, J., Goto, K., Yamakawa, A., Shibata, M., Takenawa, T., van Blitterswijk, W.J. (1997). Cloning of a Novel Human Diacylglycerol Kinase (DGKθ) Containing Three Cysteine-rich Domains, a Proline-rich Region, and a Pleckstrin Homology Domain with an Overlapping Ras-associating Domain. *J. Biol. Chem.* 272: 10422-10428.

Imai, S-i., Sakane, F., Kanoh, H. (2002). Phorbol ester-regulated oligomerization of diacylglycerol kinase δ linked to its phosphorylation and translocation. *J. Biol. Chem.* 277 (38): 35323-35332.

Imai, S-i., Kai, M., Yamada, K., Kanoh, H., Sakane, F. (2004). The plasma membrane translocation of diacylglycerol kinase δ1 is negatively regulated by conventional PKC-dependent phosphorylation at Ser-22 and Ser-26 within the pleckstrin homology domain. *Biochem J.* 382: 957-966.

Imai, S-i., Kai, M., Yasuda, S., Kanoh, H., Sakane, F. (2005). Identification and characterization of a novel human type II diacylglycerol kinase, DGKκ. *J. Biol. Chem.* 280 (48): 39870-39881.

Jennings, M. L. (1989). Topography of membrane proteins. *Annu. Rev. Biochem.* 58: 999-1027.

Kohyama-Koganeya, A., Watanabe, M., Hotta, Y. (1997). Molecular cloning of a diacylglycerol kinase isozyme predominantly expressed in rat retina. *FEBS Letters* 409: 258-264.

Liscum, L., Ruggiero, R.M., Faust, J.R. (1989). The intracellular transport of low density lipoprotein-derived cholesterol is defective in Niemann-Pick type C fibroblasts. *J. Cell. Biol.* 108: 1625-1636.

Liu, L.P. and Deber, C.M. (1998). Guidelines for membrane protein engineering derived from de novo designed model peptides. *Biopolymers (Peptide Science)* 47: 41-62.

Luo, B., Prescott, S.M., Topham, M.K. (2003). PKCα phosphorylates and negatively regulates DGKζ. *J. Biol. Chem.* 278: 39542-39547.

Luo, B., Regier, D.S., Prescott, S.M., Topham, M.K. (2004). Diacylglycerol kinases. *Cellular Signalling* 16: 983-989.

MacDonald, M.L., Mack, K.F., Williams, B.W., King, W.C., Glomset, J.A. (1988). A membrane-bound diacylglycerol kinase that selectively phosphorylates arachidonoyl-diacylglycerol. *J. Biol. Chem.* 263 (3): 1584-1592.

Mafalda, N., Berneche, S., Roux, B. (2000). Anchoring of a monotopic membrane protein: the binding of prostaglandin H2 synthase-1 to the surface of a phospholipid bilayer. *Eur. Biophys. J.* 29: 439-454.

Master, S.C. (2004). Co-immunoprecipitation from transfected cells. *Methods in Molecular Biology*: Protein-Protein Interactions: Methods and Protocols 261: 337-348.

Murakami, T., Sakane, F., Imai, S-i., Houkin, K., Kanoh, H. (2003). Identification and characterization of two splice variants of human diacylglycerol kinase η. *J. Biol. Chem.* 278 (36): 34364-34372.

Musto, A. and Bazan, N.G. (2006). Diacylglycerol kinase epsilon modulates rapid kindling epileptogenesis. *Epilepsia* 47(2): 267- 276.

Nagaya, H., Wada, I., Jia, Y-J., Kanoh, H. (2002). Diacylglycerol kinase δ suppresses ER-to-Golgi traffic via its SAM and PH domains. *Mol. Biol. Cell* 13: 302-316.

Noble, M.E., Endicott, J.A., Johnson, L.N. (2004). Protein kinase inhibitors: insights into drug design from structure. *Science* 303: 1800-1805.

Ohanian, J. and Heagerty, A.M. (1994). Membrane-associated diacylglycerol kinase activity is increased by noradrenaline, but not by angiotensin II, in arterial smooth muscle. *Biochem J.* 300: 51-56.

Ottaway, L. (2006). Characterization of the mammalian diacylglycerol kinase epsilon isoform. McMaster University
Ref Type: Thesis/ 4th year project

Pettitt, T.R. and Wakelam, J.O. (1999). Diacylglycerol kinase ε, but not ζ, selectively removes polyunsaturated diacylglycerol, inducing altered protein kinase C distribution in vivo. *J. Biol. Chem.* 274 (51): 36181-36186.

Pierce Biotechnology Inc. (2005). Protein Structure: Cross-linking instruction book
http://www.piercenet.com/files/0418as4.pdf
Ref Type: Electronic Citation

Pike, L.J. (2004). Lipid rafts: heterogeneity on the high seas. *Biochem J.* 378: 281-292.

Prescott, S.M. and Majerus, P.W. (1981). The fatty acid composition of phosphatidylinositol from thrombin-stimulated human platelets. *J. Biol. Chem.* 256: 579-582.

Ramjeesingh, M., Huan, L., Garami, E., Bear, C. (1999). Novel method for evaluation of the oligomeric structure of membrane proteins. *Biochem J.* 342:119-123.

Rodriguez de Turco, E. B., Tang, W., Topham, M.K., Sakane, F., Marcheselli, V.L., Chen, C., Taketomi, A., Prescott, S.M., Bazan, N. (2001). Diacylglycerol kinase ε regulates seizure susceptibility and long-term potentiation through arachidonoyl-inositol lipid signaling. PNAS 98 (8): 4740-4745.

Sapay, N. (2006). In-plane Membrane Anchoring Peptides: structural characterization by NMR and molecular dynamics & development of a bioinformatics prediction method. Institut de Biologie et Chimie des Protéines, Lyon, France
Ref Type: Thesis/ Dissertation

Sapay, N., Guermeur, Y., Deleage, G. (2006). Prediction of amphipathic in-plane membrane anchors in monotpic proteins using a SVM classifier. *Bioinformatics* 7: 255-279.

Schagger, H., Cramer, W.A., von Jagow, G. (1994). Analysis of molecular masses and oligomeric states of protein complexes by blue native electrophoresis and isolation of membrane protein complexes by two-dimensional native electrophoresis. *Analytical Biochemistry* 217: 220-230

Schlegel, A., Pestell, R.G., Lisanti, M.P. (2000). Caveolins in cholesterol trafficking and signal transduction: implications for human disease. *Frontiers in Bioscience* 5: 929-937.

Singer, S. J. and Nicolson, G.L. (1972). The fluid mosaic model of the structure of cell membranes. *Science* 175: 720-731.

Spisni, E., Tomasi, V., Cestaro, A., Tosatto, S.C.E. (2005). Structural insights into the function of human caveolin 1. *Biochem. Biophys. Res. Comm.* 338: 1383-1390.

Takeuchi, H., Kanematsu, T., Misumi, Y., Sakane, F., Konishi, H., Kikkawa, U., Watanabe, Y., Katan, M., Hirata, M. (1997). Distinct specificity in the binding of inositol phosphates by pleckstrin homology domains of pleckstrin, RAC-protein kinase, diacylglycerol kinase and a new 130kDa protein. *Biochim. Biophys. Acta* 1359: 275-285.

Tang, W., Bunting, M., Zimmerman, G.A., McIntyre, T.M., Prescott, S.M. (1996). Molecular cloning of a novel human diacylglycerol kinase highly selective for arachidonate-containing substrates. *J. Biol. Chem.* 271:10237-10241.

Tang, W., Bardien, S., Bhattacharya, S.S., Prescott, S.M. (1999). Characterization of the human diacylglycerol kinase ε gene and its assessment as a candidate for inherited retinitis pigmentosa. *Gene* 239: 185-192.

Thirugnanam, S., Topham, M.K., Epand, R.M. (2001). Physiological implications of the contrasting modulation of the activities of the ε- and ζ- isoforms of diacylglycerol kinase. *Biochemistry* 40:10607-10613.

Topham, M.K., Bunting, M., Zimmerman, G.A., McIntyre, T.M., Blackshear, P.J., Prescott, S.M. (1998). Protein kinase C regulates the nuclear localization of diacyglycerol kinase ζ. *Nature* 394: 697-700.

Topham, M.K. and Prescott, S.M. (2002). Diacylglycerol kinases: regulation and signaling roles. *Thromb. Haemost.* 88: 912-918.

Topham, M.K. (2006). Signaling roles of diacylglycerol kinases. *J. Cellular Biochemistry* 97: 474-484.

Torshin, I. (1999). Activating oligomerization as intermediate level of signal transduction: analysis of protein-protein contacts and active sites in several glycolytic enzymes. *Frontiers in Bioscience* 4: 557-570.

van Blitterswijk, W.J. and Houssa, B. (1999). Diacylglycerol kinases in signal transduction. *Chemistry and Physics of Lipids* 98: 95-108.

van Blitterswijk, W.J. and Houssa, B. (2000). Properties and functions of diacylglycerol kinases. *Cell Signal.* 12: 595-605.

Walsh, J.P., Suen, R., Lemaitre, R.N., Glomset, J.A. (1994). Arachidonoyl-diacylglycerol kinase from bovine testis. Purification and properties. *J. Biol. Chem.* 269:21155-21164.

Wang, Y., Castoreno, A.B., Stockinger, W., Nohturfft, A. (2005). Modulation of endosomal cholesteryl ester metabolism by membrane cholesterol. *J. Biol. Chem.* 280 (12): 11876-11886.

Yamada, K., Sakane, F., Matsushima, N., Kanoh, H. (1997). EF-hand motifs of α, β, and γ isoforms of diacylglycerol kinase bind calcium with different affinities and conformational changes. *Biochem J* 321: 59-64.

Yang, Z., Lui, Y., Mao, L., Zhang, J., Zou, Y. (2002). Dimerization of human XPA and formation of XPA2-RPA protein complex. *Biochemistry* 41, 13012-13020.

Yeagle, P.L. (1993). The membranes of cells. Ch.6: *Membrane proteins*. Ch 7: *Lipid-protein interactions and the roles of lipids in biological membranes*. 2nd edition. Academic Press Inc. 191-196, 202-227

Zhu, Y., Lim, W.G., Tan, B.J., Tian, S. T., Duan, W. (2005). Identification of an integral plasma membrane pool of protein kinase C in mammalian tissues and cells. *Cellular signaling* 17(9):1125-1136